Sensibilité neuronale à la stimulation lumineuse : implications pour la thérapie par photostimulation

Anistasha Lightning

Université Claude Bernard Lyon 1

THESE de DOCTORAT DE
L'UNIVERSITE CLAUDE BERNARD LYON 1

Ecole Doctorale N° 476
NSCO Neurosciences et Cognition

Discipline : Neurosciences Cellulaires et Moléculaires

Soutenue publiquement le 11/12/2023, par :
Anistasha LIGHTNING

Sensibilité neuronale à la stimulation lumineuse : implications pour la thérapie par photostimulation

---

Devant le jury composé de :

CREPEL, Valérie : Directrice de Recherche, INSERM Marseille U1249-Inmed - Rapporteure
GAIARSA, Jean-Luc : Directeur de Recherche, CNRS Marseille U1249-Inmed - Rapporteur
MARTIN, Claire : Chargée de Recherche, INSERM Paris UMR 8251–BFA - Examinatrice
RHEIMS, Sylvain : Professeur des Universités/Praticien Hospitalier, Université Lyon 1 UMR5292-CRNL - Président

KUCZEWSKI, Nicola : Maître de Conférences, Université Lyon 1 UMR5292-CRNL - Directeur de thèse

Université Claude Bernard Lyon 1

DOCTORAL THESIS from
THE UNIVERSITY OF LYON CLAUDE BERNARD 1

Doctoral School N°476
NSCO Neuroscience and Cognition

Discipline: Cellular and Molecular Neuroscience

Defended Publicly on the 11/12/2023, by:
Anistasha LIGHTNING

Neuronal sensibility to light stimulation: implications for photostimulation therapy

---

In front of a jury composed by:

CREPEL, Valérie: Research Director, INSERM Marseille U1249-Inmed - Reviewer
GAIARSA, Jean-Luc: Research Director, CNRS Marseille U1249-Inmed - Reviewer
MARTIN, Claire: Head of Research, INSERM Paris UMR 8251–BFA - Examiner
RHEIMS, Sylvain: Professor / Hospital Practitioner, University of Lyon 1 UMR5292-CRNL - President

KUCZEWSKI, Nicola: Professor, University of Lyon 1 UMR5292-CRNL – Thesis Director

ACKNOWLEDGEMENTS

There are many people to thank, all of whom were invaluable in making this work possible. First and foremost, I need to thank my thesis supervisor and mentor through this whole process: Nicola Kuczewski. You found a cognitive psychology researcher interested in switching fields and decided that motivation and a desire to learn were enough. I came into this doctoral project with little background in biophysics and cellular physiology, and the learning curve was both steep and rapid. It's only thanks to your abilities as a teacher and your patience as a mentor that I was able to succeed. I'm sorry I broke so many things in your lab. In my defense, I also fixed a lot of things. In any case, rest assured that once I leave the CRNS you will no longer have to worry about walking into the electrophysiology lab and finding a doctoral student disassembling various parts of your electrophysiology equipment.

I also need to thank my spouse, Max, for all of their support and encouragement over the course of this project. Thank you for sitting through countless hours of presentation practice, helping me talk through tangled thoughts, and most importantly for pushing me to keep going even when I felt like I couldn't. A special mention as well to my brother, Shane, who got so tired of me talking about this work every time I saw him that he crashed his motorcycle halfway through the project, presumably to avoid all further discussion via coma. I appreciate the theatric dramaticism of the avoidance tactic but am nonetheless overjoyed that it didn't work. Unfortunately, he now gets to hear me talk even more about how light stimulation therapy may also be applicable to his new head injuries.

I extend my heartfelt appreciation to the members of my thesis following committee, Nadia Urbain and Marco Canepari, who offered great insight and commentary at our yearly check-in meetings. I offer a separate and sincere thank you to Nadia, who also provided encouragement and warm words during my brother's aforementioned theatrics and subsequent recovery. Your kindness and that of others in the lab was instrumental in keeping me in the doctoral program throughout that time. And of course, I must thank the CRNL and the University of Lyon 1, who funded my participation in conferences and formative coursework throughout the doctoral program. Finally, I would like to thank the two interns that assisted on various aspects of this project: Hajar El Yaqoti and Fabrice Abate. You were both fantastic to work with and I wish you every success in your lives and academic journeys.

ABSTRACT

Mammalian biological tissues are capable of interacting with light. In the early 2000s, the development of optogenetics allowed for the introduction of genetically modified opsin (photoreceptors) to rodents, which facilitates real time optical control of neuronal behavior in research settings. A growing body of recent work suggests that neurons in the central nervous system may be sensitive to light without prior optogenetic modification. These effects include changes to neuronal firing rates and effects on the membrane physiology. Naïve neuronal light sensibility presents potential problems for optogenetic experimentation, which relies on the light stimulation of brain tissues. Additionally, it is possible that light-mediated reduction in naïve neuronal firing activity could be adapted for medical use. The present work provides an overview of the current literature concerning neuronal light sensitivity. Further, it presents two studies with the aim of (a) making recommendations for optogenetic research to avoid artefactual data produced by naïve neuronal light sensitivity and (b) investigating the possibility that blue light stimulation may be adaptable as a treatment for neural pathologies where the chief component is uncontrolled neuronal hyperexcitability.

SUMMARY (ENGLISH)

Light is experienced as electromagnetic radiation. This radiation is classified by its wavelength and energy levels, and experiences various transformations as it moves through space and matter before ever reaching those who perceive it. Visual spectrum light, as the name suggests, is naturally perceivable by photoreceptors in the human eye. Our eyes can interact with the electromagnetic radiation and transform it into a type of energy that neurons can understand (phototransduction), thus granting us our sense of vision. Mammalian tissues that are sensitive to light are not contained only within the eye, and indeed the question of whether biological tissues outside of the eye are sensitive to light can be traced as far back as the 1800s. The light sensitivity of neurons, specifically, traces back to the 1960s.

While this line of questioning has existed for some decades, it was the advent of optogenetics in the early 2000s that reinvigorated a cascade of investigative work concerning neuronal light sensitivities in the central nervous system (CNS). Optogenetics employs the use of genetically modified opsin—light sensitive g-protein-coupled receptors—to selectively modulate rodent brain activity during neuroscientific research. A growing body of research is demonstrating that neurons in the brain exhibit natural light sensibility even without any optogenetic modification. This naïve neuronal light sensitivity has been demonstrated in the mammalian CNS, with several recent studies reporting light-mediated decreases to action potential firing rates and membrane hyperpolarization *in vitro* concomitant with light-induced increases to tissue temperature. Visual spectrum light appears to also be capable of modulating naïve rodent behaviors *in vivo*. The totality of the biological mechanism behind this effect is currently still under investigation, though researchers have begun to uncover evidence for components that are mediated by light-induced tissue temperature increases and light-induced changes to inhibitory synaptic activity.

The effect of light on naïve neuronal physiology presents a concern for optogenetic experimentation. As these assays rely on the stimulation of the brain with light, it is possible that the natural light sensitivity of the surrounding naïve neurons may be confounding the results of these studies. Thus, the first goal of the present work is to investigate several light stimulation patterns commonly used in optogenetics to evaluate their varying effects of naïve neuronal physiology. The aim is twofold. In one part, to make recommendations for the light stimulation parameters that may prevent artefactual data due to naïve neuronal light sensibility. The other is to understand the effect of the light on several different neuronal subtypes. This serves to both broaden the argument for caution in optogenetic assays and to set up the second research question: is the neuronal effect of light medically adaptable?

The medical adaptability of CNS light stimulation is not a new question. Both visual and infrared (IR) light appear to be capable of penetrating through the rodent and human skull, which opens the possibility for minimally invasive or non-invasive brain light stimulation. Non-invasive transcranial IR light stimulation has already been adapted in a pre-clinical medical context. It has sown promise for the treatment of traumatic brain injuries and appears to be effective in improving cognitive functions such as problem solving and emotional cognition. Transcranial white light stimulation delivered via the ear canals has also shown promise for treating depression symptoms in human patients.

Very recent evidence suggests that one-photon blue light stimulation is capable of decreasing neuronal activity and generating a hyperpolarizing membrane current in several mouse neuronal subtypes *in vitro*. The effect is, however, often transient, with activity levels recovering to baseline after the end of the light stimulation. The magnitude of light's effect on naïve neurons does appear to be mediated by light power levels and stimulation durations. Therefore, it is possible that increasing these parameters could produce a non-transient effect. If a long-lasting reduction in neuronal firing can be produced and validated with human

neurons *in vitro*, then it may be possible to apply blue light stimulation to the treatment of pathologies where the primary component is uncontrolled neuronal hyperexcitability.

Specifically, I seek to understand whether this could be a viable therapeutic tool for epileptic syndromes. Around 30% of epileptic patients are not able to control their seizures pharmacologically. The sole recourse in these cases is the surgical removal of the epileptic tissues. Blue light mediated neuronal activity reduction may become a less invasive alternative for these patients. For now, this hope is purely speculative, and the second study will aim to establish more of the background necessary for continuing an investigation in this direction.

Consequently, the second study uses greater light power and stimulation duration (compared to previous studies) to create a long-lasting action potential firing suppression in mouse cortical neurons and attempts to replicate the suppression in human cortical neurons. Additionally, it attempts to gather more information concerning the light's effect on neuronal membrane physiology and how this may be related to the observed suppression of action potential firing rates. This includes investigating the light-mediated changes to the sodium and potassium ion currents associated with the action potential.

From the results of these studies, I will make recommendations for future studies investigating the applicability of light stimulation therapy to the treatment of epileptic syndromes. I thank you for your time in reading the overview of the established literature on the subject in addition to the two studies meant to further the case for light stimulation therapy.

RÉSUMÉ (FRANÇAIS)

La lumière est perçue comme les rayonnements électromagnétiques. Ces rayonnements sont classés selon sa longueur d'onde et ses niveaux d'énergie, et sont subit à diverses transformations pendant ses déplacements au travers l'espace et la matière avant d'atteindre ceux qui le perçoivent. La lumière du spectre visuel, comme le nom indique, est naturellement perceptible par les photorécepteurs de l'œil humain. Nos yeux peuvent interagir avec les rayonnements électromagnétiques et les transformer en un type d'énergie que les neurones peuvent comprendre (la phototransduction). Celle-ci nous accordant ainsi notre sens de la vision. Les tissus des mammifères qui sont sensibles à la lumière ne sont pas contenus uniquement dans l'œil, et en effet, la question de savoir si les tissus biologiques situés à l'extérieur de l'œil sont sensibles à la lumière remonte au XIXe siècle. La sensibilité à la lumière des neurones, en particulier, remonte aux années 1960.

Bien que cette ligne de questionnement existe depuis quelques décennies, c'était l'avènement de l'optogénétique au début des années 2000 qui a relancé une cascade de travaux concernant les sensibilités neuronales à la lumière dans le système nerveux central (SNC). L'optogénétique utilise l'opsine (des récepteurs couplés aux protéines G sensibles à la lumière) génétiquement modifiée pour moduler sélectivement l'activité cérébrale des rongeurs au cours de la recherche neuroscientifique. Récemment, de plus en plus de recherches démontrent que les neurones du cerveau présentent une sensibilité naturelle à la lumière, même sans aucune modification optogénétique. Cette sensibilité neuronale naïve à la lumière a été démontrée dans le SNC des mammifères, avec plusieurs études récentes faisant état de diminutions des taux de déclenchement du potentiel d'action et d'une hyperpolarisation membranaire *in vitro* concomitantes à des augmentations de la température des tissus induites par la lumière. La lumière du spectre visuel semble également capable de moduler les

comportements naïfs des rongeurs *in vivo*. La totalité du mécanisme biologique à l'origine de cet effet est actuellement encore à l'étude, bien que les chercheurs aient commencé à découvrir des preuves de composants médiés par des augmentations de température des tissus induites par la lumière et des modifications de l'activité synaptique inhibitrice induites par la lumière.

L'effet de la lumière sur la physiologie neuronale naïve présente une préoccupation pour l'expérimentation optogénétique. Comme ces tests reposent sur la stimulation du cerveau par la lumière, il est possible que la sensibilité naturelle à la lumière des neurones naïfs environnants confondrait les résultats de ces études. Ainsi, le premier objectif du présent travail est d'étudier plusieurs modèles de stimulation lumineuse couramment utilisés en optogénétique afin d'évaluer leurs effets variables sur la physiologie neuronale naïve. L'objectif est double. Dans une partie, de faire les recommandations concernant les paramètres de stimulation lumineuse qui peuvent empêcher les données artéfactuelles dues à une sensibilité neuronale naïve à la lumière. L'autre partie consiste à comprendre l'effet de la lumière sur plusieurs sous-types neuronaux différents. Cela sert à la fois à élargir l'argument en faveur de la prudence dans les tests optogénétiques et à introduire la deuxième question de recherche : l'effet neuronal de la lumière est-il médicalement adaptable ?

L'adaptabilité médicale de la stimulation lumineuse du SNC n'est pas une question nouvelle. La lumière visuelle et infrarouge (IR) semble être capable de pénétrer à travers le crâne des rongeurs et des humains, ce qui ouvre la possibilité d'une stimulation lumineuse cérébrale peu invasive ou non invasive. La stimulation lumineuse transcrânienne non invasive par lumière IR a déjà été adaptée dans un contexte médical préclinique. Il semble applicable pour le traitement des traumatismes crâniens, de telle sort qu'il semble d'améliorer la récupération. Il existe également des preuves que la ce type de stimulation IR peut améliorer les fonctions cognitives telles que la résolution de problèmes et la cognition émotionnelle. La

stimulation transcrânienne par la lumière blanche délivrée via les conduits auditifs s'est également révélée prometteuse pour traiter les symptômes de la dépression chez les patients humains.

Quelques études très récentes suggèrent que la stimulation par la lumière bleue à un photon est capable de diminuer l'activité neuronale et de générer un courant membranaire hyperpolarisant dans plusieurs sous-types neuronaux de souris *in vitro*. Cependant, l'effet est souvent transitoire et les niveaux d'activité revenant à leur niveau de base après la fin de la stimulation lumineuse. L'ampleur de l'effet de la lumière sur les neurones naïfs semble être médiée par les niveaux de puissance lumineuse et les durées de stimulation. Il est donc possible que l'augmentation de ces paramètres pourrait produire un effet non transitoire. Si une réduction durable du déclenchement du potentiel d'action peut être produite et validée avec des neurones humains *in vitro*, il pourrait être possible d'appliquer la stimulation par la lumière bleue au traitement de pathologies dont la composante principale est une hyperexcitabilité neuronale incontrôlée.

Plus précisément, je cherche à comprendre si cela pourrait constituer un outil thérapeutique viable pour les syndromes épileptiques. Environ 30 % des patients épileptiques ne parviennent pas à contrôler pharmacologiquement leurs crises. Le seul recours dans ces cas est l'ablation chirurgicale des tissus épileptiques. La réduction de l'activité neuronale médiée par la lumière bleue pourrait devenir une alternative moins invasive pour ces patients. Pour l'instant, cet espoir est purement spéculatif, et la deuxième étude essayera à établir davantage le contexte nécessaire pour poursuivre une enquête dans cette direction.

Par conséquent, la deuxième étude utilise une puissance lumineuse et une durée de stimulation plus grandes (par rapport aux études précédentes) pour créer une suppression de déclenchement de potentiel d'action durable dans les neurones corticaux de souris et tente de reproduire la suppression dans les neurones corticaux humains. De plus, il tente de recueillir

davantage d’informations sur l’effet de la lumière sur la physiologie de la membrane neuronale et sur la manière dont cela peut être lié à la suppression observée des taux de déclenchement des potentiels d’action. Cela comprend l'étude des changements induits par la lumière dans les courants ioniques sodium et potassium associés au potentiel d'action.

À partir des résultats de ces études, je formulerai des recommandations pour de futures études portant sur l'applicabilité de la thérapie par stimulation lumineuse au traitement à syndromes épileptiques. Je vous remercie d'avoir pris le temps de lire cette revue de la littérature établie sur le sujet et les deux études destinées à faire avancer les arguments en faveur de la thérapie par stimulation lumineuse.

ABREVIATIONS

1P: One-photon

ACSF: artificial cerebrospinal fluid

AHP: Afterhyperpolarization

AP: Action Potential

bPBM: brain photobiomodulation

CCO: cytochrome c-oxidase

CI: Confidence interval

CNS: central nervous system

EEG: electroencephalogram

EMR: Electromagnetic Radiation

ES: Effect size

FSI: fast-spiking interneuron

FWHM: Action potential full width at half maximum

GABA: Gamma-aminobutyric acid

GC: hippocampal granular cell

IR: infrared

Kir: Inwardly rectifying potassium channel

LED: light-emitting diode

MC: Mitral cells

MSN: Medium spiny neurons

NIR: Near infrared

NMDA: N-methyl-D-aspartic acid

NMDG: N-methyl d-glucamine

NO: Nitric oxide

OB: olfactory bulb

PNS: Peripheral nervous system

PYR: cortical pyramidal neuron

Rm: membrane resistance

SAD: Seasonal affective disorder

sIPSC: spontaneous inhibitory post-synaptic current

SLD: seizure-like discharge

T.I.: total illumination time

TLLT: Transcranial laser light therapy

UV : Ultra-violet

Vm: Membrane potential

LIST OF FIGURES

This list does not include figures within the studies.

TABLE OF CONTENTS

INTRODUCTION

The capacity to modify neuronal behavior with light has been known since the early 1960's and accumulating evidence shows that several neuronal subtypes in the central nervous system (CNS) appear to be naturally sensitive to light stimulation (e.g., Ait-Ouares et al., 2019; Lightning et al., 2023; Owen, Liu, & Kreitzer, 2019; Stujenske et al., 2015). The question of whether tissue behavior is sensitive to light can be traced back even further, with one of the first known studies on the subject taking place in 1891, where Arsonval (1891) investigated the activation of muscular fibers via light stimulation. This line of questioning continued through the late-19th century through the mid-20th century, ultimately culminating on the work of Arvanitaki, Chalazonitis, and Costa (1964), which showed definitive results for the excitation of the giant squid axon with luminous stimulation.

A growing body of more modern research suggests it is possible to modify neuronal behavior with visible light stimulation. This is true for the naïve (read: non-genetically modified) neurons in both invertebrates and vertebrates, with promising examples in mammalian species as well (Ait-Ouares et al., 2019; Anders et al., 2015; Deng et al., 2014; Duke et al., 2013; Owen, Liu, & Kreitzer, 2019; Senova et al., 2017; Stujenske et al., 2015). This underlines the key investigative target of the present work—the specific light sensibility of individual neurons in the mammalian CNS. This idea capitalizes on the apparent "natural sensitivity" to light of certain cellular subtypes in the CNS to create cellular behavior modification (Ait-Ouares et al., 2019; Gutiérrez-Menéndez et al., 2020; Huang, 2022). Possibly due to either light sensitive neuronal receptors or to light induced modification of thermo-sensitive ion channels (Anders et al., 2015; Deng et al., 2014; Fernades et al., 2013).

We are interested in two key offshoots of visible light effect on neuronal activity, all of which are primarily related to the sensibility of individual neurons to photostimulation. First, we are interested in possible physiological artefacts that may result from brain photostimulation in those assays that use light to achieve specific system effects, such as in optogenetics manipulations. In the most simplistic of summaries, optogenetics requires genetic modification resulting in the expression of exogenous light-sensitive proteins, called opsins, in a specific subpopulation of neurons. These neurons can then be selectively stimulated or inhibited with defined wavelengths of light, allowing researchers to develop insights into their interconnected functionalities (Deisseroth, 2015; Fenno, Yizar, & Diesseroth, 2011). However, this approach becomes concerning when one considers the aforementioned effects of light on the naïve neurons that risk producing an out of target effect of the optogenetic stimulation, leading to a misleading interpretation of the experimental outcome. Thus, the present investigation is first interested in the single neuron level physiological and activity changes associated with brain photostimulation, so that we might (a) speculate on possible confounds for optogenetic research and provide appropriate recommendations and (b) better understand the processes involved in a neuronal level light effect.

Second, it will explore the neuronal sensibility to visible light in a speculative, pre-clinical medical context. If light can affect the behavior of neurons both at the individual neuronal level and systemically (at the level of larger brain communication networks and the CNS) then it stands to reason that light may be capable of becoming a therapeutic tool to counteract the pathological alteration of neuronal activity in specific brain regions. Indeed, brain photobiomodulation (bPBM) therapies, such as those based on infrared (IR) stimulation of the CNS (Transcranial laser light therapy: TLLT), already exists in the pre-clinical and clinical research, and more recently has been adapted to patient-level treatments in medicine (Huang, 2022). This approach has shown promising results for pathologies such as psychiatric

conditions, neurodegenerative diseases such as Alzheimer's, tissue inflammation both within and without the nervous system, and some aspects of traumatic brain injury (TBI) (Hamblin, 2016; Huang, 2022). The cellular targets and mechanisms of action of IR light in bPBM are still debated but some of them could be the same or similar to ones that are involved in the visible light effect on neurons. These include the thermosensitive ion channels mentioned earlier, but also voltage gated channels, inhibitory networks, naturally occurring extra-ocular brain opsins, and photon interactions with the cellular nucleus (Richter & Tan, 2014; Huang, 2022). Understanding the neuronal mechanisms of visible light may therefore aid in understanding the mechanism behind bPBM therapies and may also provide new speculative avenues for the medical treatment of brain pathologies that are not actually targeted by bPBM.

In order to properly frame the points of investigation as they relate to neuronal light sensitivity, I will first examine and present the literature concerning what is currently known about the effects of light on the neuronal environment, the physiological mechanisms behind these effects, and the general methodology behind the optogenetic assays that we predict may be affected by naïve neuronal light sensitivity. This must, however, begin with the development of an appropriate level of understanding surrounding the physical mechanics of light and how light is able to reach and interact with biological tissues in the first place.

CHAPTER 1

THE PROPERITES OF LIGHT AND ITS INTERACTION WITH BIOLOGICAL TISSUE

1.1 The physical properties of light

Before any deeper discussion concerning the effect of light on neuronal tissue and behavior can begin, it is important to understand the physical properties of light itself. Humans experience light as electromagnetic radiation, which is composed of high energy particles called photons. Electromagnetic radiation (EMR) can be visualized (approximately) as a sine wave oscillation (Figure 1, top). It is thus classified by the varying wavelengths (λ), expressed in meters, observable within solar radiation or by the frequency of the oscillations in Hz (ν). Wavelength is defined as the distance between two peaks in the continuous oscillation of EMR particles, and frequency is defined as the number of waves per seconds. Light higher frequency has higher energy, where light with lower frequency has lower energy.

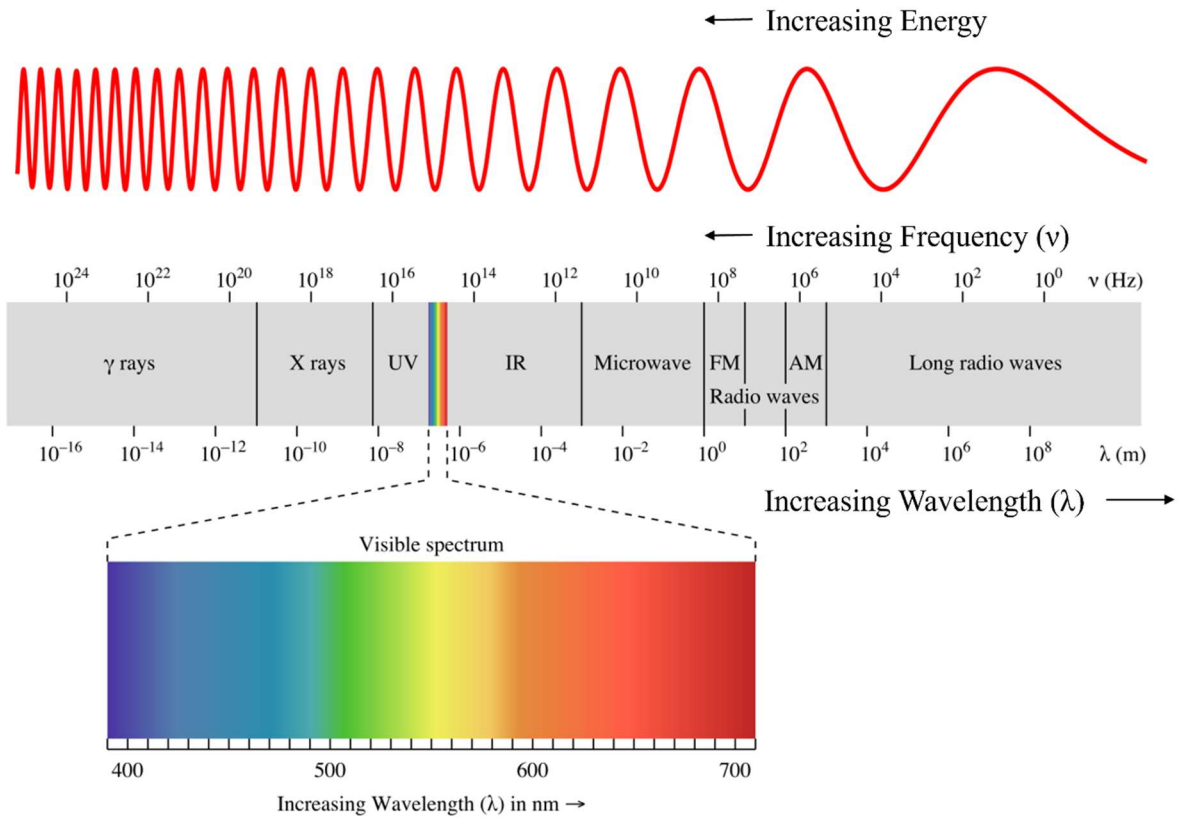

Figure 1. The electromagnetic spectrum. Frequency (waves per second) is expressed in Hz. Light contains photons that move through space via a series of oscillations, which contain both an 'up' and 'down' wave movement. Wavelength (the distance between two peaks in an oscillation) is expressed in meters. Adapted from: Phillip Roman, CC BY-SA 3.0, Wikimedia Commons.

When light reaches a certain energy threshold (around λ = 380nm), the individual photons contain the amount of energy necessary to interact with photosensitive molecular structures in the human eye, and thus becomes visible. The first color of visible light is violet, thus the EMR directly before this point is classified as ultraviolet light (UV, λ = 100nm – 380nm). As EMR energy lessens, it eventually reaches a point where the individual photons no longer have sufficient energy to interact with these molecular structures, and thus ceases to be visible to humans (around λ = 750nm). Since the last color on the visible spectrum is red, the EMR immediately beyond this point is classified as infrared light (IR, λ = 750nm-1mm). Of course, EMR does not exist only on the UV, visual, and IR spectrums. Indeed, there are huge variation in wavelength, from those that are the width of an atomic nucleus to those that are as wide as buildings. The varying classifications of EMR are displayed in Figure 1 (bottom). It is important, at this point, to note that though the frequency of EMR is used in the calculation of wavelength (λ = velocity/ frequency), one can change without necessarily changing the other. This is because frequency is fundamentally tied to the energy of the photons emited from the source, which remains constant, and wavelength is tied to the oscillations of the waveform of those photons moving through space. This principle will become very important shortly when I talk about light refraction (section 1.1c). But to get to that point, I must first finish discussing some more fundamental light properties.

There are many sources of EMR, the most well-known of course being the sun. The speed of light is defined by the velocity of solar radiation travels to earth through the vacuum of space, exactly 299, 792, 458 m/s. Since everyone on earth has not spontaneously dropped dead recently, it is reasonable to assume that the planet is not, itself, a vacuum. While good for our health, it creates some complications for how we must think of EMR. This is because as light passes through substances containing ordinary matter (e.g., anything that isn't a vacuum), its behavior changes. For example, the velocity of light through water is roughly ¾ of its

velocity in a vacuum. The remainder of this section will talk about four such behavior changes that are deeply important to the question of neuronal light stimulation: reflection, absorption, scattering, and refraction.

1.1a Light can be either reflected or absorbed

Light can also be absorbed by or reflected off matter it encounters. The property of reflection, incidentally, is what allows us to see. Certain wavelengths of visible light are selectively reflected by certain materials, which causes only those wavelengths to be observed when viewing an object, thus creating its color. The perception of color and the color itself are not a type of reflection, but rather the consequence of it.

There are two types of reflection. The first is specular, or mirrored reflection, which occurs when the light reflected from a surface retains both its energy and its image. This is often the case with things like mirrors and still polls of water. The second type is diffuse reflection, in which the light retains its energy but loses the image. This is the case when light reflects off a non-smooth surface. Looking back to the example of color: a mirror (specular reflection) reflects the range of visual spectrum light evenly, allowing it to retain the original image of the light being reflected. Conversely, a grey rock is reflecting light, but does not reflect each

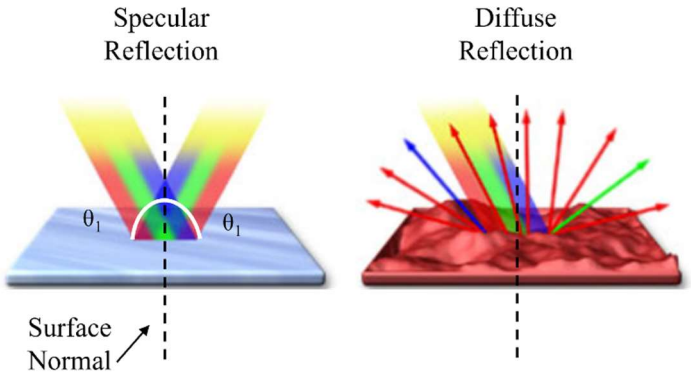

Figure 2. An illustration of the different types of light reflection. Left: Specular reflection on a smooth mirror, where all the components of white light (light on the visible spectrum) reflect almost equally and follow the same angle (θ_1) with respect to the surface normal (point of perpendicularity). Right: Diffuse reflection off a rough reddish surface, which does not reflect all wavelengths and scatters the light in all directions. From the Florida State University: https://micro.magnet.fsu.edu/primer/java/reflection/specular/

wavelength evenly or in a steady direction (diffuse reflection). One would therefore not see their own image reflected by a rock they observe but would still perceive it as grey from the mix of visible wavelengths still being reflected. This difference is illustrated in Figure 2.

This is certainly interesting and will be important to remember later when discussing some aspects about how light interacts physically with biological tissues. But what is far more important when considering neuronal light stimulation is the reciprocal property: absorption.

Light can also be absorbed by a material it contacts. Broadly speaking, light absorption is a type of energy conversion. In being absorbed by a medium, the EMR is converted into energy. Photosynthesis is one such conversion where light energy is converted into chemical energy that can be used by the plant. In earlier example of color perception with visual spectrum light, the wavelengths of EMR being absorbed by the material (rater than reflected) are equally important to the perceived color of the object.

Which wavelengths of light are absorbed by a material is directly related to their frequency. Thus, the absorption of EMR is dependent on the nature of the material (more specifically, the vibration frequency of its electrons) and its proportionality to the EMR frequency. In simple terms, a complementary interaction will result in the wavelength being absorbed, with non-complementary interactions resulting in either reflection or transmission through the substance (Figure 3). During the anatomical interaction between the photons and electrons that takes place during light absorption, the vibrations of the electrons interact with nearby atoms and covert their vibrational energy into thermal energy. That is to say: absorption always results in heat generation. This is why a black surface under the sun will feel much warmer than surfaces of other colors—these surfaces are absorbing most wavelengths of visible light, and thereby producing more heat.

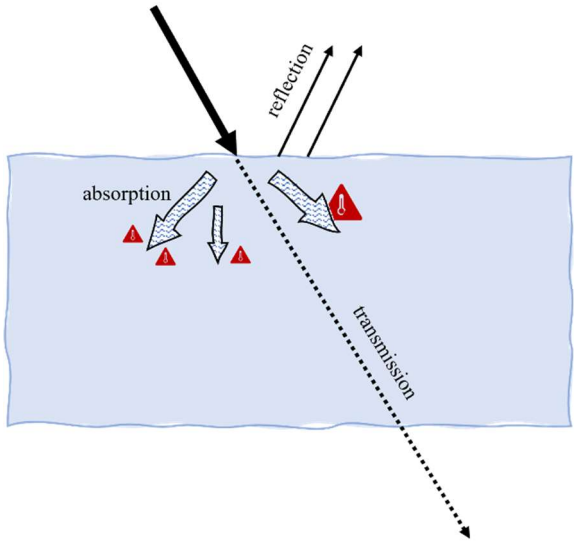

Figure 3. Absorption of EMR by a medium creates heat. Light can also be reflected or transmitted.

Though reflection and absorption are reciprocal properties of light, it would not be correct to say: "light that is not reflected is absorbed" or vise verse. Indeed, Figure 3 shows that light can also be transmitted through the medium. It can also be scattered. Scattering occurs as light moves though different mediums; the photons change direction as they interact with other particles.

1.1b Light scatters when photons collide with other particles

First, scattering is not just something that occurs with light. It is an incredibly complex property of physical matter. The term itself describes a broad range of behavior concerning many different types of radiation and particles. In short, it refers to the consequences of one particle striking another. These particles can be of any type—electrons, atoms, molecules, and of course, photons. In EMR, the scattering of photons is often referred to as diffusion and refers to the multi-directional re-emission of light after it strikes another set of dispersed particles. This diffusion is not random, and indeed physicists have defined several different scatter patterns, so to speak, depending on the properties of the origin particle. Here, the focus will be

placed on the Mie Theory, or Mie Scattering (Figure 4), which is often used for spherical particles like photons and thus is most commonly applied in optics to explain the behavior of photons of smaller wavelength (which includes the UV, visible, NIR, and low-level IR spectrums of concern in this review).

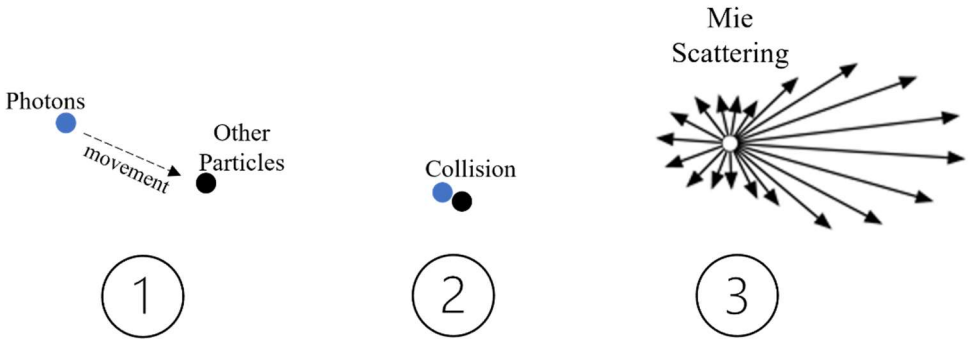

Figure 4. Mie scattering pattern. Photons in light move through space (1) and collide with other particles (2), which causes them to scatter (3)

In the figure above, the scatter lines are shown as a 2D x/y axis of movement. This is done for simplicity, but since we live in a 3D, note that the movement of the photons composing the EMR occurs *in all directions* following the collision with other matter. Depending on the angle and speed of impact, the scattering of the composite photons will be more pronounced in some directions than in others (hence the varying arrow size in Figure 4), but for all intents and purposes in this simplified context, consider the movement to be random.

Mie Scattering is defined by an incredibly complex mathematical theorem published by Gustav Mie in 1908 (later translated from the original German) and applies specifically when the scattering dimension (the distance particles are scattered from their origin point) is greater than the wavelength of the particles being scattered (Mie, 1908). For the optical stimulation of the neuron that concerns light in the UV, visual, and IR ranges of the electromagnetic spectrum (λ = 100nm - 1mm), the scattering dimension will very often be larger than the wavelength, particularly so in the case of UV and visible light. Thus, Mie Scattering is the most relevant to

the present investigation, and indeed is used as the mathematical model for Monte-Carlo simulations that model the diffusion of light through stimulated cortical tissue (Jiang et al., 2022).

Of course, this is only one of several ways in which light can be scattered. There are additional offshoot scattering behaviors that deal with how light properties change when EMR interacts with different surfaces and mediums. Here, I will discuss only one: refraction.

1.1c Light refracts when it changes mediums

Where the basic principle of scattering describes what happens to light as it moves through one medium, refraction describes a particular type of consequent scattering behavior when light transfers from one medium to another. When you observe something that has been dipped in water, the angle of the object will appear distorted. This is because the light reflected from the object is being refracted by the change from air to water, causing your perception of the object to skew.

This happens because when light crosses the boundary between two different mediums, the wavelength of the light changes due to the physical interaction between the photons and the media (i.e., the change in the velocity with which the photons can move—recall: λ = velocity/frequency), but the frequency of the light moving into the new medium remains constant. While it may seem a bit counterintuitive, frequency is a preserved energy constant and a characteristic of the photons themselves with respect to the source of the light, but wavelength depends on the velocity of their movement through a specific medium. Therefore, when light must move through a different medium with different properties resisting the photons' movement, its velocity, and therefore its wavelength, will be altered. Noether's Theorem, a theoretical physics proof taking the variations in space into account when discussing

energy conservation, is often used in the complex mathematical models of refraction, and any particularly interested parties are encouraged to read his work (Noether, 1918).

Light always follows the path between two points that takes the shortest time (Fermat's principle), so if a beam of light is not perpendicular to the boundary between the mediums the change in wavelength changes its direction as it naturally seeks out the new 'shortest path', resulting in distortion. Since the light that humans perceive is composed of many beams, most of them will, of course, not be perpendicular to the medium and this distortion will be perceived as refraction.

The mathematical model of refracting light is another important component to the Monte-Carlo simulations used to model light propagation through biological tissue. This is because refraction describes the behavior of light moving through transparent or semi-transparent mediums. When it does this, it behaves according to Snell's law:

$$n_1 \sin\theta_1 = n_2 \sin\theta_2$$

Where $\boldsymbol{n}$ represents the indices of refraction for the different mediums, and $\boldsymbol{\theta}$ is the angle between the beam of light and the surface normal (point of perpendicularity) in the medium (Figure 5A).

This is an incredibly useful light property, with one of the most common applications of refraction being corrective eyeglasses, which refract incoming light in order to better focus it on the retina, thus improving vision (Figure 5B). You will find more information concerning just how the light is interacting with the retinal tissues later. For now, it is just important to understand the governing principle behind refraction itself.

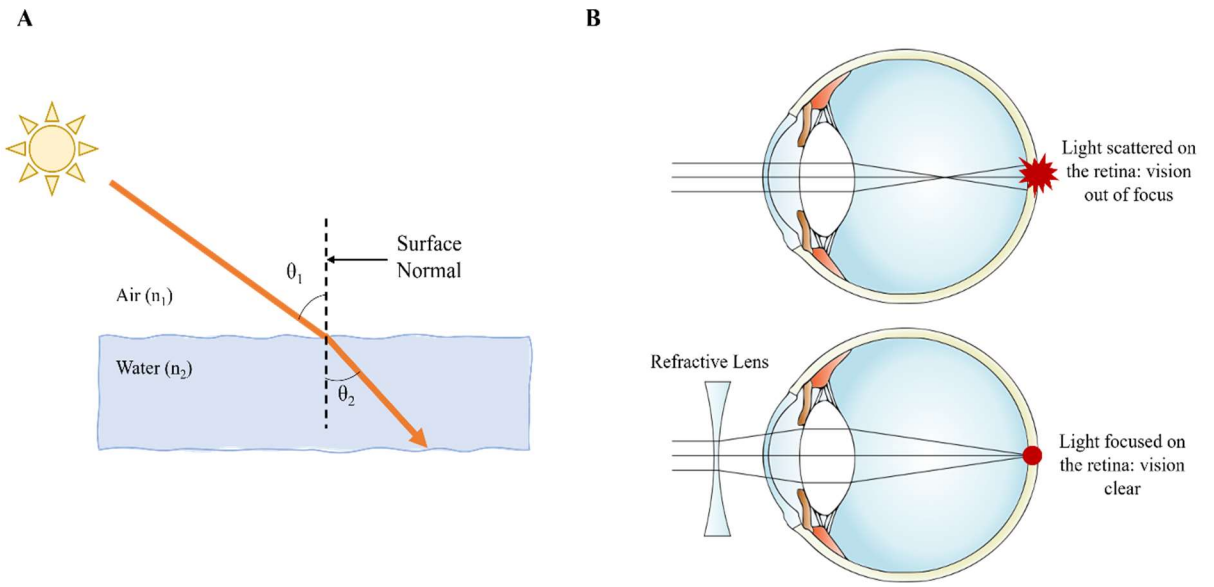

Figure 5. A visualization of refraction and one of its common applications. A) Light moves between the air and the water, distorting according to Snell's law, resulting in refraction. B) Top: light passing through the lens of a human eye exhibiting nearsightedness; Bottom: Light is filtered through a corrective lens, which refracts the light and allows the human eye to better focus the light on the retina, making vision clearer.

Considering that EMR is being constantly altered and redirected by its interactions with matter, one would expect that light penetration into CNS tissues would be very low. However, several studies have both mathematically modeled and physically demonstrated that light is, in fact, capable of penetrating CNS tissues and reach adequate depths for brain and neuronal photostimulation.

1.1d Light stimulation reaches sufficient penetration depths in the brain

In order for light to act on neuron in the brain it need to penetrate both the scalp and the brain tissue. When light is able to reach the cortical tissue, either through direct tissue stimulation or through transcranial stimulation, the depth it can penetrate must account for both light scattering and absorption. Thus, the effective penetration depth of light into brain tissue can be mathematically modeled with the following equation (as derived by Jiang et al., 2022, using Mie scattering theory and calculations for the refractive index and absorption of light):

$$\delta_{eff} = \frac{1}{\sqrt{3\mu_{\alpha}(\mu_s + \mu_{\acute{s}})}}$$

Where $\boldsymbol{\delta_{eff}}$ is the effective penetration depth of light into the tissue, $\boldsymbol{\mu_{\alpha}}$ is the mean absorption (calculated according to Jiang et al., 2022, eq. 5 and 6), $\boldsymbol{\mu_s}$ is the average distance between two scattering events (eq. 2 and 3), and $\boldsymbol{\mu_{s'}}$ describes a model of completely random photon scattering (eq. 4). When the authors modeled light behavior in tissue according to this Mie derived model, also accounting for the light intensity decay (eq. 9) found that IR light of λ = 1070nm achieved the maximum tissue penetration depth (Jiang et al., 2022).

Models like these have long been used in Monte-Carlo simulations and have a history of allowing teams to simulate tissue penetration from optical EMR stimulation. Stujenske, Spellman, and Gordon (2015), for example, modeled green light (λ = 532nm) tissue penetration as a function of preserved intensity, finding that at least 50% of initial light intensity could be preserved up to 1mm from a 62µm optical fiber tip, and that by 2mm less than 0.01% of the initial intensity remained (Figure 6A).

These measurements are not only performed on a simulation basis, however. Direct measurement of light penetration into real tissue was performed by the Deisseroth lab (the creators of optogenetics) in 2007. They first modeled light propagation from their optical LED fibers developed for *in vivo* optogenetic research. Aravanis et al. (2007) suspended a microLED optical fiber (blue light, λ = 473) in rat and mouse cortical tissue and then validated the model in real tissue *ex vivo*, finding that the light was able to penetrate through 1mm of cortical tissue in both species. The propagation of light through the tissue fit neatly into mathematical models for the diffuse scattering of light in media, and the light power transmitted into the tissue reduced by 50% after 100µm, and 90% by the 1mm mark (Figure 6B). Despite the limited diffusion, the authors found that the blue light stimulation was still sufficient to produce reduced

motor movements (whisker movement) in their optogenetically modified (see chapter 3) animals.

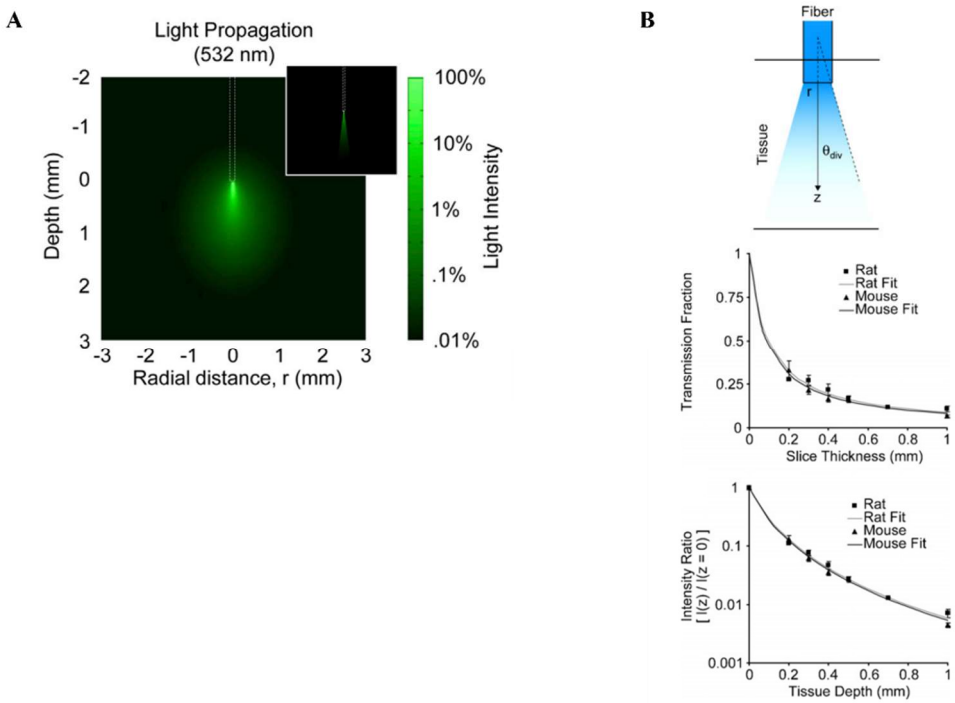

Figure 6. Adapted from (A) Stujenske, Spellman, & Gordon, 2015 and (B) Aravanis et al., 2007. Light propagation through cortical tissue has been both simulated (A) and modeled on tissues (B). A) Light intensity prentration depth predicted for green (λ = 532nm) light from a 62µm optical fiber tip. Calculated using a Monte Carlo simulation with tissue parameters established for cortical tissue. B) Top: experimental setup used on rodent cortical tissue showing the mathematical relationship between the optical fiber radius (r), the tissue (z = tissue depth), and the angle of blue light (λ = 473nm) delivery (θdiv) used to calculate the fit to models of diffuse light scattering in media. Middle: transmission of the light through different thicknesses of cortical tissue. Bottom: Light intensity as a function of tissue depth.

The same lab used a similar methodology to test other wavelengths of visible light for adequate penetration depth and light power dispersion, though this time with a purely simulation-based model. Their simulation showed similar penetration depths and light power dispersion with green, yellow, and red light in addition to demonstrating that increasing the wavelength decreased scattering and increased the penetration depth into the tissue (Yizhar et al., 2011, Figure 7). Note that for blue light (λ =473nm), these data showed slight differences

in total penetration depth from the earlier data from live animals, with the simulated depth (Yizhar et al., 2011) being shorter than the real depth shown by Aravanis et al (2007).

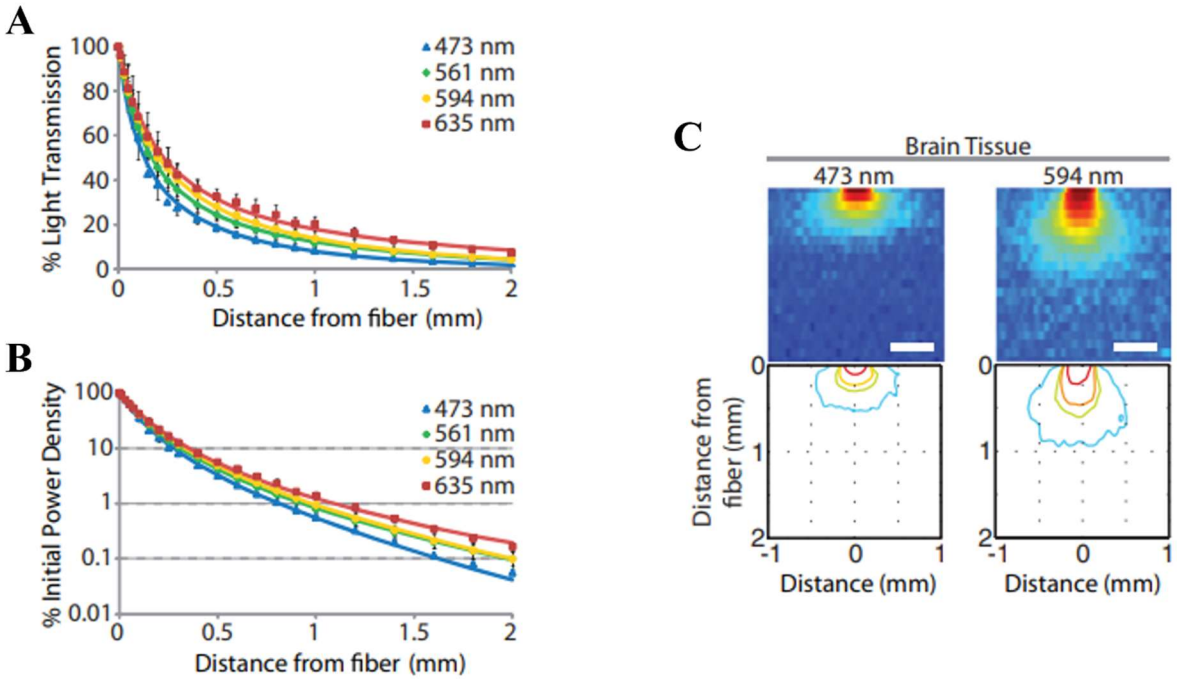

Figure 7. Light propagation through the tissue as a function of simulated light parameters. Adapted from Yizhar et al., 2011. A) Measured percent transmission of light power at 473 nm, 561 nm, 594 nm, and 635 nm light from a fiberoptic (200 mm, NA = 0.37) shown as a function of distance from the fiber tip in brain tissue. Solid lines represent fits to the measured data (Aravanis et al., 2007). B) Predicted fraction of initial light power density as a function of depth in brain tissue for the same fiber; includes effects of absorption, scattering, and geometric light spread. C) Lateral light spread as a function of sample thickness, simulated rat gray matter (bottom) was illuminated by either blue (473 nm; left) or yellow (594 nm; right) light delivered through a 200 mm optical fiber (NA = 0.37). Contour maps of the image data show iso-intensity lines at 50% (red), 10% (orange), 5% (green), and 1% (blue) of maximum.

In a study on irradiance toxicity and thermal propagation under light stimulation, Senova and colleagues (2017) later demonstrate the difference in penetration depth between blue (λ = 476nm) and red (λ = 638nm) light delivered via optical fiber to anesthetized rat cortical tissue. Their results noted that the majority of blue light did not penetrate more than 500μm into the tissue, while the majority of the red light was able to penetrate much deeper (1.5mm) due to decreased scattering and absorption (Senova et al., 2017). This paper serves as an interesting demonstration of the relationship between wavelength and penetration depth (recall: greater wavelength = greater penetration depth) in cortical tissue. However, even lower wavelengths of visible light have been shown to adequately penetrate even very deep structures despite the

greater diffusion and absorption. Indeed, Zhang et al. (2020) successfully used violet light (peaked at λ = 380nm) to transcranially stimulate OPN5 (a naturally occurring non-image forming extraocular photoreceptor) in the preoptic area of the mouse hypothalamus, a structure located near the bottom of the brain and several millimeters away from the optical stimulation point.

This brings up an interesting point about the ability of light to reach neuronal tissue transcranialy. Several studies have demonstrated the permeability of both the mouse and human skull to light. Wu et al. (2012) used varying laser-light wavelengths (λ = 665nm & 810nm) to transcranialy stimulate the cortex in a pre-clinical mouse TBI treatment model of low-level laser light therapy (LLLT), noting that the light penetrated the skull enough to result in significantly greater post-TBI improvement for mice exposed to the light. The next year, Litsher, D. & Lishter G. (2013) tested the transmission factors of light of varying wavelengths through the human skull, noting that transmission increased with wavelength (Figure 8A).

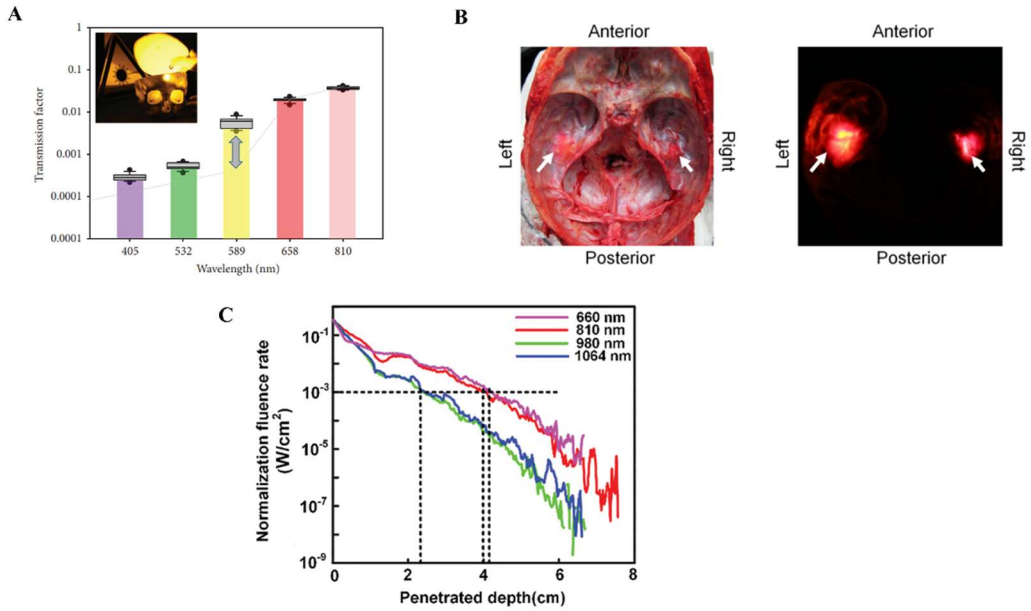

Figure 8. The human skull is permeable to light, and the light can propagate through the tissue even with transcranial stimulation. Adapted from (A) Litsher, D. & Litcher, G. (2013), (B) Sun et al. (2016), and (C) Wang & Li (2019). A) Boxplot showing the transcranial transmission factor of violet (405nm), green (532nm), yellow (589nm), red (658nm), and IR (810nm) light. B) Left: A human skull cadaver dissected and prepared with white-light LEDs in the ear canals (arrows). Right: Observation of the light being clearly transmitted through the skull. C) a simulated model of the cortical penetration depth of transcranial light (humans) of varying wavelengths. The fluence rate measures the number of particles crossing into a space per unit time (here: watts per cm^2)

Sun et al. (2016) also used human cadavers to show that white light (which contains wavelengths on the entire visual spectrum) can penetrate the skull and reach the brain through the ear canals (Figure 8B). Finally, Wang and Li (2019) used a simulated tissue model to predict the propagation of transcranial near infrared (NIR) and IR light through human cortical tissue, finding that the light can penetrate up to 8cm, with longer wavelengths once again penetrating deeper and 810nm appearing to be the optimal wavelength for LLLT (Figure 8C).

Clearly, the light can adequately reach the brain for effective photostimulation both from stimulation directly on the cortex and with transcranial stimulation. The next question, of course, becomes: can the light interact with those tissues, and if so, how? To answer this question, I will need to start with the eye. Of course, this is not an investigation into ocular biology but rather an investigation that is concerned with how light has been shown to interact with extraocular tissues in the CNS. The mechanics of that interaction and the effects produced are paramount, and several theories have been proposed to explain different components. Fortunately, I will talk all about them in chapter 2. I will, however, need work up to the currently proposed mechanisms of action for extraocular photo sensitivity by starting with the first known photosensitive human tissue: the retina at the back of the eye. More specifically, how the biological properties of the retinal cells allow it to interact with light.

1.2 Light can interact with biological tissues

If you have ever been subjected to a high school biology lecture, you might remember that the eye is able to process light and transmit it to the brain as an image, otherwise known as our sense of vision. I will spare you another lecture on eye anatomy in the interest of time and skip right to the retina, which contains the photoreceptors (rods and cones) necessary to interact with ERM and transmit it as information the brain can understand. When light enters the eye, it initially passes through ganglion and bipolar cells to reach the rods and cones (Figure 9A).

These photoreceptors are specialized, non-action-potential-generating neurons that are then able to interact with the light and start the chain of neuronal communication via the release of glutamate. A key component of the mechanism that allows them to do this lies in a specific type of protein present in their cell membrane called opsin. Opsin is a unique g-coupled protein complex bound to retinal (also called retinaldehyde). Retinal is a polyene chromophore—the chemical basis for photoreception—that gives the opsin its ability to respond to light. In the dark cyclic GMP (cGMP) channels permeable to Na^{+} and Ca^{2+} ions are opened by the high intracellular concentration of cGMP (Figure 9A, right), resulting in a resting membrane

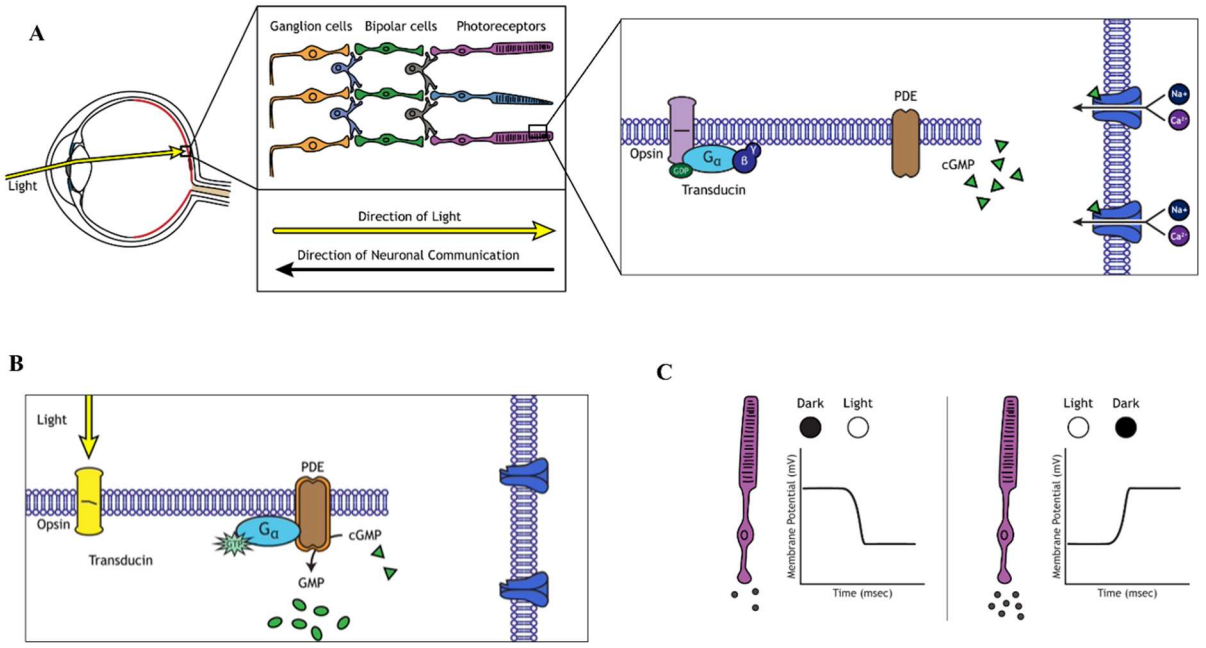

Figure 9. Light interacts with opsin, resulting in the dissociation of cGMP into GMP, closing cGMP gated ion channels. Adapted from Hanley, 2021, Creative Commons Attribution Non-Commercial Share-Alike (CC BY-NC-SA) 4.0 International License. A) Light moves through ganglion and bipolar cells before reaching the photoreceptor. The photoreceptor contains light-reactive opsin and cGMP gates ion channels. B) Light reacts with opsin to activate g-protein tranducing, which activates an enzyme that dissociates cGMP into GMP, closing the ion channels and hyperpolarizing the cell. C) The neuron is depolarized in the dark and hyperpolarizes when exposed to light.

potential of around -40mV, quite a bit more depolarized than other neuron types (see chapter 2 for more information). When a photoreceptor is exposed to light, the interaction of EMR with opsin triggering a g-protien transduction signal that lead to the activation of the membrane enzyme phosphodiesterase (PDE) what reduce the intracellular concertation of cGMP. Without

cGMP the ion channels close, stopping the influx of positive ions across the membrane and hyperpolarizing the photoreceptor (Figure 9B, C). When the light is removed, the cGMP can once again bind to the ion channels, again depolarizing the cell (from Henley, 2021).

Everything that happens thereafter is related more to the biological processes involved in vision more than photoreception. What we are interested here is that protein that made the initial biological interaction with EMR possible: opsin. If opsin bound cells are photosensitive, then the next question becomes whether or not they exist in other areas of the body and, if so, whether they are also photosensitive when expressed in extraocular regions. Interestingly, naturally occurring extra-ocular photo receptors have been identified in both vertebrates and invertebrates, with some evidence emerging in recent years for their photosensitivity. Gong et al. (2016) identified photoreception in the LITE-1 taste receptors of *C. elegans* (the roundworm), additionally noting that it is UV sensitive and helps the animal display UVA/UVB light avoidance. This same type of photoreceptor-mediated UV light avoidance is present in *Drosophila* (fruit fly) as well (Hardie & Franz, 2012).

Opsin has also been identified in vertebrates and even in mammals. These include rhodopsin, encephalopsin (OPN3, Blackshaw & Snyder, 1999), melanopsin (OPN4, Provencio et al., 1998), and neuropsin (OPN5, Tarttelin et al., 2003). Immunohistochemistry analysis of mouse cortical tissue had shown that OPN3 has a particularly notable presentation in the mouse brain, specifically within the cerebral cortex, paraventricular area of the hypothalamus, in cerebral Purkinjie cells, in the striatum, and in the thalamus (Blackshaw & Snyder, 1999; Nissila et al., 2012). OPN5 has been identified in the retina, brain, spinal cord, and testes of both humans and mice using a bioinformatics approach to genetic sequencing (Tarttelin et al., 2003).

Concerning the photosensitivity of extra-ocular vertebrate opsin: Fischer et al. (2013) used culture staining techniques to identify TMT-opsin in the brain neurons of *Danio rerio*

(zebrafish) and VAL-opsin in both *Danio rerio* and *Oryzias latipes* (medaka fish). The authors note that though neither opsin displayed natural photosensitivity in culture, these two species are known to have particularly light sensitive circadian rhythms and often display light-avoidance locomotion (Fischer et al., 2013). They do not, however, show that light avoidance locomotion is due to these extraocular receptors. Some knowledge in this vein did come from Friedman et al. (2015) two years later, who showed that the curling behavior of opsin-expressing translucent zebrafish embryos could be suppressed by green light stimulation (λ=508nm, intensity = 13.2μW/mm^2). The authors linked this locomotive effect to the Gαi class of G-protein-coupled receptors present in this species. They note that light-slowing of biological processes may be influencing the light avoidance locomotion observed in *Danio rerio* as part of a survival tactic preserving the ability to flee or hide from predators (Friedman et al., 2015). Very recently, Zhang et al. (2020) suggested that transcranial stimulation with violet light (λ = 380nm) can activate the OPN5 localized in the hypothalamic preoptic area of mice in this way affecting their body's thermal regulation system. Outside of these three studies, which already provide shaky evidence themselves, there is little in the literature directly linking natural extra-ocular opsin photosensitivity to light-mediated effects on the brain and behavior in vertebrates.

If there is not much evidence that the light reaching neuronal and cortical tissues is acting on natural extra-ocular brain opsins, then how might it be interacting with those tissues? Recall that one of the fundamental properties of light and its interaction with media is absorption, and that the absorption of EMR into a substance always generates heat. Heat, then, has been proposed as a key component in how light interacts with tissues in the CNS.

1.3a Light heats tissue it encounters, and heat interacts with biological mechanisms

One of the earliest quantifications of head radiation and propagation through tissue comes from Pennes (1948), who derived an equation for in-tissue heat distribution from known laws of thermodynamics and the theory of conductance-based heat flow. He confirmed the model using blood temperature measurements following thermal stimulation of the human arm (Pennes, 1948). Nearly five decades later, Wang, Jacques, and Zheng (1995) mathematically derived and coded their Monte Carlo simulation of light and heat transport through multi-layered tissues (Figure 10A). Stujenske, Spellmen, and Gordon (2015) would note that this simulation serves as an accurate model for heat and light propagation through cortical tissues *in vivo* and used it as a component in their own simulation model of light-induced tissue heat propagation. The team was able to accurately model the propagation of thermal energy through cortical tissue, validating their model against green light stimulation (λ = 532nm) of anesthetized mice *in vivo* and noting that the light also changed firing activity (Figure 10B, C). Their model also demonstrated that heat propagation through the tissue is inversely related to wavelength, with higher wavelengths of light generating smaller temperature changes (Stujenske, Spellman, & Gordon, 2015, Figure 10D, E), but since they only tested green light *in vivo*, they were not able to validate this part of the model in real tissue. Their model displays the inverse of the relationship wavelength has with tissue penetration depth, as noted in section 1.1d, where penetration depth increases with wavelength. This simulated conclusion, however, would be debunked by two subsequent studies that used real tissue to show that heat propagation was not linked to wavelength, thereby rounding out how light is interacting with cortical tissue temperature increases.

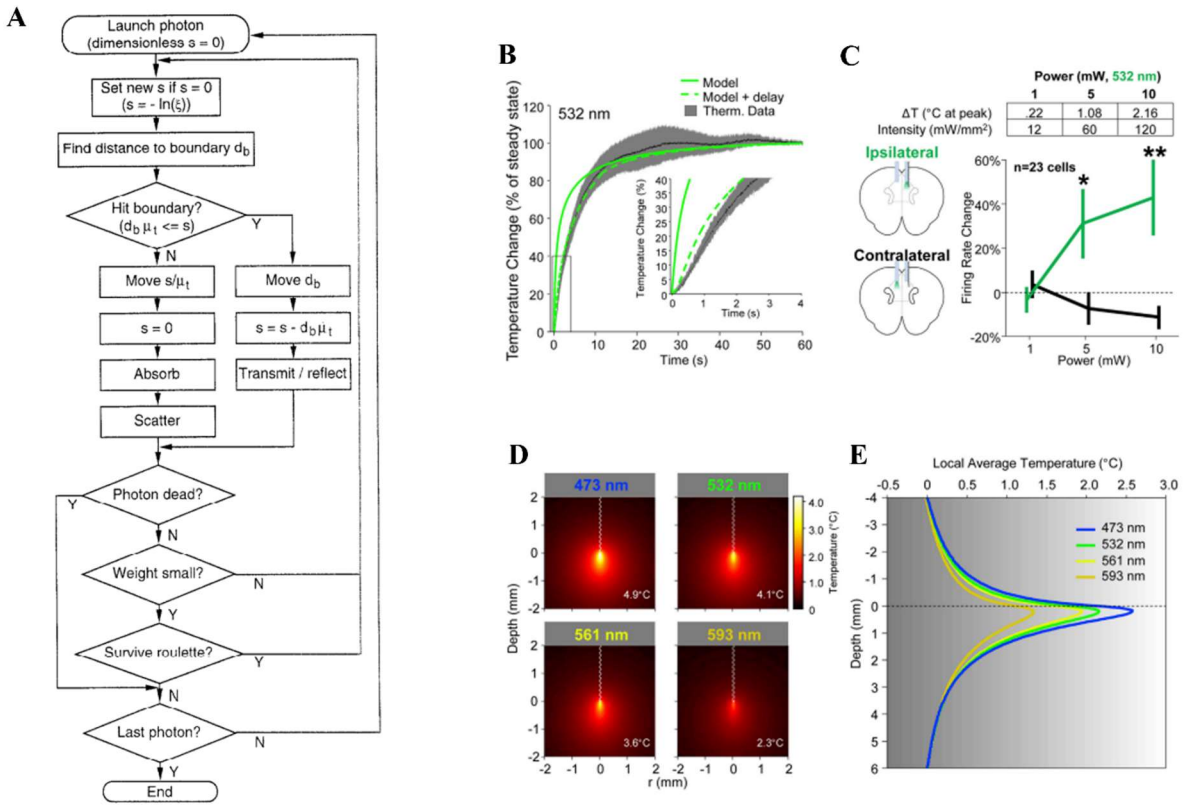

Figure 10. Light induced temperature change propagates through cortical tissue. (A) from Wang, Jacques, & Zheng, 1995. (B-E) Adapted from Stujenske, Spellman, & Gordon, 2015. A) Flowchart for tracing the logic of the Monte-Carlo simulation based on photon origin position. (B) Temperature change as a function of time from light onset for 20 mW light power at 400 mm away from an optical fiber. Super-imposed are the predictions for the model with (green, dashed) and without (green) a compensatory delay measured for the thermistor instrument used. C) Left: Schema for single-unit recordings in the mouse PFC. During ipsilateral stimulation, light (532 nm) was delivered on the same side that the single units electrode while during contralateral stimulation, light was delivered on the opposite side. Right: Predicted peak temperature changes (after 30s of illumination) plotted in the box above for the three light powers tested in the study (1, 5, and 10 mW). Firing rate of single units in the PFC during 30s periods of light illumination are plotted as averaged across five repetitions. *p < 0.05, **p < 0.01, Wilcoxon signed-rank test between ipsilateral and contralateral conditions. D) Predicted temperature change as a function of distance from the optical fiber (62 mm, 0.22 NA) for 473, 532, 561, and 593 nm light. All plots have the same color scale. Text indicates peak temperature. E) Predicted temperature change as a function of depth as in (D) for the same wavelengths as in (D). Here, 0 represents the tissue surface where the light is placed, positive values represent the temperature in the tissue, and the negative values represent simulated changes to local solution temperature near the diode but above the tissue.

Podgorsky and Ranganathan (2016) would similarly look at the tissue heating produced by light in anesthetized awake mice *in vivo* using two-photon laser microscopy, noting the opposite wavelength-temperature relationship for NIR and IR light (tested λ = 650-652nm, 800nm, 920nm, and 1040nm). Remember, however, that this concerns two-photon microscopy illumination with temperatures measured following 20s of illumination and 180s, the point where a steady state temperature was attained. This illustrates light-induced heating though the

tissue but is ultimately not the same type of stimulation used in neuronal light stimulation and brain photobiomodulation (typically 1-photon laser light delivered though microLED diodes). What is, however, important to pull from this in addition to the knowledge of tissue heating is that prolonged heat toxicity can irreparably damage the tissue. According to the team, this can be mitigated with reductions in the light power intensity to below 250mW, with intensities below this level not producing irreversible tissue damage. Further, they were also able to propose (from their steady state temperature measurements) a useful estimator for tissue temperature: continuous illumination appeared to heat the tissue at an approximate rate of 1.8°C/100mW per 1mm^2 cubic area (Podgorsky & Ranganathan, 2016).

Senova et al. (2017) conducted a study of heat propagation and thermal toxicity more suited to the optical fibers used in neuromodulation studies. The team exposed anesthetized rat brains to increasing levels of red-light irradiance and increasing stimulation frequencies (λ=638; irradiance = 200, 400, and 600mW/mm^2; frequency = 20, 40, and 60Hz). Their goal was to evaluate the related temperature change and tissue damage under light sufficient to reach the optical irradiance level necessary for optical neuromodulation (1-5mW). They found that (a) the spatial distribution of temperature effect was larger than the spatial distribution of the light itself, (b) the overall temperature change remained under 1°C even at the highest power levels they used, (c) that temperature change increased with frequency for given irradiance levels, and (d) that these levels of irradiance and frequency, which are sufficient for neuromodulation, do not appear to be resulting in permanent damage. They also demonstrated that red light (λ=638) produces a larger temperature change than blue light (λ=476), at least for the lower low stimulation energy (200 and 400W/mm²), but a smaller change at higher power (600W/mm²). This is another contrast to Stujenske et al.'s (2015) simulated model (Figure 10E) that can be explained by a final important point in Senova et al. (2017): **temperature increases**

linearly with optical stimulation parameters (Figure 11), **which are not wavelength dependent**.

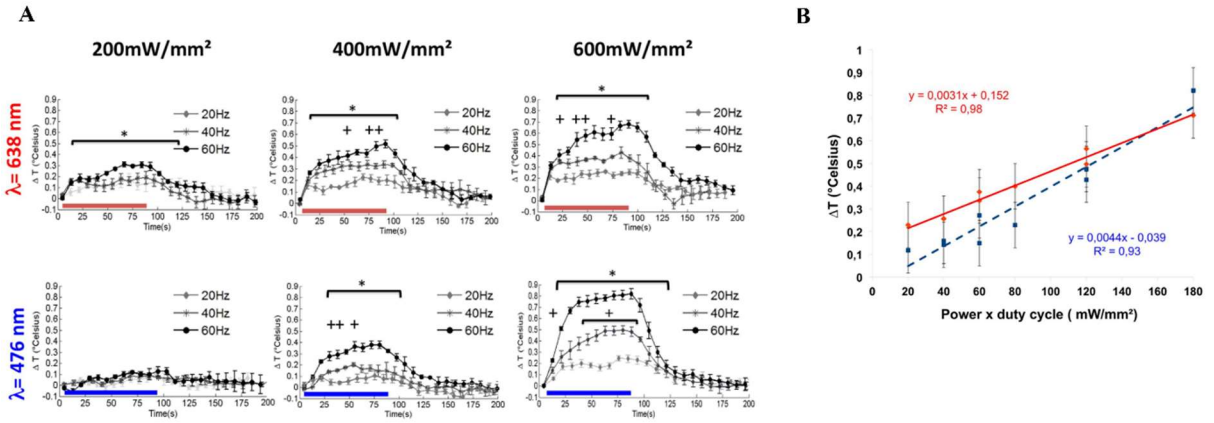

Figure 11. Light-induced tissue temperature increases linearly with the light stimulation parameters. Adapted from Senova et al., 2017. A) Temperature change over time for different irradiance power levels and light stimulation frequencies separated between blue and red light. Horizontal bars indicate when the light is turned on. The authors binned the data in 8s temporal windows for clarity. Stars and crosses indicate statistical significance for Wilcoxon signed-rank tests (comparisons between data obtained at 60 and 20Hz and data obtained at 40 and 20Hz, respectively ($p<0.05$)) B) Regardless of wavelength, light-induced temperature change follows a linear pattern with respect to the stimulation parameters. ΔT = Maximal temperature = averaged max temperature from (A). Solid line for red light, dashed for blue.

These are all important conclusions that, in combination with the other literature in this section, demonstrate that heat can propagate through the tissue in a manner sufficient for optical stimulation and that the thermal change is not irreversibly toxic. Understanding this, however, this is only a small part of the picture. There are several proposed interactions that heat is having with the neuronal and cortical tissues that lead to the effects of activity touched on in the introductory section. The most prominent appears to be effects on the ion transfer activity across neuronal membranes that control their activity.

The most direct way temperature can affect membrane permeability is through transient receptor potential (TRP) cation channels. TRP channels are widely expressed in numerous bodily tissues, including in peripheral and central neurons. Their role in the CNS has been summarized to include involvement in synaptic transmission, neurogenesis, brain development, and as components affected by some neurological diseases (Vennekens, Meningoz, & Nilius, 2012). The TRP protein complex family that encodes TRP channels is also quite large, with 28

individual encoding genes identified in mammals (Nilus & Szallasi, 2014), and this type of protein complex is found in both voltage and lipid-gated ion channels (Yang et al., 2010).

While all TRP channels are thermos-sensitive, a subfamily of TRP channels are sensitive to elevations in temperature. These are TRPV1, 3, and 4, TRPM2 and 3, and TRPA1. The TRPM8 channel is sensitive to both cold and warm temperatures, with activation occurring for cold temperatures and inhibition occurring for warm. Some of these channels have been confirmed in the rodent brain, with TRPM2 channels found in the rodent pre-optic area and TRPM8 displaying in the hypothalamus (Kashi & Tominaga, 2022).

Rhee et al. (2008) demonstrated a light induced TRP effect for IR stimulation on rat sensory neurons in culture (from ganglion cells dissociated from the vagus nerve). These neurons contain heat sensitive TRPV1 channels, which are known to open in response to temperature elevation above 37°C. They have a higher permeability to Ca^{2+} ions overall, so the authors used a florescent indicator for calcium to demonstrate that even very brief 2ms pulses of IR light (λ=1850nm) rapidly and reversibly activated the TRPV1 channels. The team confirmed the involvement of these channels by eliminating the light-induced calcium influx by introducing a TRPV1 blocker (capsazepine) to the culture (Rhee et al., 2008).

TRP channels are not the only channels that can be affected by temperature modification, indeed the gating properties and permeability of almost all membrane channels are potentially affected by temperature changes. A classic example is the heat-related component and heat dependence within the waveform of the Hodgkin and Huxley model for action potential generation (Hodgkin & Katz, 1949; Hodgkin & Huxley, 1952a; Portela et al., 1978; see chapter 2 for more information). The next chapter will therefore discuss how light can affect neuronal activity thought the modification of the synaptic and biophysical properties of neuronal cells.

CHAPTER 2

NEURONAL BIOPHYSICS AND THE EFFECT OF LIGHT ON NEURONS AND THE BRAIN

2.1 The Biophysical Properties of Neuronal Activity

A typical CNS neuron is composed of three basic component parts, the cell body (the soma), dendrites branching from the soma, and a myelinated axon extending from the soma to connect with other cellular dendrites via the synapse, thus facilitating intercellular signaling. The soma contains the nucleus of the cells and the component organelles (such as the mitochondria) necessary for the creation, transmission, and processing of both incoming and outgoing neuronal signals, which may be electrical and/or chemical in nature, and action potentials (Byrne, Heidelberger, & Waxham, 2014, Figure 12).

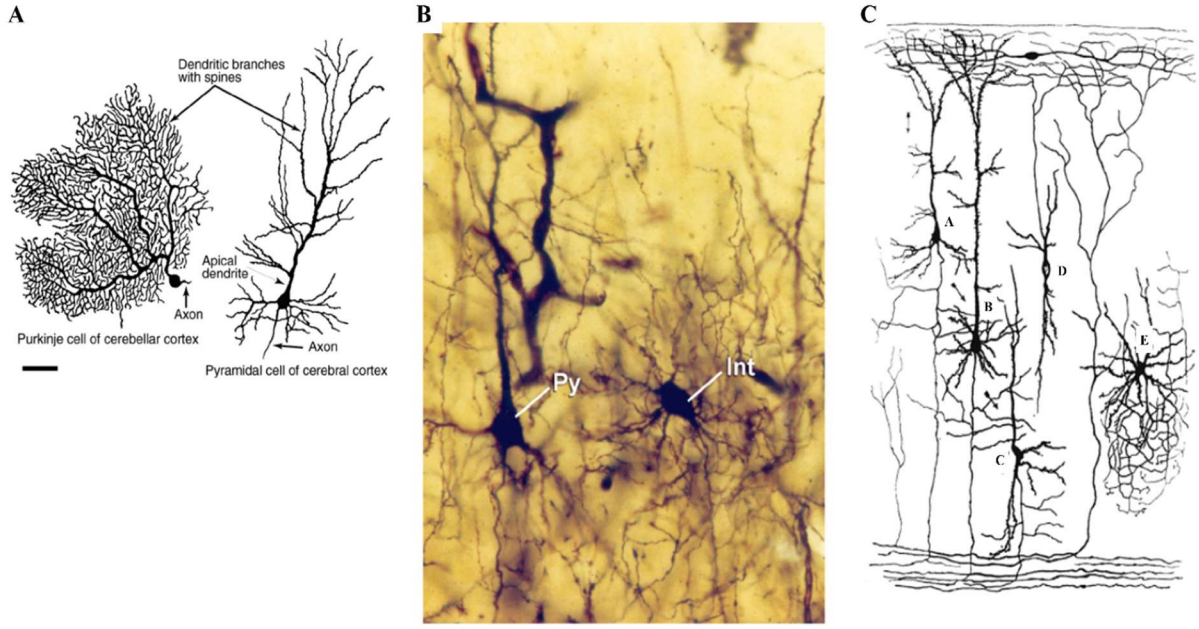

Figure 12. Examples of neuron anatomy and morphology, adapted from Byrne, Heidelberger, & Waxham (2014). A) The typical composition of projection neurons with wide spreading dendritic connections to other neurons. Left: a Purkinje neuron in the cerebellum. Right: a pyramidal neuron in the cerebral cortex. B) Cat cortical neurons stained with the Golgi method, py = pyramidal neuron, int = interneuron; C) examples of different neurons found in the cerebral cortex; a = medium sized pyramidal neuron, b = giant pyramidal neuron (typically found in layers 4 and 5), c = a polymorphic neuron, d = a neuron with an ascending axon, e = a golgi cell.

The biophysical properties that are responsible for the activity of neurons in the central nervous system are so numerous as to warrant extensive, textbook length analyses in order to explain their nuances. For the purposes of this investigation, I will focus only a brief review on

the mechanisms responsible of the maintaining of neuronal resting membrane potential (V_{rest}) and on those responsible for the generation of the action potential.

A neuron has a negative V_{rest} which results from differing ion concentrations on either side of the cell membrane. First, note that ions in the intracellular and extracellular spaces are separated by a lipid bilayer that is impermeable to both water and ions in its base state. Channel proteins within this cellular membrane allow for the inflow and outflow of select ion types, resulting in changes to the intra-and extracellular ion concentrations and thereby changes to the difference in charge on either side of the membrane, which can dynamically change the membrane potential (V_m). Among the many different types of membrane channels are passive ion channels, sometimes called leak channels, that allow ions to freely move across the membrane in order to maintain the proper V_{rest}. Although many ions participate in the maintaining of the V_{rest}, K^+ cations are undoubtedly predominant. To illustrate the mechanism that determines a cell's V_{rest}, consider, a simplified example where only passive K^+ channel participate in this process.

When the V_m moves away from the V_{rest}, potassium ions begin to move freely through the leak channels in a direction that brings the V_m back toward the V_{rest}. K^+ flux is arrested only when this value is attained. In this simplified example, the V_{rest} is equal to the potassium equilibrium potential (E_K) and can be determined by the Nernst equation:

$$E_{rest} = E_K = \frac{RT}{z_i F} ln \frac{[K]_{out}}{[K]_{in}}$$

Where E_k is the "Nernst potential" of the ion K^+, R and T are the universal gas constant and temperature in Kelvins, respectively, z_i is the number of electrons transferred, and F is the Faraday Constant (representing the amount of electric charge carried by one mole of atoms). $[K]_{out}$ and $[K]_{in}$ are the extracellular and intracellular concentrations of the ion, respectively. When a cell membrane is at E_{rest}, it is in a state of equilibrium where there is neither an influx nor an outflux of K^+ ions.

However, leak channels other than those for K^+ are present in a neuron. Thus, this equation was expanded on in the 1940s to also account for the free movement of other ions, such as Na^+ and Cl^-, resulting in a completed equation for predicting the overall cellular equilibrium potential (the GHK equation; Goldman, 1943; Huxley & Katz, 1949):

A: Nernst-like equation for single ion permeability:

$$E_{m,I} = \frac{RT}{F} ln\left(\frac{P_{ion}[I]_{out}}{P_{ion}[I]_{in}}\right) = \frac{RT}{F} ln\left(\frac{[I]_{out}}{[I]_{in}}\right)$$

B: Expanded GHK equation accounting for the permeability of Na^+, K^+, and Cl^- channels:

$$E_{Rest} = \frac{RT}{F} ln\left(\frac{P_{Na}[Na+]_{out} + P_K[K+]_{out} + P_{Cl}[Cl-]_{in}}{P_{Na}[Na+]_{in} + P_K[K+]_{in} + P_{Cl}[Cl-]_{out}}\right)$$

Where $\boldsymbol{P_{Na}}$, $\boldsymbol{P_K}$, and $\boldsymbol{P_{Cl}}$ are the membrane permeabilities of the leak channels for those ions.

Leak channels are not the only ones on the neuronal membrane. There are also various types of gated channels (ligand gated, voltage gated, lipid gated, temperature gated, etc.). The opening of these channels tends to move the $\boldsymbol{V_m}$ toward the reversal potential of the ions that permeate through them. In this way, the movement of ions either depolarizes or hyperpolarizes the neurons. Membrane depolarization can, in some cases, lead to the generation of action potentials. Moving forward, the ionic mechanism behind the action potential itself will be oversimplified for brevity, and particularly interested parties are encouraged toward further reading on the established complexity of the AP generation mechanism via both Byrne, Heidelberger, & Waxham (2014) and Huguenard & McCormick (1994).

AP generation requires a depolarization of the membrane, until $\boldsymbol{V_m}$ reaches the AP activation threshold, which varies by neuron type and condition. When the activation threshold is attained, a much faster and more important depolarization takes place, which in many cases causes the $\boldsymbol{V_m}$ to reach positive values. This huge depolarization is short lasting and the $\boldsymbol{V_m}$ rapidly returns to negative values. In some neuronal types, this can be followed by the $\boldsymbol{V_m}$ transiently becoming more negative than neuronal $\boldsymbol{V_{rest}}$, producing what is called the

afterhyperpolarization or AHP. This AHP is very brief, and afterward the neuron V_m returns to the initial V_{rest}.

The biophysical mechanisms of AP generation were first discovered by the works of Hodgkin and Huxley (1952b), who found that the rapid depolarization phase results from the activation of voltage dependent Na^+ channels. This produces a massive influx of Na^+ ions into the neuron. The repolarization is due to both the inactivation of these channels and to the late activation of voltage gated K^+ channels that produces an outflux of these ions. As illustrated in Figure 13 the dynamics of activation inactivation of voltage dependent Na^+ and K^+ channels shape the modification of V_m during the AP.

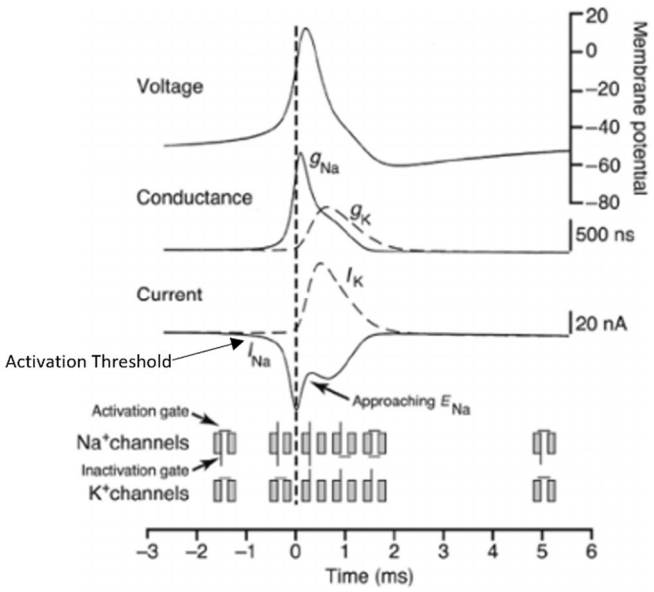

Figure 13. From Huguenard & McCormick, 1994. Action potential generation is associated with an increase in membrane Na+ conductance and Na+ current followed by an increase in K+ current and K+ conductance. Before AP generation, Na+ channels are neutral, being neither activated or inactivated (bottom). When these channels are activated, Na+ enters the cell depolarizing the membrane potential. Depolarization also activates K+ channels, which briefly remain open after the Na+ channels close post-AP generation. The continued activation of the K+ channel is one of the membrane properties that result (in some cells) in the afterhyperpolaization (the dip following the AP).

Hodgkin and Huxley's (1952a,b) original observation that the generation of the action potential itself and the repolarization of the cell thereafter depends primarily on the transfer of

Na^+, K^+ across the cell membrane was later expanded upon when Carbone & Lux (1984) noted that a voltage-gated Ca^{2+} channel triggers calcium ion flux in response to the voltage change across the cell membrane during end-phase hyperpolarization, which aids in the slight depolarization necessary to restore resting state V_m. Carbone & Lux's (1984) conclusions clearly implicated voltage-gated calcium in the AP lifecycle as well.

The brief review of the physiology of neuronal activity can stop here, as it has established the necessary background concerning the resting membrane potential, ionic flux, the early establishment of thermal components, and the voltage-gated ion channels implicated in the action potential necessary to move forward in the context of the present investigation. Though heavily truncated, it provides a sufficient launching pad to move deeper into the cellular physiology associated with the effect of photo stimulation at the neuronal level and the main theories that have been put forward around the mechanisms associated with light-induced neuronal activity change.

2.2 Light Effects on Neural Systems

The knowledge that neurons are sensitive to light stimulation is not recent. The investigation started in the peripheral nervous system (PNS) where Aravanitaki and Chalazonitis (1961) demonstrated that the giant nerve cells of *Aplysia californica* and *sepia* (the California sea hare – a type of sea slug) could be inhibited by a broad spectrum of visible light (λ= 400-700nm) and either excited or inhibited by IR light (λ = 750-4000nm). Concerning the IR light, authors were unable to differentiate the conditions under which cells were excited or inhibited; simply noting that cells displayed both behaviors in the IR light condition. At the time, the authors proposed that this was possible due to EMR absorption by yet unnamed cellular components (Aravanitaki & Chalazonitis, 1961). Fork (1971) would investigate the abdominal ganglion cells of the same species under blue (λ = 488nm), green (λ=515) and IR

(λ=1060) laser light stimulation, finding that the stimulation produced polarization changes (both depolarization and hyperpolarization) in the in the cells, causing changes AP firing. The author noted that the blue and green lights sometimes produced firing when the light was on, but other times firing was only observed when the light was off (indicating light-induced firing inhibition). The effect was reversible so long as the light stimulation intensity was low enough to avoid rapid and permanent cell depolarization, what the author described as irreversible damage (Fork, 1971).

These two studies looked at light stimulation on neurons in the PNS in their natural stage, i.e., without concurrent electrical stimulation to evoke firing activity. But other early work was studying light effects on PNS nerve fibers concurrent to such stimulation. Booth et al. (1950) studied the effects of continuous UV irradiation (λ < 370nm, stimulation >2min) on the nodes of Ranvier within myelinated nerve axons. The authors found that the light both increased the activation threshold for AP generation and decreased the AP amplitude (Booth et al., 1950). Decades later, Balaban et al. (1992) would provide some of the first results differentiating light effects on silent neurons from spontaneously active ones in on more complex invertebrates and within the same species (*Helix pomatia*, the European burgundy snail). The team was not able to evoke APs in silent esophageal ganglia, but they were able to demonstrate that that 10mW red laser irradiation (λ = 632.8nm) depolarized the neurons. Further, cells that were already spontaneously active increased their activity following irradiation in an intensity-dependent manner (Balaban et al., 1992).

In the mammalian PNS, the results of neuronal light stimulation have been quite different than those observed in early invertebrate PNS studies. In an exploratory study concerning the effect of pulsed laser IR (λ = 1064) light stimulation on rat sciatic nerve axons, Wesselmann, Kerns, and Rymer (1994) demonstrated reductions to electrically evoked AP amplitude and generation that occurred at the same time as irradiation-induced tissue heating,

though the authors did not model any links between the different factors. Orchardson et al. (1997) followed the same investigative line to (a) determine the factors associated with laser IR suppression of spinal nerve activity and (b) speculate on whether the effect could be adapted for analgesic treatments. The team found that pulsed IR laser light (λ = 1064nm, power levels between 0.3 and 3mW) reduced AP generation dorsal root nerve cells in a power-dependent manner (greater power = larger effect), an effect that did not appear to irreparably damage the tissue at the low power levels investigated. The authors further speculated that the effect may have something to do with light-evoked tissue temperature changes (Orchardson et al., 1997).

This last point on temperature would become an important component of the investigation into the light sensibility of neurons in mammalian CNS, which took off following the advent of optogenetics. In the early 2000s, the Deisseroth lab discovered that genetically modified opsin could be engineered to respond to specific wavelengths of light and coupled to different neuronal subtypes, allowing them to act as a sort of "switch" to selectively deactivate or activate them, allowing for greatly improved investigative prospects for fundamental neurosciences (Boyden et al., 2005; Diesseroth, 2015, see chapter 3 for more information).

Because the correct interpretation of effects produced by optogenetic manipulation requires that light only affects the activity of those neurons that have been modified to express exogenous opsins, researchers began to question whether optogenetic protocols could produce off-target effects through the interaction of light with naïve brain tissue. Several studies since have addressed this point. Christie et al. (2013) demonstrated that blue light stimulation can produce fMRI artifacts in the rat, which a later study identified as the result of temperature-induced vasodilation (Rungata et al., 2017). And though Wade, Taylor, and Siekevitz (1988) identified cortical effects of light on the naïve rat cerebral cortex *in vitro* more than thirty years ago, describing an effect on the potassium-induced release of synaptic GABA, only recently have several studies targeting light effect at the individual neuronal level been able to clearly

demonstrate a light effect on naïve neuronal activity and specific cellular physiology (Ait-Ouares et al., 2019; Acharya et al., 2021; Feng et al., 2010; Lightning et al, 2023; Owen et al., 2019; Stujenske, Spellman, & Gordon, 2015; Tyssowski & Gray, 2019).

The following sections will discuss these and other studies in detail as they unravel the proposed physiological mechanisms behind such neuronal and synaptic communication level light effects.

2.2a Light induced modification of firing activity is associated with light induced temperature modification

Three very recent studies demonstrated that luminous stimulation could reduce neuronal firing rates concomitant to light-induced tissue temperature change. First, when Stujenske, Spellman, and Gordon (2015) validated their thermal propagation model (section 1.3a) in mice, they a surgically implanted optrode (diameter = 200μm) to stimulate the PFC of anesthetized mice *in vivo* with green light (λ = 532, intensities = 1, 5, and 10mW). The authors noted a change in temperature associated under the light stimulation in tandem with light induced increases to the AP firing rate. They recorded firing activity on both the stimulation-ipsilateral and -contralateral sides. The authors found that both temperature and AP firing increase were higher as a function of increasing light power. Further, they reported that AP firing increased on the stimulation-ipsilateral side of the PFC, but slightly decreased on the stimulation-contralateral side (Stujenske, Spellman, & Gordon, 2015, see Figure 10C in section 1.3a). Three years later, Ait-Ouares et al. (2019) demonstrated a similarly temperature-paired blue (λ = 430-490nm) and green/yellow (λ = 470-570nm) light, though this time with a light-mediated reduction *in vitro* for mitral cells (MC) in the mouse olfactory bulb (Figure 14A,C). But this is not the only neuronal type investigated by this team. They also looked at the effect of 13mW blue light on olfactory tufted cells, medium spiny neurons (MSN) in the striatum, Purkinje

neurons, and CA1 hippocampal neurons. They found light-associated AP firing reduction in both tufted cells and MSNs, but not in Purkinje neurons or CA1 neurons (Ait-Ouares et al., 2019), demonstrating that the effect of light varies by neuronal subtype. Further, this team showed incredibly solid evidence for a temperature mediated light effect in the olfactory bold, demonstrating that the AP frequency reduction in MCs was reproducible simply by raising the temperature of the tissue in the absence of light (Ait-Ouares et al., 2019, Figure 14E). Ait-Ouares et al. (2019) also noted that blue light reduced excitatory post synaptic potentials (Figure 14D). Speculatively, this may suggest an inhibitory synaptic component to the neuronal light effects observed, but it should be noted that our own results with blue light ($\lambda = 473$, see study 1) weakened the argument for this component, as the luminous inhibition of cortical fast spiking interneurons was not necessarily any greater than the inhibition produced in other neuronal subtypes.

This same year, Owen, Liu, and Kreitzer (2019) used green light ($\lambda = 532$nm) simulation of MSNs in the naïve mouse striatum to demonstrate that the light altered neuronal activity at level sufficient to alter animal behavior *in vivo* and that this reduction occurred parallel to a light-induced tissue temperature increase (Figure 14B, F). The Owen team also investigated multiple cell types in addition to MSNs, those being CA1 hippocampal pyramidal neurons, granular cells from the dentate gyrus, cortical pyramidal neurons, and cortical fast-spiking interneurons *in vitro*, finding that light reduced firing rates in all but the CA1 neurons (Owen, Liu, & Kreitzer, 2019), and giving more evidence to the idea that light effect varies by neuronal subtype.

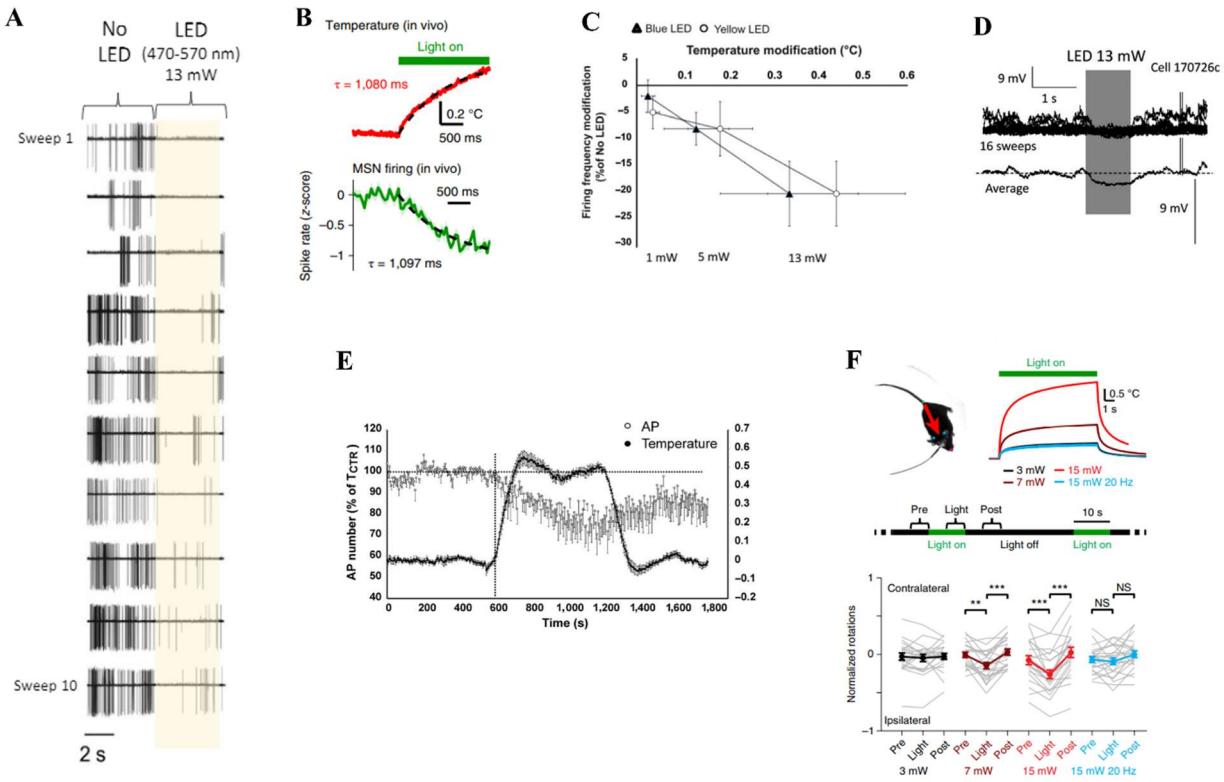

Figure 14. Light mediated changes to neuronal activity. Adapted from Ait-Ouares et al., 2018 (A [unpublished pilot study], C, D, C) and Owen, Liu, & Kreitzer, 2019 (B, F). A) LED-induced reduction in neuronal firing across 10 sweeps of light stimulation. Cell attached recording in mitral cells. B) in vivo green light stimulation of the naïve mouse striatum in vivo produces changes in tissue temperature. C) Blue and yellow light-induced firing reduction in olfactory mitral cells occurs concomitant to tissue temperature increase. D) Light-stimulation (grey) reduces spontaneous synaptic activity (top) and hyperpolarizes the cell membrane (bottom). E) Tissue temperature increase can reduce neuronal firing in olfactory MC by itself, absent light. F) Green light produces contralateral rotation bias during green light stimulation of MSN neurons. Top: experimental setup with the modeled temperature change, bottom: the degree of effect appears to be associated with the light power and duty cycle of the light.

The results of the studies so far suggest that temperature mediated AP firing changes with neuronal subtype and indeed can either be excitatory (as in Stujenske, Spellman, & Gordon, 2015) or inhibitory (as in Ait-Ouares at al., 2019 & Owen, Liu, & Kreitzer, 2019). Of course, neuronal activity reduction under light is not a one-size-fits-all conclusion and you will find an example later in study 2, where we note in our own work that some cells displayed AP activity increases. This is true even concerning temperature modifications in the absence of light. Kim and Connors (2012), for example, described a depolarization and increased spiking in mouse CA1 and CA3 pyramidal neurons under induced hyperthermia (41°C). They further demonstrated that the temperature sensitivity varied based on neuronal subtype (Kim &

Connors, 2012). However, it should also be noted that the Kim and Connors (2012) paper was looked at the effects of a global hypothermic temperature increase on the tissue (to 41°C) far outside of the realm of biological safety for living mammals, while light other induced effects reported here are associated with a much lower local tissue temperature increases (less than 1°C) (Ait-Ouares et al., 2019; Owen, Liu, & Kreitzer, 2019; Senova et al., 2017). Thus, the increase may simply be a function of the hyperthermia, but it could also be a function of the different anatomical area, as the studies in this section have reported varying AP firing effects in different brain areas and on different neuronal subtypes. Temperature increases following tissue cooling have indeed been shown to be responsible for changes to AP parameters, such as decreases in AP spike threshold, and increases to AP latency in the rat visual cortex (Volgushev et al., 2000a). Keeping in mind that these parameters are deeply tied to cation activity and membrane physiology provides a great introduction to the next points concerning light effect mechanisms.

2.2b Light stimulation affects AP properties and induces an outward current at neuronal Vrest

The strong temperature corollary of the effects described in the previous section is not surprising. After all, one of the first studies demonstrating tissue temperature increases causing inverse linear neuronal activity decrease took place in the 1960s, though on cells from the PNS rather than the CNS. Frankenhauser and Moore (1963) investigated the effect of temperature on myelinated nerve fibers of *Xenopus laevis* (the clawed toad) and found it to be linearly correlated with increases to Na^+ and K^+ membrane permeability. Thompson, Musukawa, and Prince (1985) later investigated changes in ion conductance for *in vitro* guinea pig CA1 hippocampal neurons, finding that cooling with as little as 5 – 10°C reduced K^+ and Ca^{2+} conductance. Notably, they observed that this increased the amplitude and duration of the

afterhyperpolarization (AHP), increased the AP half-maximum amplitude, increased time between action potentials (AP latency) and, interestingly, decreased the action potential firing rate. All of the effects were reversible when the cells were re-warmed (Thompson, Musukawa, & Prince, 1985).

There is, however, much more to unravel. Fifteen years later, Volgushev et al. (2000a;b) would report temperature-increase dependent changes to AP latency and AP threshold. They also noted that temperature increases from 12°C to 31°C in the rat visual cortex produces an outward hyperpolarizing current, where the V_{rest} change is approximately -1.3 ± 0.09mV/°C. The biophysical properties of this change appeared to be mainly due to an increase in the permeability ratio between potassium and sodium leak channels (Volgushev et al., 2000b).

Since the literature demonstrates that light is both capable of modulating neuronal activity and heating the tissue, these earlier studies bring up interesting questions about the involvement of ion conductance in the neuronal light effect. Ait-Ouares et al. (2019) explored their light's effect on action potential components, finding significant light-induced changes to the AP amplitude, maximum AP threshold, AP rising slope and half width, and the after hyperpolarization, all of which are associated with voltage-gated sodium and potassium ion activity. In contrast to the Thompson study discussed in the previous paragraph but in accordance with Volgushev (2000a;b) studies, their results (which occurred in tandem to temperature increase) also showed decreases to AP amplitude and latency and an increase to AHP amplitude (Ait-Ouares et al., 2019).

Membrane potential is also known to be determined by ion conductance (Hodgkin & Huxley, 1952a;b; Hodgkin & Katz, 1949), and Ait-Ouares et al. (2019) observed that 13mW light stimulation resulted in a membrane hyperpolarization of MCs (Figure 15A), a change which they estimated to occur at a rate similar to that described by Volgushev et al. (2000b): -&.7mv/°C. In an earlier stage using varying power intensities of light (13, 5, and 1mW) they

do note that light power has varying effects on firing frequency, with higher powers producing greater effect. Since they did not investigate varying intensities when reporting membrane polarization, it is unclear if that variance from light power is also present there or is the varying effects on AP frequency are related to the membrane hyperpolarization (Ait-Ouares et al., 2019). Owen and colleagues later show that the light induced membrane current in MSNs can be produced by temperature modification (Figure 15B). Additionally, due to the I-V profile (Figure 15C), they suggested that this is due to the activation of lipid-gated inward rectifier potassium channels (K_{ir}) (Owen, Liu, & Kreitzer, 2019).

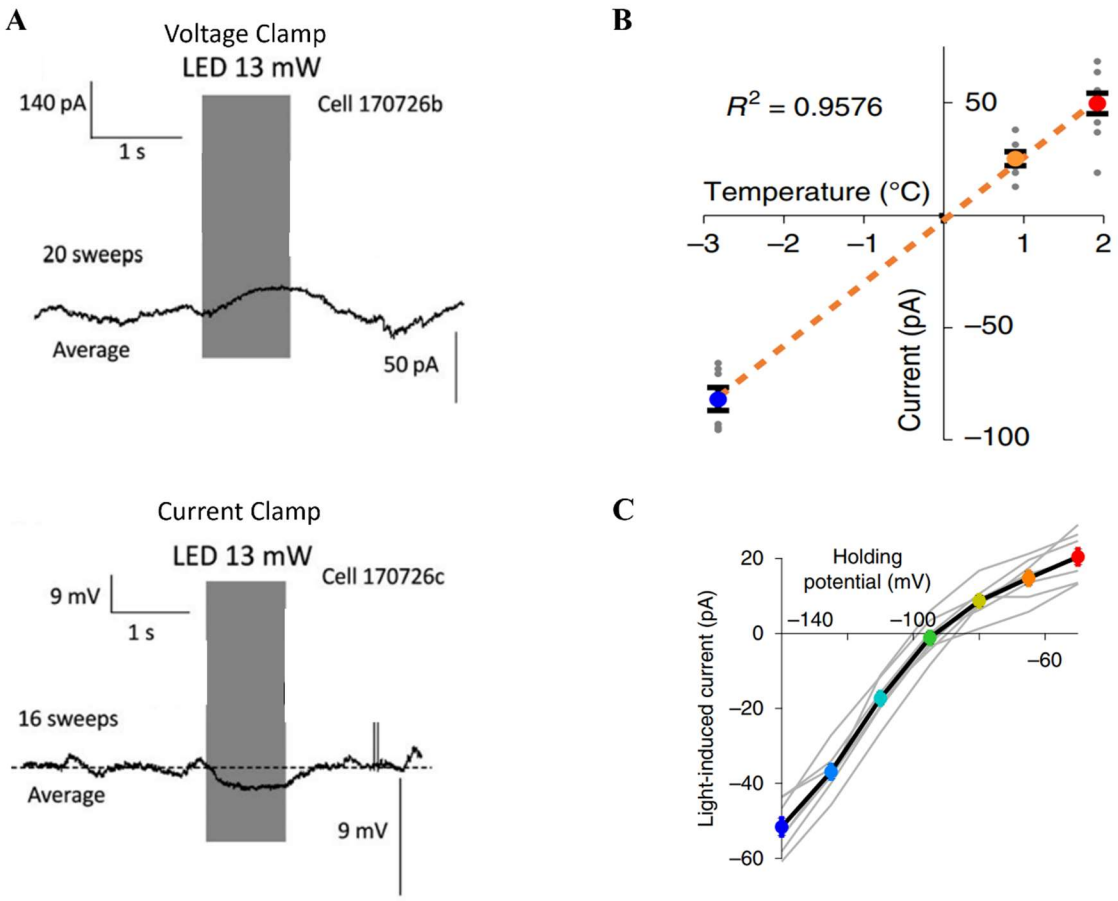

Figure 15. Adapted from (A) Ait-Ouares at al., 2018 and (B, C) Owen et al., 2019. Light stimulation depolarizes the membrane current. Temperature increase is, however, linearly correlated with potassium outflow. A) Visualization of light-induced membrane hyperpolarization in electrophysiological traces. Top: Voltage clamp configuration. Bottom: current clamp configuration. B) Representation of the strong linear correlation between temperature increase and putative potassium current. C) I-V profile of light-induced current modifications in MSNs (voltage sensitivity of light activated currents).

K_{ir} channels are known to have component proteins from the thermos-sensitive TRP family (Yang, Cui, Wang, Zheng 2010) and immunohistochemistry staining has identified a particularly widespread presentation of $K_{ir}2$ channels (a neuron-specific subtype implicated in both excitation and inhibition) in the telencephalon, diencephalon, mesencephalon, metencephalon, and myelencephalon of the rat brain (Prüss et al., 2005). Interestingly, K_{ir} genes have been identified on chromosome 21 of both the human and mouse genomes, and fetal tissue analysis implicates them in normal brain development for both species (Thiery et al., 2003). In their study, Owen et al. (2019) tested light effect on firing activity of CA1/dentate gyrus hippocampal neurons, striatal MSNs, and cortical layer 5 pyramidal neurons and fast spiking inter-neurons (FSI), finding that the light-induced AP spiking suppression correlated with brain region known to express K_{ir} channels (i.e., the dentate gyrus, the cortex, and the striatum).

Aside from the direct the modification of gating properties and/or permeability of membrane channels, visible light may also be affecting the firing activity of brain neurons trough the activation of brain opsin or through modifications to the efficacy of synaptic transmission. Earlier, I mentioned how extraocular opsins, though identified in many brain regions, are rarely functional (section 1.2). Accordingly, Ait-Ouares et al. (2019) show that in the presence of G-protein inhibitors, light stimulation was still able to reduce MC firing activity, suggesting that extraocular brain opsins do not play a major role in this effect. However, the same author shows some evidence of a reduction of synaptic activity by light (see figure 14F). Indeed, as we will see in the next chapter light stimulation has been shown to affect synaptic GABAergic transmission.

2.2c Light has some effects on GABA inhibitory systems

The question of any direct light effect via GABA-ergic systems is a bit more complex. In the 1980s, Wade, Taylor, and Seikevitz (1988) demonstrated that low intensity (1.3 mX/cm^3)

white light stimulation could enhance potassium-induced GABA release in rat cortical slices. The slices were placed in Ringer's solution with additive aminooxyacetic acid (AmoA), which allowed them to absorb radioactive [^{3}H]GABA while the AmoA prevented its metabolization. This allowed the team to evaluate the presence of GABA by measuring the levels of released radioactivity in the slices during experimentation. The slices were then rinsed and transferred to a Ringer's solution with elevated potassium (K^+) under either light or dark conditions. The researchers observed that tissue in the white light condition released more radiation, allowing them to conclude that the white light triggered an increase in potassium-mediated GABA release, an effect that appeared to vary based on the intensity of the light stimulation (Wade, Taylor, & Siekevitz, 1988). It should be noted that high K^+ concentration on slices is typically used to activate the neurons, but these researchers only collected radiolabeled GABA during their study and did not evaluate any effect of the light on neuronal firing rates.

Later, Leszkiewicz and Aizenman (2003) looked at light mediated $GABA_A$ receptor activity (a Cl^- selective ion channel) in a culture of rat cortical neurons. They applied GABA to the cultured cells before and after brief pulses of light stimulation (λ>270nm, 1-2s of stimulation) and used whole-cell patch clamp to record the resultant effect on cellular current. They observed an enhancement to GABA-mediated current response following the light stimulation, suggesting that light can increase the permeability of $GABA_A$ receptors and/or GABA affinity for the receptor. This effect was reversible after allowing the culture to rest for 3-5min.

In a more recent paper Sun et al. (2020), recorded spontaneous inhibitory post synaptic currents (sIPSC) in rat hippocampal CA1 pyramidal neurons *in vitro* and were able to selectively suppress the sIPSCs with blue (λ=480nm) light. The authors noted that the presence of the $GABA_A$ receptor antagonist bicuculine blocked this effect, and thus concluded that the light was acting on GABA transmission. Moreover, the authors concluded that the effect was

one of photosensitivity and not thermal sensitivity since increasing the perfusion bath temperature from 0.1°C to 1°C did not similarly suppress sIPSC activity (Figure 16B).

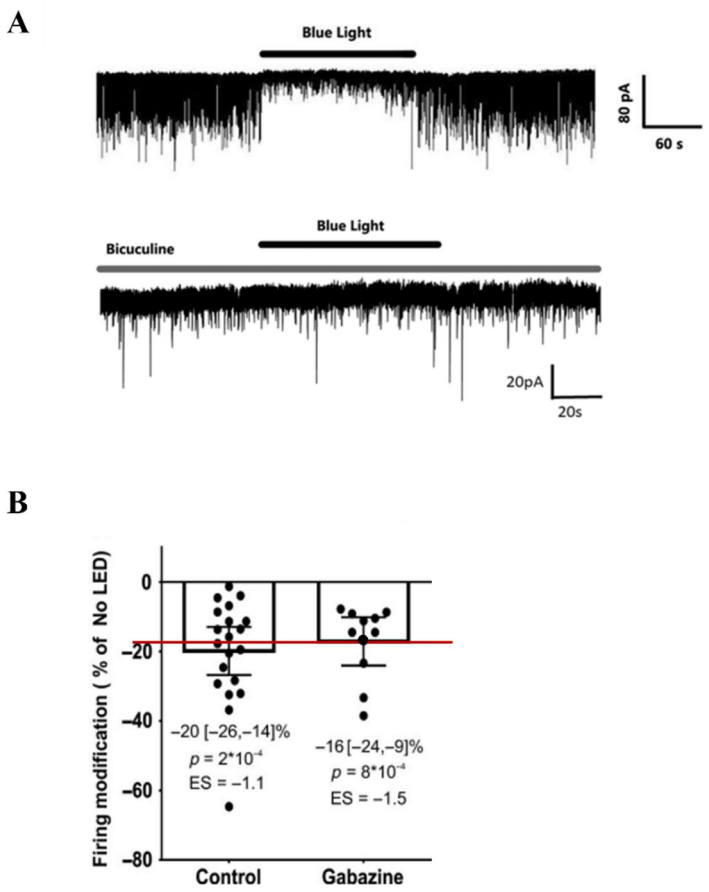

Figure 16. Light inhibition of neuronal firing may only be liked to GABA for specific subtypes and/or non-evoked activity. Adapted from (A) Sun et al., 2020 and (B) Ait-Ouares at al., 2018. A) Blue light inhibition of sIPSC activity is not reproducible in the presence of GABAa antagonist bicuculine. B) Light still reduces firing in mouse MCs in the presence of GABA antagonist gabazine. The red line is illustrative for the average effect.

All together these results established a baseline for exploring whether light-induced changes to neuronal firing were mediated by these changes to GABA synaptic transmission. However, Ait-Ouares et al. (2019) ruled out a direct effect from increased GABA inhibition by showing that in the presence of the $GABA_A$ receptor antagonist, gabazine, the inhibitory effect of light on MC firing was not modified (Figure 16A). This result was supported by our recent work (Lightning et al., 2023) where the effect of light on different neuronal types were observed in the presence of antagonists of both GABAergic and gutamatergic transmission (see results section). All together these studies demonstrate that, though evidence for a GABA-mediated

component to the neuronal light effect is present, its participation on the effect of light on neuronal firing is negligible, at least *in vitro* conditions.

Thus far, I have discussed the biophysical and synaptic mechanisms participating in the visible-light-induced modification of neuronal activity. As you will see, one of the aims of my thesis project was to investigate whether neuronal sensitivity to visible light could be used as a therapeutic tool for brain pathology. As I mentioned in the introduction, this is not a completely new idea, as there is already a biomedical field of research on brain light therapy, bPBM. But this therapy is based on NIR and IR light stimulation. It is therefore important to review the proposed mechanisms that account for bPBM as well as other possible effects of light on brain function that are not directly related to modification of neuronal activity.

2.2d Other possible mechanism of light effect on brain activity

The first law of photochemistry states that in order for light to affect biological chemistry, it first needs to be absorbed. I have talked extensively about the light absorption into cortical and biological tissues, along with the chromophores and opsins implicated in the effect. I have also spoken extensively about the thermal consequences of that absorption and how both temperature dependent and temperature independent components have been proposed surrounding the neuronal light effect. I have also discussed the relationship between wavelength and absorption into the tissue. IR and NIR light, with their longer wavelengths and higher tissue permeability, have been ties to a unique mechanism of action based on the absorption of photons alone. Multiple reviews have described Ca^{2+} transfer following photon absorption by the mitochondria and the subsequent activation of cytochrome c oxidase (CCO, a known photosensitive molecule) and reactive oxygen species (such as nitric oxide, NO) as the key mechanism of action behind IR and NIR light effects on the brain (Figure 17A), but any degree of conclusiveness for the entire mechanism remains largely speculative (Hamblin, 2016;

Hamblin, 2018; Huang, 2022; Pierroz & Folcher, 2018). The speculation is, however, highly scientific and based on a history of studies that show IR and NIR light are capable of stimulating the component parts of the effect in both neurons and other mitochondria-containing cells.

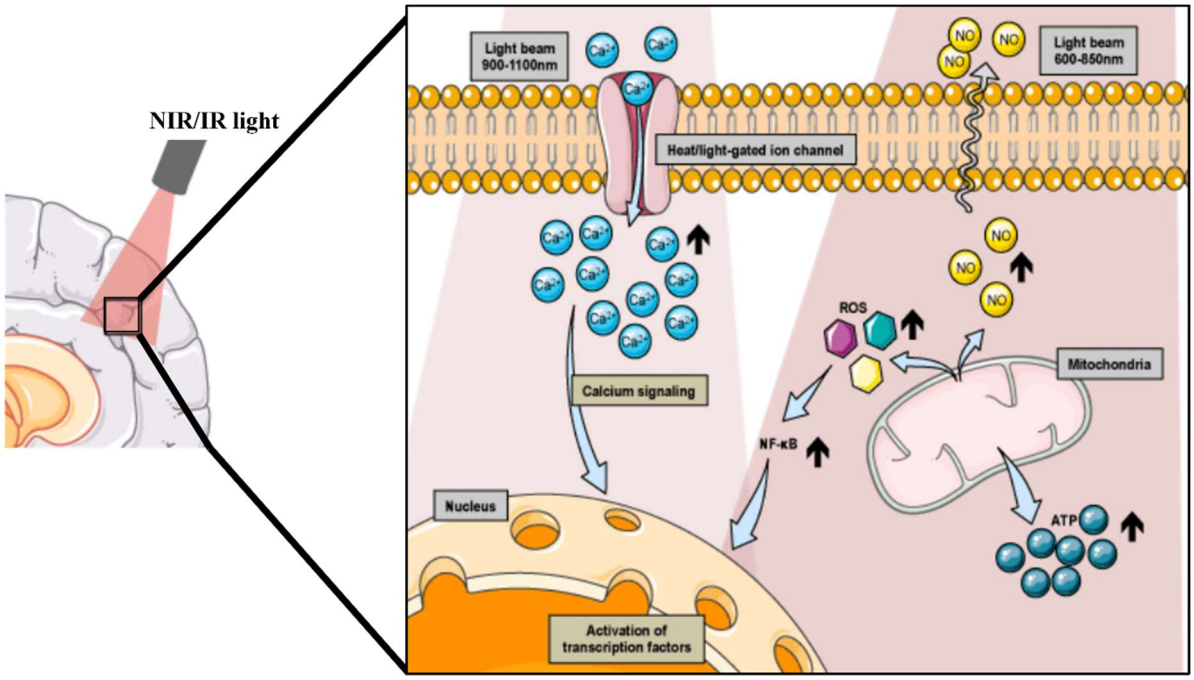

Figure 17. NIR and IR light stimulation activate cortical CCO and may be dissociating reactive oxygen species, such an NO, when the photons are absorbed by neuronal mitochondria. Adapted from Pierroz & Folcher, 2018. Light reacts with both CCO and heat activated TRP channels to facilitate the transfer of calcium and the metabolization of ATP. CCO effects can be either inhibitory or excitatory for the cell metabolism, seeming to depend on the redox state of the receptor (see Pastore, Greco, and Passarella, 2000)

Pastore, Greco, and Passarella (2000) were some of the first to demonstrate the interaction between NIR laser light ($\lambda = 632.8$nm) and purified mitochondrial CCO. The authors isolated and purified CCO from horse heart cell mitochondria and catalyzed its activation with and oxidative reaction (COX) under control and NIR laser stimulation conditions. They not only found that CCO was activated under NIR light, but that its activation was dependent on the CCO to oxidizer ratio, with activation only occurring at lower CCO ratios and inhibition occurring when the ratio was high (Pastore, Greco, & Passarella, 2000). Wong-Riley et al.

(2005) would later link CCO directly to brain photostimulation (using cultured rat visual cortex neurons) under NIR and IR (λ = 670, 728, 770, 830, and 880nm) light. They used KCN to irreversibly inhibit the CCO in their test cultures, hypothesizing that the inhibition should interfere with the light effect (heightened neuronal ATP metabolization), which is indeed what they discovered (Wong-Riley et al., 2005).

Many other studies involving NIR and IR irradiation of the mitochondria from multiple cell types took place throughout the 2000s, such that a recent systematic review was able to quantify their collective conclusions and declare CCO activation a consequence of NIR/IR light absorption in mitochondrial cells (Passarella & Karu, 2014). Recent advances in optical spectroscopy have even allowed researchers to confirm this effect in humans (aged 18-85 years) undergoing TLLT (λ = 1064). Recall that TLLT stands for transcranial low-level laser therapy, and is an acronym commonly used in bPBM research. Saucedo et al. (2021) used broadband NIR and IR spectroscopy to evaluate cellular changes to CCO following 8 minutes of TLLT stimulation on the right forehead and demonstrated a, increase in CCO activation (measured via observed modifications in the concentration) on both the stimulation-ipsilateral and stimulation contralateral sides of subject pre-frontal cortexes (Figure 18A).

They did note, however, an aged-based difference, as older patients seemed to have higher CCO activation on the ipsilateral side, while younger patients had higher activation on the contralateral side (Saucedo et al., 2021; Figure 18B, C). This demonstration in human patients is incredibly important, both for the definitive identification of cellular mechanisms for NIR/IR stimulation and to demonstrate that the light effects on the human brain appear to be variable with age. Since I will be speculating later concerning the possible medical applications of neuronal light stimulation, having evidence of age-difference is very useful, even if it is only in NIR/IR light therapies.

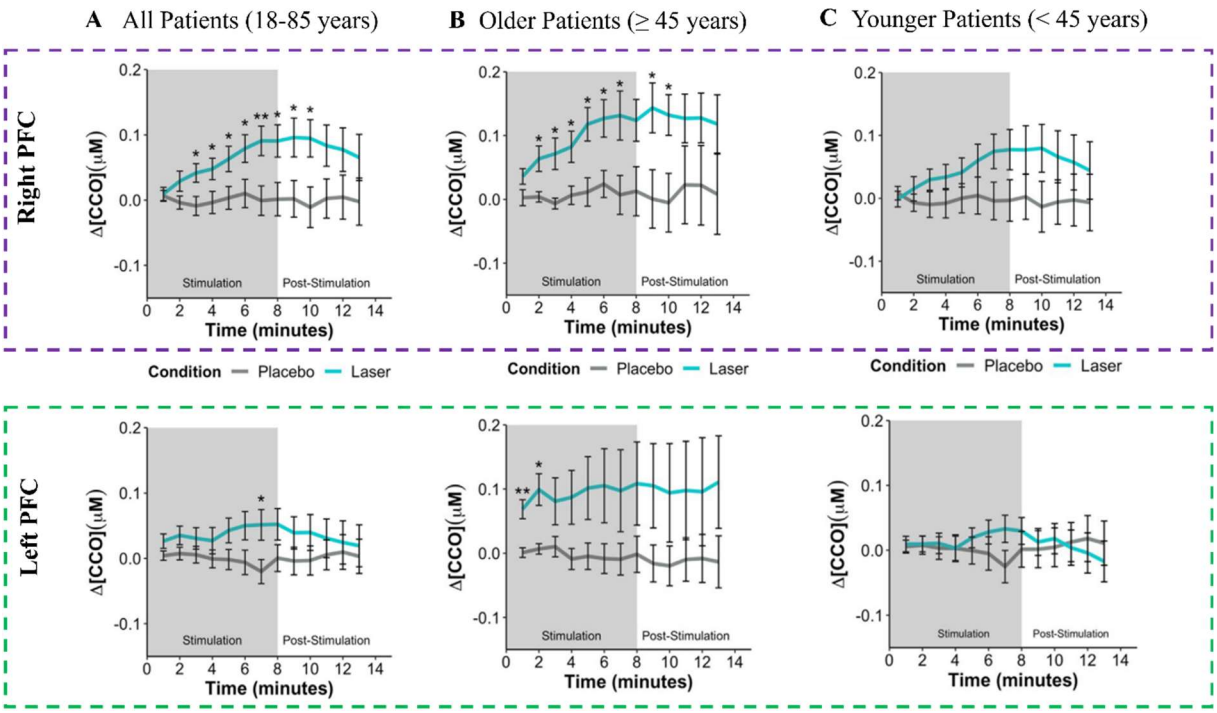

Figure 18. Transcranial IR stimulation during TLLT therapy is activating CCO in human cortical mitochondria. Adapted from Saucedo et al., 2021. Stimulation ipsilateral (top, purple) and contralateral (bottom, green) CCO activation in the human PFC, measured via NIR/IR spectroscopy in A) All patients, B) Older patients, and C) younger patients.

So, the effects of NIR and IR light on the activation of CCO appear to be well demonstrated in the literature. The speculative side of the proposed mechanism depicted in Figure 17 appears to be the specific dissociation of NO the additional activation of Ca^{2+} (recall that heat-associated ion exchange is associated with TRP channels and voltage gated ion channels). This speculation appears largely due to a few pieces of knowledge gathered in several systematic reviews. First, NO increases cellular respiration and ATP concentration (a known consequence of NIR/IR neuronal light stimulation). Second, when PBM is used for analgesia, the damaged cells targeted and affected by the light therapy tend to have higher inhibitory NO concentrations, leading reviewers to speculate that this may be a part of the reason the light is effective. And finally, the dissociation of NO from the mitochondria allows it to serve as a vasodilator through the activation of Ca^{2+} exchange channels sensitive to reactive oxygen species (Hamblin, 2016; Hamblin, 2018; Huang, 2022; Pierroz & Folcher, 2018).

The vasodilation is also a possible mechanism tied to brain light stimulation. Vasodilation and constriction in the CNS are reactive consequences to changes to neuronal activation, as the change in activity changes the energy needs of the active area. Thus, blood flow (and therefore oxygenation and nutrient exchange across the blood brain barrier) changes necessarily result from neuronal activity changes. This is one of the principles behind readable fMRI response, which Christie et al. (2013) used on naïve rat brains both *in* and *ex vivo* to study the effect of blue light (λ = 445nm) on BOLD response readings. The authors found that not only did prolonged stimulation (30s) from the blue light produce marked temperature changes (Figure 19A), but that the stimulation generated both positive and negative "activation" of the stimulated brain areas both *in* and *ex vivo* (Figure 19B). They further tied the activation to the light power, using several different light intensities (1.2, 3.9, 8, 12, and 16mW) to stimulate the tissue and demonstrating greater effects for larger light powers (Christie et al., 2013).

This result was reproduced and extended by Rungta et al. (2017) who stimulated naïve rat brains via optical fiber (blue light, λ = 473nm; two photon mixed blue/red light, λ = 473/561nm, or red light λ = 594 or 638nm) with the intensities and duration commonly used in brain optical stimulation experiments (durations = 20ms, 20Hz pulsed light, and 2s; power levels = 5 – 45mW/ mm^2). The authors found that the blue light triggered vasodilation (Figure 19C), which they tied to the heat-induced release of Ca^{2+} ions in the smooth muscle cells using two photon calcium imaging (Rungta at al., 2017).

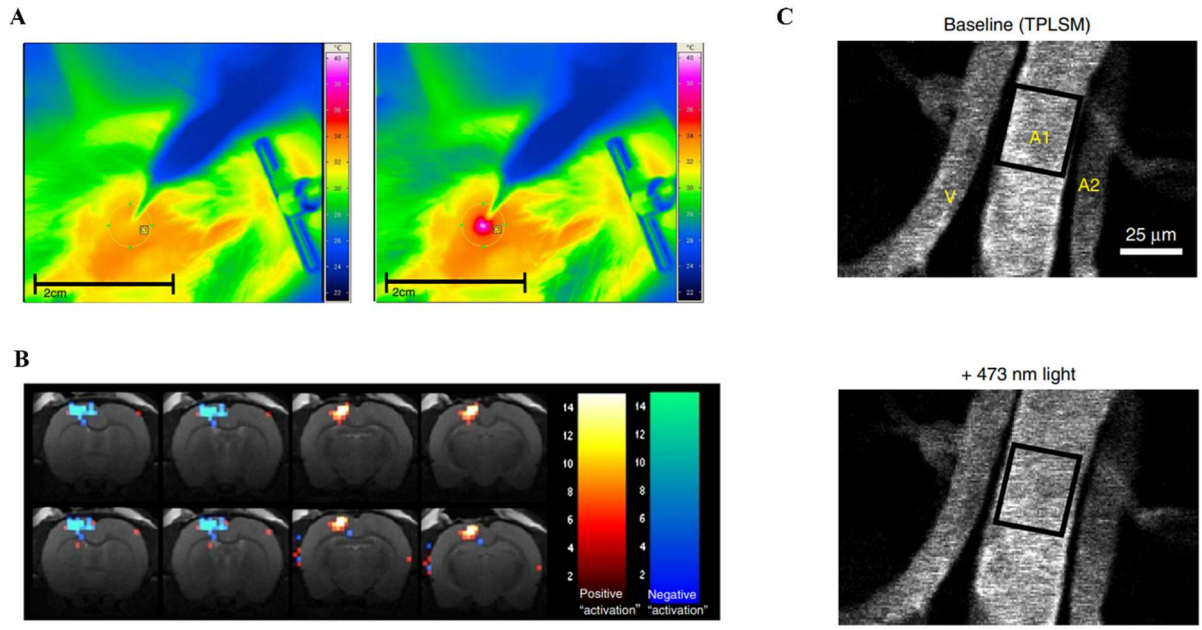

Figure 19. Blue light stimulation produces tissue temperature increases in vivo and pseudo activation of the cortex under fMRI. This is facilitated by light-activated vasodilation in stimulated areas. Adapted from (A & B) Christie et al., 2013 and (C) Rungta et al., 2017. A) Thermal map of a resting rat brain (left) in vivo compared to the thermal map of the same animal stimulated with blue optical fiber light (right). B) BOLD fMRI responses to blue light stimulation in vivo (top) and ex vivo (bottom). C) Blue light induces vasodilation in the rat cortex. Pre light vascular size (top) compared with intra-light vascular size (bottom).

I have now provided an overview of the current literature surrounding neuronal and brain light stimulation showing that light is able to act on the naïve mammalian brain via several known cellular mechanisms, the question finally becomes: what should we do with this information? In addition to further exploring mechanisms of action, effect duration, and neuronal subtype differences, our work will center on two possibilities. First, on the fact that naïve neuronal light sensibility may be providing confounds to optogenetic studies. Second, that light stimulation suppression of action potential firing activity may be a viable tool to treat epileptic pathologies since the common marker of epileptiform family disorders is uncontrolled neural hyperexcitability. The final chapter will therefore provide a brief overview of optogenetics and the mechanics of optogenetic research, as well as an introduction to epileptiform disorders and existing medical uses of light stimulation.

CHAPTER 3

AN OVERVIEW OF OPTOGENETICS, EPILEPSY, AND CURRENT MEDICAL APPLICATIONS FOR BPBM

The fact that that light can indeed modulate the activity of naïve (read: non-genetically modified) neurons brings up a major concern in modern neuroscience research. Namely, the possible off-target effect that could be produced by techniques using light as a tool to study the brain, such as calcium imaging, photometry and optogenetics. On the other hand, the neuronal sensitivity to visible light, and in particular the light-induced inhibition of firing activity, could open up new perspectives for the use of brain light stimulation in pathologies associated with neuronal hyperactivity, such as epileptic syndromes. The aim of this chapter is to provide a brief overview of these two aspects.

3.1 What is optogenetics and how does it work?

According to the inventor of the technique, Karl Deisseroth, optogenetics is at its very core a research tool for identifying deep neural processes, giving it the capability to expand neuroscientific knowledge in diverse ways (Deisseroth, 2015). In section 1.2, I discussed how opsins are associated with light-mediated cellular excitation and inhibition. This principal association is what allowed them to be adapted for use in what would become the field of optogenetics (Boyden et al., 2005; Diesseroth, 2015).

As the name suggests, optogenetics genetically adapts natural algal or microbial opsins in a way that allows them to be expressed by mammalian neurons. The modified opsins are engineered to couple to specific neuronal subtypes and give them pre-defined wavelength sensitivities, thus allowing for the luminous control of neural activity. They can be adapted as a neural "switch" of sorts that facilitates real-time behavioral control through selective activation or inactivation of neuronal activity (Boyden, 2011; Deisseroth, 2015; Fenno, Yizhar, & Deisseroth, 2011; Figure 20).

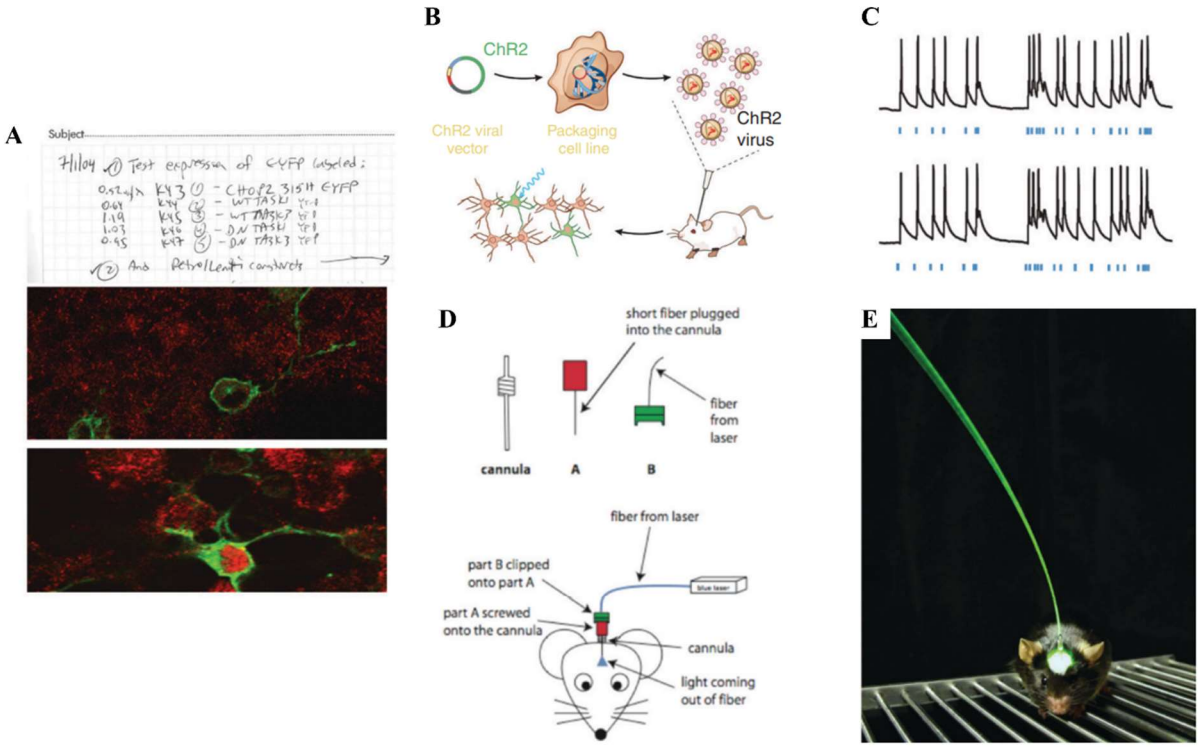

Figure 20. The creation of optogenetics allowed for the light-mediated control of neuronal activity in vivo. Adapted from Deisseroth, 2015. A) Original notebook page and florescence staining of neurons during the development of viral vector optogenetics. B) The introduction of the opsin virus to mice. C) An example of the stable and reproducible neuronal activity control achievable with optogenetics (here with blue light). D) Prototype engineering sketch of the in vivo optical fiber setup, later perfected into E) the setup that finally allowed the optical control of behavior in vivo.

Various opsins are used for optogenetics, though those in the rhodopsin family, such as halorhodopsins (Halo/NpHR) and channelrhodopsins (ChR2), are among the most common due to their ease of implementation, diverse wavelength sensitivities, and adaptability toward varying neuronal firing effects (Boyden, 2011). Optogenetic techniques can provide selective activation or inhibition of different neuronal subtypes, leading to a high degree of spatial selectivity and closed-loop control of neuronal networks (Deisseroth, 2015). It is a powerful research tool, with the primary goal being to understand neuronal and neural circuit behavior via animal models (Williams & Deisseroth, 2013). The light-based spatial selectivity also allows electrical signaling to be recorded without interference from electrical stimulation that might be used for selective activation/inactivation in place of optogenetic techniques (Richardson et al., 2020).

The lack of electrical interference unfortunately does not result in the complete elimination of artefactual risk. Optogenetic changes to the behavior of neurons and neuronal networks are achieved through changes to ion channel activity that either polarizes or depolarizes the cells (Chen et al., 2022; Hallet et al., 2016; Yao et al., 2012; Yizhar et al., 2011). Studies that measure any electrophysiological changes also beholden to these mechanisms (e.g., membrane potential, action potential, and synaptic transmission) may be particularly sensitive to artefacts from naïve neuronal light sensitivity. Brain light stimulation can also affect EEG alpha and beta wave oscillations in naïve subjects (Wang et al., 2021). So, it is possible that even optogenetic studies reporting EEG information, such as Cardin et al. (2009) who used optogenetic tools to identify the strength of gamma oscillations produced by interneurons, may also be sensitive to data pollution.

This ends the brief introduction to optogenetics. Parties who may be particularly interested in this technique and its mechanics are encouraged toward further reading of publications from the Deisseroth lab and the ever-growing literature using optogenetic methodologies. For the purposes of this review, I have provided a truncated summary for clarity, as I am sure you can now imagine how naïve neuronal light sensibility might confound such studies and produce artefactual data. Our work in study 1 will make methodological recommendations toward exactly that point. But light effects on neuronal activity are not only confounding factors. They have the potential to be adapted for medical use, as well. Particularly, the inhibitory effects observed upon blue light stimulation on several neuronal subtypes could potentially counteract brain disorders due to neuronal hyperexcitability, such as epileptic syndromes.

3.2 Current and speculative applications of naïve neuronal light sensitivity in medicine

Using light to treat pathology in the brain is not a completely new idea. In earlier chapters I have touched on TLLT therapies, a transcranial application of bPBM that uses NIR and IR light as a therapeutic tool for various brain pathologies (Huang, 2022). Naeser et al. (2016) reported on a series of studies by the team where they used transcranial mixed NIR/IR (λ = 633nm and 870nm) laser stimulation on patients with mild TBI, resulting in improvements to cognitive functioning. More specifically, they treated TBI patients who had lasting injury-related cognitive impairments with a United States FDA-approved laser therapy helmet (9min 45sec stimulation at power density 22.2mW/cm^2 and energy density 13J/cm^2). Patients who underwent the treatment has statistically significant improvements in cognitive reasoning tests used for TBI patients and reported both improved sleep and better social interaction ability. TLLT stimulation (IR, λ = 1064) has also repeatedly proven effective at increasing cognitive functioning and emotional reasoning in healthy humans (Gutiérrez-Menéndez et al., 2020; Huang 2022). For example, Barrett and Gonzalez-Lima (2013) demonstrated that human subjects treated with TLLT had improved sustained attention ability (via psychomotor vigilance task scores) and improved memory retrieval task performance compared to controls. Blanco, Maddox, and Gonzalez-Lima (2015) used the same type of stimulation to generate improvements in executive functioning, which they evaluated via performance in the Wisconsin Card Sorting Task.

White light also shows some promise for transcranial neural pathology treatment. In 2012 Timonen and colleagues demonstrated that bright light therapy (a therapy using full spectrum white light exposure to treat seasonal affective disorder [SAD]) delivered via the ear canals of human patients resulted in the reduction of depression symptoms found in SAD. Four

years later, Sun et al. (2016) conducted an EEG study on human subjects, showing through analysis of centro-parietal P300 amplitude that transcranial light delivered via the ear canals can affect attention-emotion pathways.

These studies provide some evidence that bPBM is capable of being used as a neurological medical tool. I propose that, as demonstrative studies grow in number, the neuronal light effect may be similarly adaptable in medicine. Of particular interest is epilepsy, a family of hyperexcitability disorders characterized by the repetition of sudden electrical discharge (brain seizures). It is the most common neurological disease; 10% of the population will present at least one crisis in their lifetime, with 33% of these developing into chronic epilepsies. The type of epileptic syndrome is classified according to various factors including age of onset and (if applicable) age at offset, type and cause of seizures, and pharmacological profile.

Epileptic crises can occur in a focal (partial to one brain area) or generalized (distributed to the whole brain) manner. There are further sub classifications of the crises as either ictal activity, commonly referred to as a seizure, and inter-ictal activity, which is short duration (ms-sec.) hyperexcitability that occurs between epileptic seizures. Interictal spikes typically correspond with the seizure's origin zone, but this is not always the case (Fisher, Scharfman, & DeCurtis, 2014; Figure 21, below).

There are currently two known causes, the first being brain lesions resulting from stroke, TBI, or some other traumatic insult. These may cause the onset of seizures, which later develops into an epileptic disorder (Scharfman, 2007). These lesions account for about 50% of diagnosed cases and are termed 'symptomatic epilepsies' because they are due to an identifiable cause. The second known cause is a genetic factor, which accounts for about 10% of diagnoses, leaving the remaining 40% of occurrences with unaccounted origins. Together, these are referred to as 'idiopathic epilepsies.' According to the World Health Organization, chronic epileptic disorders affect around 50 million people worldwide, though thankfully 70% of cases are estimated to be

treatable with medication (World Health Organization, 2022; Lyon Epilepsy Institute, 2016). For the remaining 30% of cases that are termed “pharmaco-resistant”, the only recourse for treatment is surgical removal of the affected brain tissues (Lyon Epilepsy Institute, 2016).

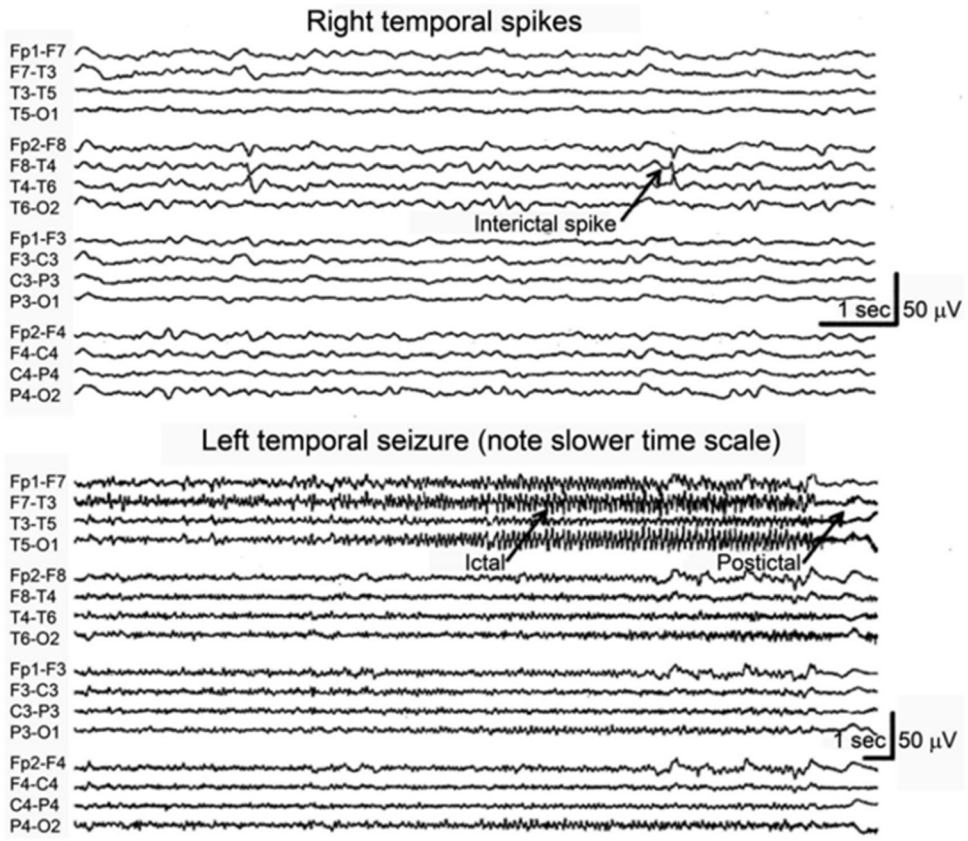

Figure 21. From Fisher, Scharfman, & DeCurtis, 2014. Interictal disparity in a single patient. Top: “Interictal-ictal disparity with spikes in the right hemisphere and seizures on the left. Bottom: Display of “interictal-ictal disparity in the same patient, with interictal spikes over the right temporal region, but seizure onset from the left temporal region.”

Seizures can arise from multiple neurobiological mechanisms, and one that is often discussed is the dysregulation of the balance between excitatory and inhibitory networks. In the first sense, this concerns synaptic transmission. Along with glutamate, the primary excitatory neurotransmitter, GABA is a major inhibitory neurotransmitter of the nervous system, and section 2.2c details the suspicion of GABA sensitivity to light. However, the relationship between these neurotransmitters and seizures may not be direct. Hyperexcitability can arise from dysfunctions in the neuronal network connectivity, but it can also arise from alterations to the neuronal biophysical properties (channelopathy). Channelopathy can come from alterations

to sodium channels, voltage-dependent potassium channels, and ion channels participating in GABAergic synaptic transmission. It also includes abnormalities in several genes coding for the different subunit of voltage-dependent sodium ion channels, which have been identified in patients with genetic epilepsies. In this case, the channelopathy concerns voltage-sensitive α-subunits that form the channel pore (Meisler et al., 2001; Scharfman, 2007). Variations in the SN1B gene of the β-subunit (adhesion molecules that determine the position of the channel) in voltage-gates sodium channels have also been liked to genetic epilepsies (Zhu et al., 2022).

Ragsdale (2008) identified two specific mutations in the SCN1A gene, coding for the α1-subunits, that are associated with febrile seizures, which occur in children 6-months to 5-years old and are caused by increases in body temperature. The mutation produces a functional change in the Nav1.1 channel (α1-subunit). When the change is a functional gain, it causes a deficit in the Na^+ channel inactivation process and a persistent sodium current (Figure 22). Epileptic activity would therefore result from the hyperactive voltage dependent Na^+ channel. However, only a few of the of SCN1A gene mutations found in epileptic subjects increase

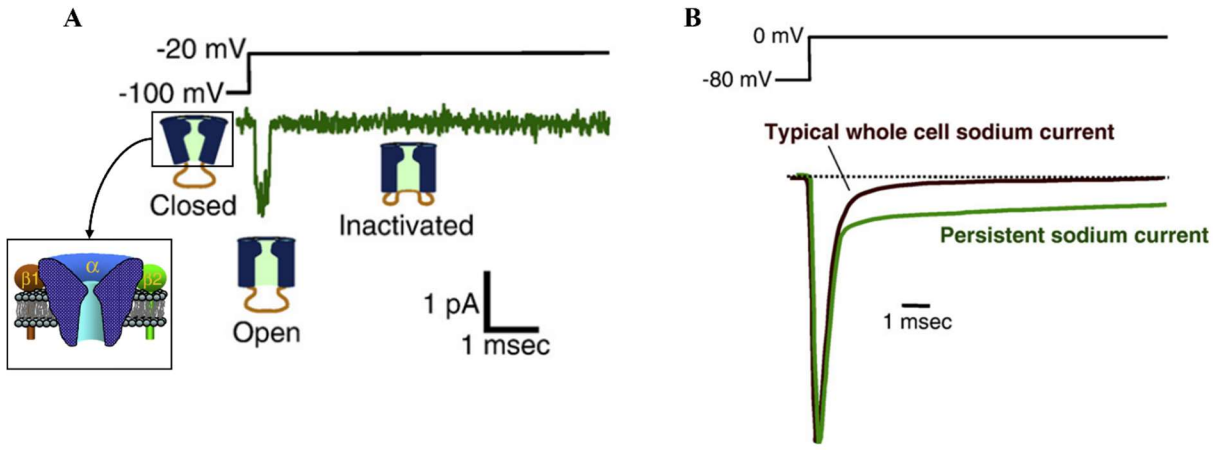

Figure 22. SCN1A mutations cause α-subunit dysfunction and are associated with febrile seizures. Adapted from Ragsdale (2008). A) A single channel current passed through a voltage-gated brain sodium channel in cell-attached patch clamp. Inlay: The structure of the α-subunit with attached β-subunit adhesion molecules. B) A normal whole cell sodium current superimposed over a sodium current with abnormally large persistence (green).

Nav1.1 channel functionality, while most of them lead to a reduction or complete loss of function (Ragsdale, 2008). In these cases, two hypotheses explain network hyperexcitability. The first is the selective reduction of Nav1.1 current in inhibitory interneurons (Yu et al., 2006).

The second hypothesis is an overcompensation for the loss of α1-subunits by an increase in the expression/or functionality of the other α-subunits (Liu et al., 2013).

As you can see from just this single example, the possible ion behavior underlays in the myriad of epileptic disorders are incredibly numerous. Thus, the question of neuronal light sensitivity applications to epilepsy is purely speculative at this point. In the upcoming presentation of our work on this light sensitivity, study 2 will aim to answer some important questions that may help establish a baseline for building a pre-clinical framework to investigate that applicability in the future.

STUDY METHODOLOGIES

In the following studies, we will seek to investigate the effect of one photon (1P) blue light stimulation on both human and mouse neurons. Study 1 examines the effect of blue light on the firing behavior, AP properties, and membrane physiology of mouse olfactory MCs. Additionally, it examines light effects on the AP and membrane physiology properties of cortical pyramidal neurons, cortical fast-spiking interneurons, MSNs in the striatum, and granular cells in hippocampus. This study seeks to make recommendations for avoiding the artefactual impacts of naïve neuronal light sensibility in optogenetic research. Because we were interested only in the isolated effect of the light, study 1 was performed in the presence of antagonists of ionotropic neurotransmission. Study 2 takes a more pre-clinical approach and examines the effect of blue light on both human and mouse cortical neurons without the presence of such chemical additions to better replicate their natural physiological condition. The second study examines the impact of blue light on the action potential firing and membrane physiology properties of human and mouse neurons and looks at the effect of the light on voltage dependent the potassium and sodium ion currents associated with the action potential.

Both upcoming studies use *in vitro* patch clamp electrophysiology, and as such, they share many similarities. In the interest of avoiding unnecessary repetition, the specific details of each study's methodology can be found in the respective manuscript. This section will serve as a summative overview of the general laboratory method used throughout the experiments. I will also highlight a couple of key differences between the two studies in addition to providing some visual references concerning the dissection techniques used for rodent experiments and the equipment used in the laboratory throughout the experimental process.

There are some methodological factors that were identical between the two studies. These include the use of rodent brain tissues sourced via ethical sacrifice and dissection and the use of oxygenated (95% O_2/ 5%CO_2) artificial cerebrospinal fluid (ACSF) to bathe the tissue, with varying compositions for dissection, pre-experimental resting, and experimental perfusion. They also adhere to strict temperature control during the various phases of the tissue preparation and experiment. We used a vibratome to cut 400µm slices (orientation dependent on the study & procedure) of brain tissue submerged in ice cold ACSF (2° - 4°C) before transferring the slices to a recovery chamber (warm ACSF) to rest prior to their use in the experiment.

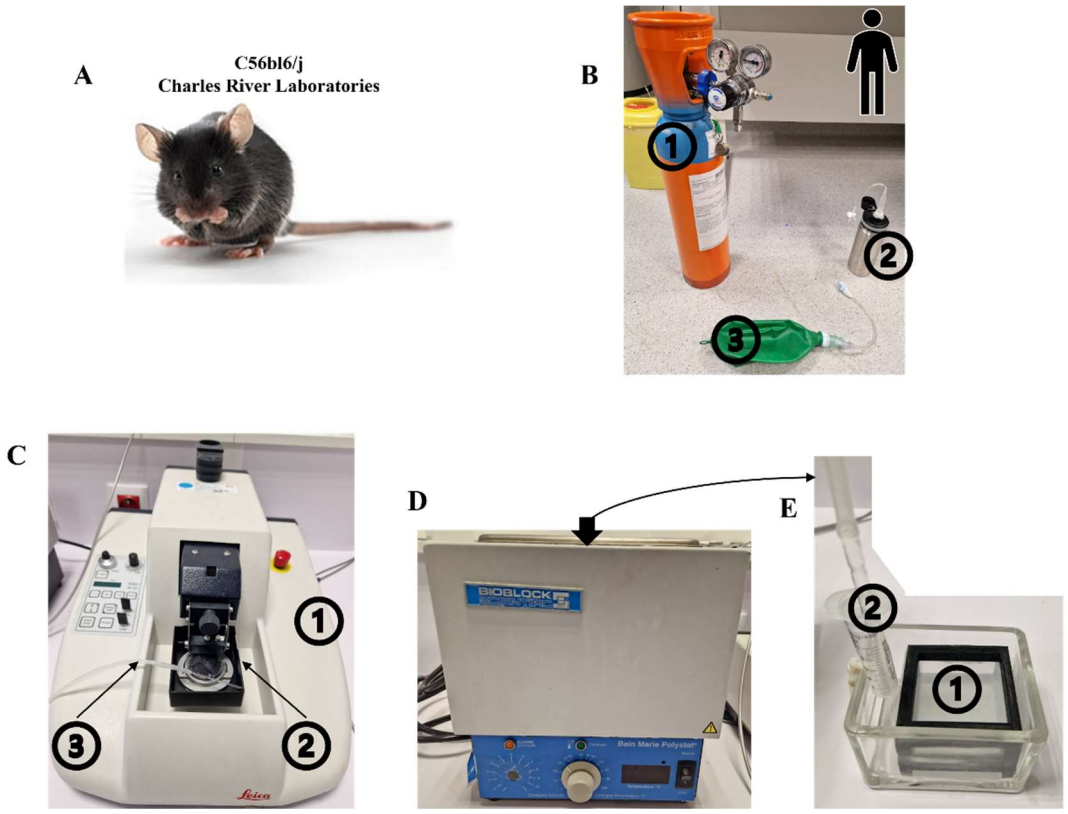

Figure M1. Laboratory Equipment Overview – slice preparation. A) The inbred strain of mice we used for the experiments involving mouse cortical tissues. B) When we sourced human cortical tissues from patient donations, we used an improvised system to oxygenate the tissue in transit. 1: Portable oxygen (95% O2/ 5% CO2 mix) container. 2: tissue transportation container filled with super chilled ACSF and fitted with an oxygenation valve. 3: When the tank in (1) was not available, we filled this balloon with the tissue oxygenation mix from out larger tanks mounted in the lab. The balloon provided approximately 1hour of oxygenation. C) The vibratome used to cut both coronal and horizontal slices. 1: the vibratome. 2: the chamber in which we mounted the brain sections for slicing, above it is the cutting tool. The chamber was filled with ice cold ACSF and continuously oxygenated via tubes attached to our mounted oxygen tanks (3). D) Device used to keep the slices at the resting temperature before transferring them to the recording chamber. E) The open slice preservation tank. 1: Slice resting chamber secured with double layered fine mesh netting to keep bubbles from forming against the slices. 2: improvised oxygen tube stabilization system. The chamber was filled with ACSF and kept at 30°C.

We used the same vibratome and slice thickness parameters whether we were cutting rodent (studies 1 & 2) or donated human tissue (study 2 only). Figure M1 (above) provides a visual overview of the animals and equipment used in the preparation of the slices.

The ACSF solutions used different concentrations of magnesium chloride ($MgCl_2$) and calcium chloride ($CaCl_2$) for the dissection (cut) solutions and the recovery/test solution. For both studies, the cut solution contained 7mM $MgCl_2$ and 0.5mM $CaCl_2$. In study 1, the recovery/test solution contained 1mM $MgCl_2$ and 2mM $CaCl_2$. In study 2, the concentrations were 0.7mM MgCl2 and 1.2mM $CaCl_2$. While the ice cold ACSF cut solution was held at the same temperature in both studies, the recovery temperature and recording temperatures varied. In study 1, they were 35°C for 5 minutes followed by 30°±1°C for the recovery and 32°C - 34°C for the recording. In study two, the recovery temperature was lower (a constant 30°±1°C), as we discovered that this prolonged the life of the slices, and the recording temperature was closer to the mammal physiological state at 36°±1°C.

Following transfer to the recording chamber, neurons were visualized using a microscope (Zeiss axioscope) with a 40X objective (Zeiss Plan-APOCHROMAT). Electrophysiological data were acquired with the amplifier RK 400 BioLogic at full sampling frequency of 25 kHz using a 12-bit A/D-D/A converter (Digidata 1440A, Axon Instruments) and PClamp software (PClamp10, Axon Instruments). The studies used a continuous perfusion system attached the microscope chamber to continuously apply oxygenated ACSF to the slices. Both studies applied 1P blue light stimulation applied peaked at 470 nm (emission spectrum between 430-495 nm), performed using a Dual Port OptoLED (CAIRN, UK) dichroic mirror 495 nm at a power of 19 mW measured at the output of the x40 objective. The microscopy equipment and perfusion system are detailed in Figure M2.

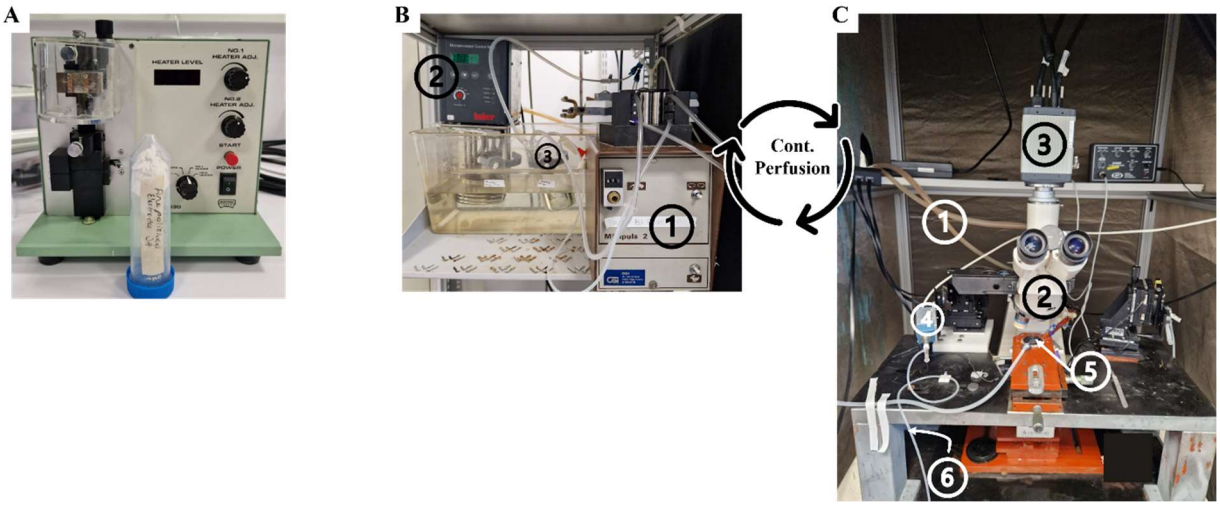

Figure M2. Laboratory equipment overview – Perfusion and Recording. A) Micro electrodes were prepared using firing polished cut pipette glass in a specialized machine. B) The perfusion system base consists of an adjustable fluid movement system (1). A heated, temperature-controlled bath (2) surrounds an oxygenated ACSF solution of a specified amount and inhibitory drug concentration (per protocol specifications) (3), which is fed through the system to continuously perfuse the tissue in the microscope recording chamber. C) the chamber is perfused via (1), and the slices/ cells are visualized with a camera attached to the microscope (2, 3). The pipette prepared in A is filled with either intracellular solution or ACSF (depending on the protocol) and attached to the moving electrode arm (4). The electrode can them be directed to the cell wall using the microscope imagery as a guide. Once the cell in the recording chamber (5) is touched, the researcher can use manual suction to patch the cell (6).

There were some slight differences in the microscopy, light stimulation, and recording equipment for the MSNs in study 1, as these cells were recorded in our co-authors' laboratory (see publication for details). In general, there were also differences in the rodent tissue preparations depending on the protocol—either coronal or horizontal slices. Study 1 used both slice types depending on the neuronal type that needed to be isolated. Study 2 used only coronal slices for mouse cortical tissue. Human tissues in study 2 were mounted to the vibratome in whatever way possible based on the tissue quality, and the orientation with respect to the human bodily planes was often difficult to determine (and thus is not reported). For the mouse cortical tissues, the dissection and mounting into the vibratome had to be performed differently depending on the desired slice orientation. These differences are detailed in Figure M3.

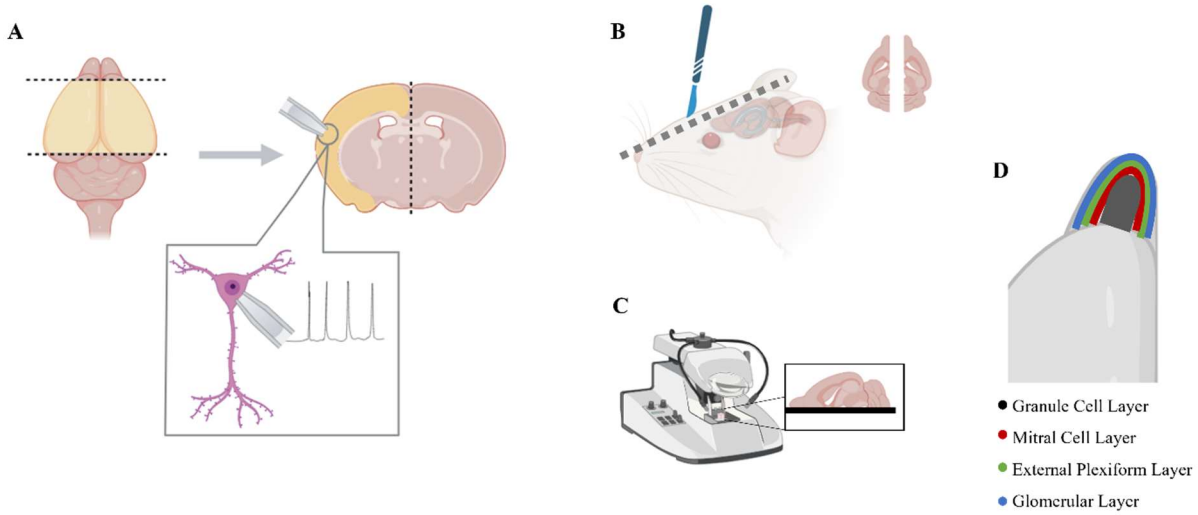

Figure M3. Preparation of mouse brain slices for studies 1 and 2. A) For all cell types except mitral cells, we used coronal slices. The olfactory bulb was removed, and the cortex was cut laterally at the level of the visual cortex to remove non-cortical structures (left). Coronal slices were cut in half to adjust their size for our recording chamber (right), where neurons were then isolated for single cell patch clam recording (bottom). B) When we needed to isolate MCs, the mice were dissected differently. The skull was bisected on the mid sagittal plane to isolate the two halves of the olfactory bulb. C) OB slices were placed cut-side-down in the vibratome to cut horizontal slices. D) The cutting of the horizontal slices allowed us to better visualize the mitral cell layer (red) to patch the MCs.

Finally, both study 1 and study 2 stimulated the patched neurons with blue light concomitant to electrical stimulation in current clamp and voltage clamp modes. The light parameters varied between the studies, with study 1 employing both varied light powers (1mW, 5mW, and 13mW), duty cycles, and total stimulation durations. Further, study 1 used both pulsed (discontinuous) and continuous light stimulation. Study 2 only used 5s continuous light stimulation at 19mW. The light stimulation protocols are introduced in the following pages as figures M4 (study 1 protocols) and figure M5(study 2 protocols). These will be the final methodological visualizations before the studies themselves, where you will find more specific reporting for the methodologies employed.

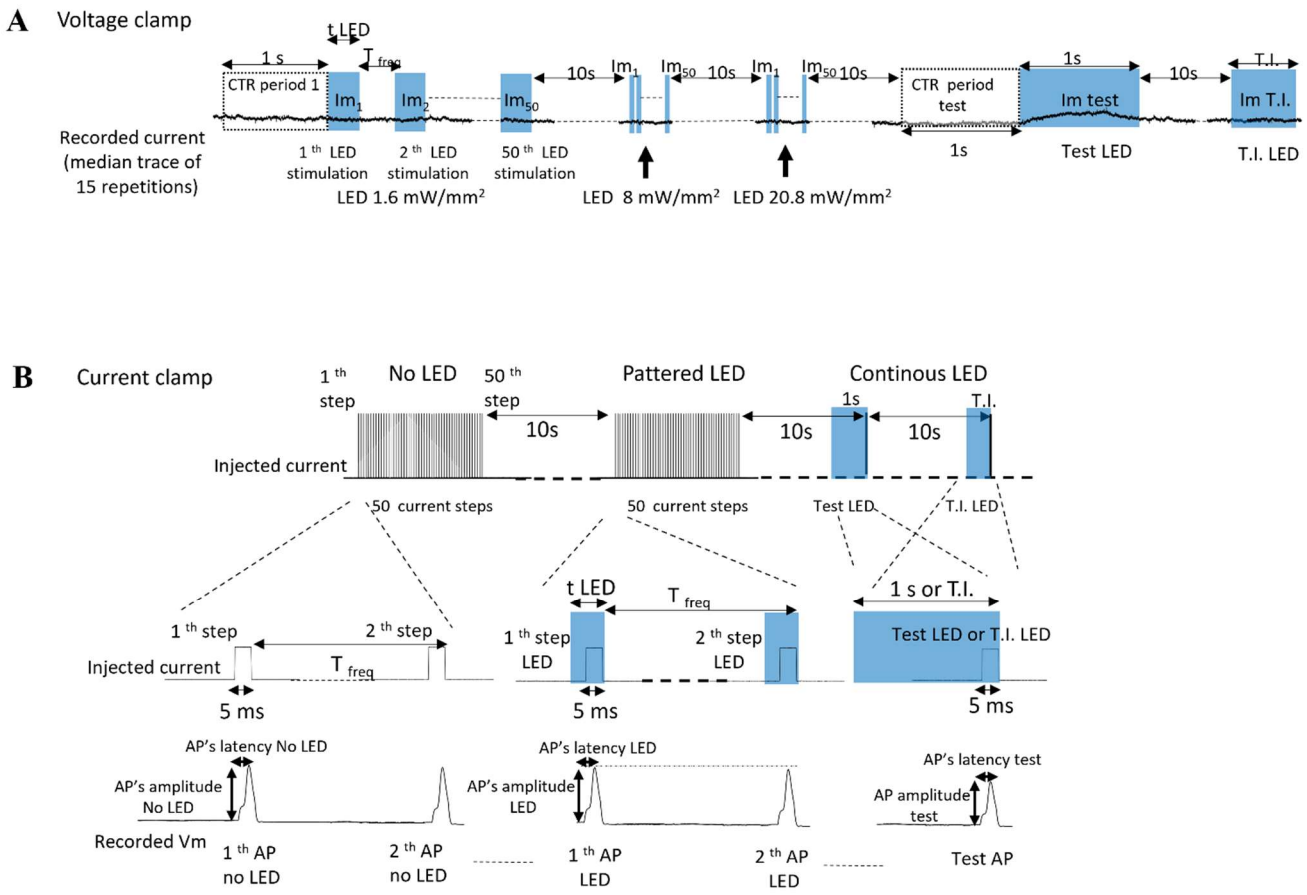

Figure M4. Overview of Light Stimulation Protocols –Study 1. A) Voltage Clamp Procedure. B) Current Clamp Procedure. See study 1 for more details.

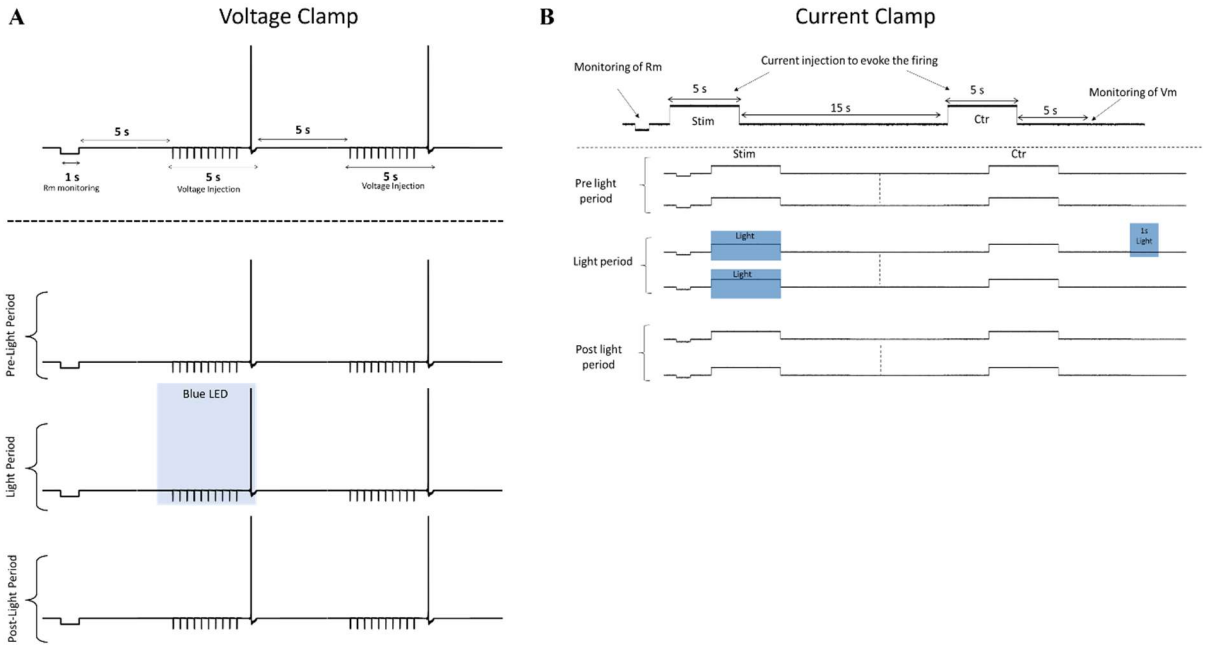

Figure M5. Overview of Light Stimulation Protocols –Study 2. A) Voltage Clamp Procedure. B) Current Clamp Procedure. See study 2 for more details.

STUDY 1

PUBLISED MANUSCRIPT

Lightning, A., Bourzeix, M., Beurrier, C., & Kuczewski, N. (2023). Effects of discontinuous blue light stimulation on the electrophysiological properties of neurons lacking opsin expression in vitro: Implications for optogenetic experiments. *European Journal of Neuroscience, 57*(6), 885–899. https://doi-org.docelec.univ-lyon1.fr/10.1111/ejn.15927

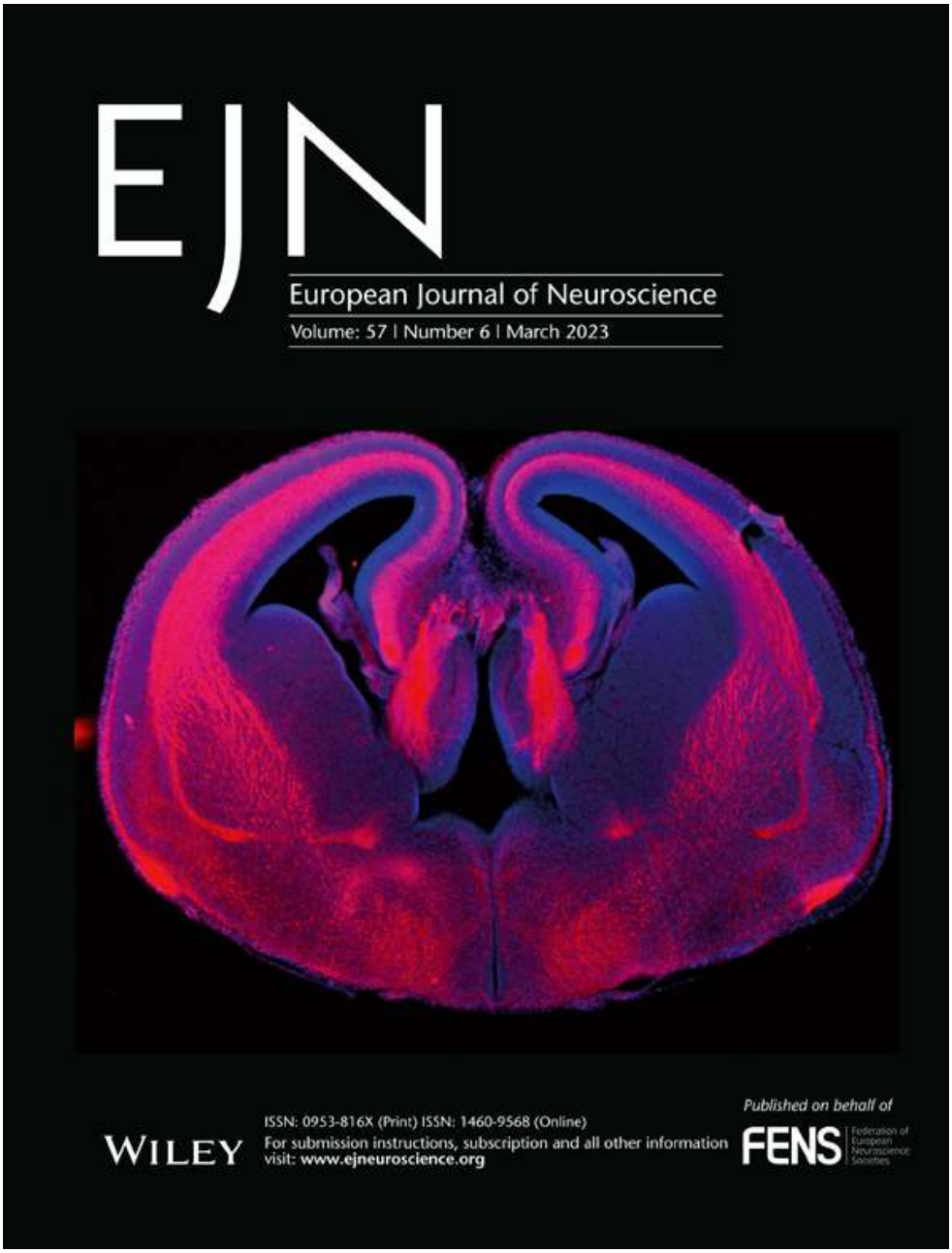

Received: 4 November 2022 | Revised: 5 January 2023 | Accepted: 26 January 2023

DOI: 10.1111/ejn.15927

REGISTERED REPORT STAGE 2

EJN European Journal of Neuroscience FENS WILEY

Effects of discontinuous blue light stimulation on the electrophysiological properties of neurons lacking opsin expression in vitro: Implications for optogenetic experiments

Anistasha Lightning[1] | **Marie Bourzeix**[2] | **Corinne Beurrier**[2] | **Nicola Kuczewski**[1]

[1]Université Claude Bernard Lyon 1, CNRS, INSERM, Centre de Recherche en Neurosciences de Lyon CRNL U1028UMR5292, NEUROPOP, Bron, France

[2]Aix Marseille Univ, CNRS UMR 7289, Institut de Neurosciences de la Timone (INT), Marseille, France

Correspondence
Nicola Kuczewski, Inserm U1028 - CNRS UMR5292 – UCBL, Centre Hospitalier Le Vinatier - Bâtiment 462 – Neurocampus, 95 boulevard Pinel, 69675 Bron Cedex, France.
Email: nicola.kuczewski@univ-lyon1.fr

Edited by: Antoine Adamantidis

Abstract

Neuronal sensitivity to light stimulation can be a significant confounding factor for assays that use light to study neuronal processes, such as optogenetics and fluorescent imaging. While continuous one-photon (1P) blue light stimulation has been shown to be responsible for a decrease in firing activity in several neuronal subtypes, discontinuous 1P blue light stimulation commonly used in optogenetic experiments is supposed to have a negligible action. In the present report, we tested experimentally this theoretical prediction by assessing the effects produced by the most commonly used patterns of discontinuous 1P light stimulation on several electrophysiological parameters in brain slices. We found that, compared with continuous stimulation, the artefactual effect of light is reduced when discontinuous stimulation is used, especially when the duty cycle and light power are low.

KEYWORDS
heat production, neurons, optogenetics, patch-clamp

1 | INTRODUCTION

The continuous wide-field 1P light stimulation of brain tissue has been shown to affect the electrophysiological properties of several neuronal subtypes, in vitro and in vivo, by producing a modification of firing rate associated with a hyperpolarizing outward current (Ait Ouares et al., 2019; Owen et al., 2019; Stujenske et al., 2015). The sensitivity of neurons to light can therefore represent a confounding factor for those assays that use light as a tool to investigate neuronal processes such as optogenetics and fluorescent imaging. Because the effect of light is primarily mediated by the increase in tissue temperature and discontinuous light has a weaker

Abbreviations: 1P, one photon; ACSF, artificial cerebrospinal fluid; AHP, afterhyperpolarization; AP/APs, action potential; CI, confidence interval; ES, effect size; FSI/FSIs, fast-spiking interneuron; FWHM, action potential full width at half maximum; GC/GCs, hippocampal granular cell (dentate gyrus); Kir, inwardly rectifying potassium channels; MC/MCs, mitral cell; MSN/MSNs, striatal medium-sized spiny neuron; NMDG, N-methyl D-glucamine; OB, olfactory bulb; PYR/PYRs, cortical pyramidal neuron; Rm, membrane resistance; T.I, total illumination time; Vm, membrane potential; Vrest, resting membrane potential.

Anistasha Lightning, Marie Bourzeix, and Corinne Beurrier contributed equally to the research and manuscript, and each retains the right to list themselves as first author on this publication.

heating action than continuous light, it can be assumed that the use of specific patterns of discontinuous 1P light stimulation is preferable to avoid non-specific effects. In particular, theoretical models (Stujenske et al., 2015) and experimental measurements (Senova et al., 2017) have demonstrated a decrease in light-induced heating concurrent with decreasing power, frequency and duty cycle of light stimulation. For example, 10 mW of discontinuous 1P light stimulation at 10 Hz with a duty cycle of 10% is responsible for a temperature increase equivalent to that produced by 1 mW of continuous light stimulation (Stujenske et al., 2015). As we previously showed that the latter protocol had no impact on neuronal activity (Ait Ouares et al., 2019), 10 mW of discontinuous light stimulation at 10 Hz should also be free of artefactual effect assuming that light effects are exclusively due to temperature increase. However, light has also been shown to be responsible for temperature independent effects (Ait Ouares et al., 2019; Tyssowski & Gray, 2019), including the activation of encephalopsins (Friedmann et al., 2015; Wang et al., 2019) or cytotoxic processes (Duke et al., 2020). It is therefore important that theoretical predictions about the "safety" of a specific pattern of optical stimulation be confirmed by empirical evidence. Based on a literature review using the PubMed query "Optogenetics," we selected 10 different patterns of discontinuous 1P light stimulation commonly used in optogenetic research and we tested their impact on several electrophysiological properties of mitral cells (MCs). More specifically, we analysed the effects of light on the generation of outward hyperpolarizing current as well as on the amplitude and latency of action potentials (APs) induced by short steps of positive current, as well as on neuronal firing produced by continuous depolarization. All these parameters were consistently modified by continuous light stimulation (Ait Ouares et al., 2019). We therefore tested whether 1P discontinuous blue light stimulation would be responsible for (1) the generation of an outward current, (2) a decrease in AP amplitude, (3) an increase in AP latency, and (4) a reduction in firing frequency. Finally, the pattern producing the most pronounced effects in MCs was also applied to cortical pyramidal neurons (PYRs) and fast-spiking interneurons (FSIs), in striatal medium-sized spiny neurons (MSNs) and in hippocampal granular cells of the dentate gyrus (GCs).

2 | METHODS

2.1 | Animals

Male C57Bl6/J mice (Charles River Laboratories, France) aged between 60 and 90 days were used. To identify FSIs, mice expressing the fluorescent tomato protein in parvalbumin neurons were generated by crossing B6;129P2-Pvalbtm1(cre)Arbr/J strain with B6.Cg-Gt (ROSA)26Sortm9(CAG-tdTomato)Hze/J strain from Jackson Laboratory.[1] All procedures were in accordance with European Union recommendations for animal experimentation (2010/63/UE). Mice were housed in groups of up to five in standard laboratory cages and were kept on a 12-h light/dark cycle (at a constant temperature of 22°C) with food and water ad libitum.

2.2 | Electrophysiology

2.2.1 | Protocols for slice preparation and recordings of olfactory bulb, hippocampal and cortical neurons

Mice were anaesthetized with an intra-peritoneal injection of ketamine (50 mg/mL) and decapitated. The head was quickly immersed in ice-cold (2–4°C) artificial cerebrospinal fluid (CutACSF) of the following composition: 125-mM NaCl, 4-mM KCl, 25-mM $NaHCO_3$, 0.5-mM $CaCl_2$, 1.25-mM NaH_2PO_4, 7-mM $MgCl_2$, and 5.5-mM glucose (pH = 7.4 oxygenated with 95% O2/5% CO_2). The osmolarity was adjusted to 320 mOsm with sucrose. Horizontal olfactory bulb (OB) slices (400 µm thick), cortical coronal slices (400 µm thick), and hippocampus coronal slices (350 µm thick) were prepared with a vibratome (Leica). Slices were then incubated in a recovery chamber at 30 ± 1°C using an ACSF solution with a composition similar to the Cut ACSF, except for changes to $CaCl_2$ and $MgCl_2$ concentrations (2 and 1 mM, respectively). Slices were transferred to a recording chamber mounted on an upright microscope and continuously perfused with oxygenated ACSF (4 mL/min) at 30 ± 1°C. Neurons were visualized using a microscope (Zeiss axioscope) with a 40× objective (Zeiss Plan-APOCHROMAT). Data were acquired with the amplifier RK 400 BioLogic at full sampling frequency of 25 kHz using a 12-bit A/D-D/A converter (Digidata 1440A, Axon Instruments) and PClamp software (PClamp10, Axon Instruments). Patch-clamp whole-cell recordings were achieved with borosilicate pipettes having a resistance 4–8 MΩ and filled with: 126-mM K-gluconate, 5-mM KCl, 10-mM HEPES, 1-mM EGTA, 1-mM $MgCl_2$, 2-mM ATP-Na2, 0.3-mM GTP-Na3, and 10-mM phosphocreatine

[1]The initial proposal planned to use wild type mice. The use of transgenic mice expressing tomato protein in parvalbumin neurons was introduced to identify the fast spiking interneurons in cortical slices. This changes in the protocol received editorial approval prior to data collection, on 9 February 2022.

(pH = 7.3, 290 mOsm). The membrane potential was corrected for the junction potential (−15 mV). All experiments were performed in the presence of ionotropic receptor antagonists (NBQX 10 μM, APV 40 μM, and gabazine 10 μM).

2.2.2 | Protocol for slice preparation and recordings of striatal neurons

Mice were deeply anaesthetized with ketamine/xylazine (100/10 mg/kg, i.p.) and transcardially perfused with an ice-cold N-methyl D-glucamine (NMDG)-based solution containing (in mM): 93 NMDG, 2.5 KCl, 1.2 NaH_2PO_4, 30 $NaHCO_3$, 20 HEPES, 20 glucose, 10 $MgCl_2$, 93 HCl, 2 Thiourea, 3 sodium pyruvate, 12 N-acetyl cysteine, and 0.5 $CaCl_2$ (saturated with 95% O_2 and 5% CO_2, pH 7.2–7.4). The brain was then removed from the skull and glued to the stage of a vibratome (Leica, VT1000S) where it remained submerged in ice-cold oxygenated NMDG-based solution. Coronal slices (250 μm thick) containing the striatum were collected. Slices were immediately transferred to recover in NMDG-based solution at 35°C for 5 min and then stored for at least 1 h at room temperature in normal artificial cerebrospinal fluid (ACSF) containing (in mM): 126 NaCl, 2.5 KCl, 1.2 $MgCl_2$, 1.2 NaH_2PO_4, 2.4 $CaCl_2$, 25 $NaHCO_3$ and 11 glucose, to which 250-μM kynurenic acid and 1-mM sodium pyruvate had been added. For the recordings, slices were transferred one at a time to a submersion-type chamber and perfused continuously with warm ACSF (32–34°C) at a rate of 3 mL/min. Solutions were continuously equilibrated with 95% O_2/5% CO_2. All experiments were performed in the presence of ionotropic receptor antagonists (NBQX 10 μM, APV 40 μM, and gabazine 10 μM). MSNs were visualized on an upright microscope (Nikon Eclipse FN1) equipped with DIC optic using an IR 40× water-immersion objective (Nikon). Patch-clamp electrodes (4–6 MΩ) were prepared from filamented borosilicate glass capillaries (PG150T-7.5, Harvard Apparatus) using a micropipette puller (PC-10, Narishige) and were filled with an intracellular solution containing (in mM): 126 KMeSO4, 14 KCl, 3 $MgCl_2$, 0.5 $CaCl_2$, 5 EGTA, 10 HEPES, 2 NaATP, and 0.5-mM NaGTP, 10 Na-Phosphocreatine, pH adjusted to 7.25 with NaOH and osmolarity adjusted to 270–280 mOsm/L. Recordings were obtained using motorized micromanipulators (MP-85, Sutter Instrument), a Multiclamp 700B amplifier, a Digidata 1550B digitizer, and pClamp 10.7 acquisition software (Molecular Devices, San Jose, CA, USA). Signals were low-pass filtered at 10 kHz online and sampled at 10 kHz. Electrode capacitances were compensated electronically during recording. In current-clamp mode, the bridge was continuously balanced and input resistances were monitored. Cells showing more than 20% input resistance variation were excluded from the analysis.

2.3 | Optical stimulation and fluorescence detection

The light stimulation applied in this study is a 1 photon visible blue light stimulation.

2.3.1 | Olfactory bulb, hippocampal and cortical experiments

1P blue light stimulation that peaked at 470 nm (emission spectrum between 430 and 495 nm) was performed using a Dual Port OptoLED (CAIRN, UK) dichroic mirror 495 nm at a power of 13, 5, or 1 mW measured at the output of the ×40 objective. Power loss at the working distance (2.5 mm from the objective), due to the presence of ACSF, was empirically estimated at 13%. The average power density in the tissue was estimated by dividing the power at the working distance by the empirically measured illumination area (~7 mm^2) which gives 1.61 mW/mm^2 for a output power of 13 mW, 0.62 mW/mm^2 for 5 mW and 0.12 mW/mm^2 for 1 mW. The excitation light for the detection of tomato expressed in cortical parvalbumin interneurons was produced by a white light LED (Dual Port OptoLED, CAIRN, UK) filtered at 545/25 nm and reflected on the sample by a dichroic mirror of 570 nm (Zeiss). The emission light was filtered at 605/70 nm (Zeiss filter). To avoid an effect of the light for tomato detection on neuronal activity, only short light pulses (<100 ms) at power <0.2 mW were used. The illumination frequency was lower than 0.5 Hz, the total time of green led illumination was lower than 2 s, and a minimum of 3 min was applied between green and blue light stimulation.

2.3.2 | Striatal experiments

1P light was delivered under the control of the acquisition software via the ×40 microscope objective lens using wide-field 475-nm LED illumination (Spectra Light Engine, Lumencor, Optoprim).

2.4 | Temperature measurement

Bath temperature in the recording chamber was measured and controlled by a ThermoClamp-1 device (Atomate Scientific).

TABLE 1 Description of the patterns of light stimulation that will be tested. Fifty stimuli will be delivered for each pattern. D. of S = duration of stimulation. T.I. = total illumination.

Duty cycle 5%	Duty cycle 10%	Duty cycle 20%	Duty cycle 40%
2 ms @ 10 Hz D. of S. = 5 s T.I. = 100 ms	20 ms @ 5 Hz D. of S. = 10 s T.I. = 1 s	20 ms @ 10 Hz D. of S. = 5 s T.I. = 1 s	20 ms @ 20 Hz D. of S. = 2.5 s T.I. = 1 s
X	10 ms @ 10 Hz D. of S. = 5 s T.I. = 500 ms	10 ms @20 Hz D. of S. = 2.5 s T.I. = 500 ms	10 ms @ 40 Hz D. of S. = 1.25 s T.I. = 500 ms
X	5 ms @ 20 Hz D. of S. = 2.5 s T.I. = 250 ms	5 ms @40 Hz D. of S. = 1.25 s T.I. = 250 ms	5 ms @ 80 Hz D. of S. = 0.625 s T.I. = 250 ms

2.5 | Experimental procedure

For MC recordings, light stimuli consisted of 50 pulses delivered according to one of the 10 different patterns showed in Table 1 ($N = 24$ MCs for each one of the different patterns). For experiments in MSNs, GCs, PYRs, and FSIs, only the pattern producing the maximal effect on MCs was tested (pattern 4, $N = 15$ for these neuronal types).

2.5.1 | Procedure 1: Determining the profile of temperature modification produced by light patterns

The thermal modifications produced by the different stimulation patterns were determined by placing the thermal probe on the surface of OB slices at the centre of the objective field. Each pattern was repeated 10 times (interstimulus time: 10 s) and the median normalized temperature trace was used to calculate the temporal profile of temperature variation for each pattern in each slice. This procedure was repeated on 10 different slices and the comparison between patterns was performed on the average trace (± 95% confidence interval).

The following experimental procedures 2, 3, and 4 were applied to each recorded neuron.

2.5.2 | Procedure 2: Calculation of the membrane resistance (*Rm*)

Cells were held at −60 mV in voltage-clamp mode. Ten steps to −65 mV (1 s duration @ 1 Hz) were generated and recorded on 15 separate electrophysiological traces and a median trace was calculated. The *Rm* was calculated on the median trace according to ohm's low $R = \Delta V/\Delta I$, where $\Delta V = -5$ mV and ΔI was the difference between the median current in the last 100 ms of the hyperpolarization and the median current in the 200-ms pre-step period. Access resistance A_R was calculated as $A_R = \Delta V/\Delta I_A$, where ΔI_A is the difference between the peak of transient current and the median current in the 200 ms pre-step period.

2.5.3 | Procedure 3: Determination of light effect on membrane currents

Cells were held at −60 mV in voltage-clamp mode. The stimulation pattern was repeated three time at 10-s intervals for the three powers (1, 5, and 13 mW). The discontinuous light patterns were followed, after 10 s, by 1 s of continuous light stimulation. Because 1-s stimulation was expected to produce a consistent outward current (Ait Ouares et al., 2019), the effect of continuous stimulation was used as positive control. In the protocols for which the total illumination time (T.I) during discontinuous stimulation was different than 1 s, a continuous T.I. light step was also applied. Fifteen electrophysiological traces were recorded for each neuron, these were aliened on the pre-light control period, and a median trace was calculated. The light effect was quantified on the median trace by subtracting, for each of the 50 light steps, the average membrane current in the 1 s preceding the application of light (the CTR period) from the average membrane current during light period. Only one of the 10 stimulation patterns was applied on each MC. Procedures 2 and 3 were performed on the same electrophysiological acquisition.

2.5.4 | Procedure 4: Determination of the light effect on AP amplitude and latency

Cells were recorded in current-clamp mode at their resting membrane potential. In cases where spontaneous firing was present, a hyperpolarization of the membrane

potential was produced by injecting negative current. Two consecutive trains of 50 APs, separated by 10 s, were generated with 5-ms depolarizing steps applied at the frequency of the light stimulation pattern chosen for that specific neuron. In half of the recorded neurons, the first train was generated in the absence of light and the second train generated during light stimulation, with the depolarizing steps concomitant to the last 5 ms of the illumination. In the other half of the neurons, light stimulation train preceded the no light train. After 10 s, a single depolarizing step (test step) was generated at the end of a 1 s continuous light stimulation. Because the latter procedure is expected to produce a consistent modification of AP amplitude and latency (Ait Ouares et al., 2019), the AP generated by the test step was used as positive control. In the protocols for which the total illumination time (T.I) during discontinuousstimulation was different from 1 s, one AP was also generated at the end of the continuous T.I. step. This protocol was repeated 10 times for each neuron. For each of the 10 acquired traces, the effect of light was assessed trough a step-by-step comparisons of AP in the absence and in the presence of light (i.e., first AP no LED vs. first AP LED, second AP no LED vs. second AP LED, ..., 50th AP no LED vs. 50th AP LED). The AP of the test step and T.I. step was compared with the first AP generated in the no LED condition. For each AP, the latency was quantified as the time of the AP peak relative to the beginning of the depolarizing step (Ait Ouares et al., 2019). AP amplitude was calculated as the difference between AP peak and the median membrane potential calculated in the 200-ms preceding the first depolarizing step. Steps presenting AP failures, or AP for which the time of AP peak exceeds the step duration, were excluded from the analysis. In half of the recorded neurons, the steps of current in the no-light condition preceded the steps of current in the light condition and vice versa for the other half of the neurons. The effect of light on each step was expressed as the average difference in AP amplitude and latency, between the light and no light conditions for that specific step. Only one out of the 10 stimulation patterns was applied on each MC.

2.5.5 | Procedure 5: Determination of the light effect on average firing frequency on MCs

The protocol was the same as that described in procedure 4 except that the current steps for AP induction were replaced by a long-lasting depolarization. The average firing frequency under light and no light condition was calculated during a 2.5-s current-induced depolarization ($N = 15$ MCs).

2.6 | Data analysis and statistics

Because the normality of the data was not known and normality tests have low statistical power for a sample size of 24 (Öztuna et al., 2006), nonparametric one-sample Wilcoxon signed rank test and one way Kruskal–Wallis test were used for the analysis. Type I error probability was kept at 5% by using Bonferroni–Holm method for correction of multiple comparisons (stats.multitest. multipletests function from Statsmodels module, Python, Holm method).

For each of the 10 patterns, the hypotheses tested were as follows:

Hypothesis 1. 1P discontinuous blue light stimulation is responsible for a decrease in AP amplitude.

Hypothesis 2. 1P discontinuous blue light stimulation is responsible for an increase in AP latency.

Hypothesis 3. 1P discontinuous blue light stimulation is responsible for the generation of an outward current.

Hypothesis 4. 1P discontinuous blue light stimulation is responsible for a decrease in the average firing frequency.

The sample sizes required to have a statistical power >90% were estimated based on the Cohen's *d* effect size observed in Ait Ouares et al. (2019) (ES = mean of light effect/standard deviation of light effect).

2.6.1 | Hypothesis 1 was tested as follows:

For each light pulse, the effect of light on AP amplitude was calculated as the difference in AP amplitude between the LED condition and the no LED condition (i.e., first AP amplitude LED − first AP amplitude no LED; ...; 50th AP amplitude LED − 50th AP amplitude no LED). For each MC, the median effect was calculated. This resulted in the median light effect for each of the 50 pulses (i.e., effect of light on the amplitude of the first AP; ...; effect of light on the amplitude of the 50th AP). The values calculated for all recorded cells were used for descriptive statistics by calculating the average population effect (±95% CI) as well as the Cohen's *d* ES (average of population effect/STD of population effect). Similar analyses were performed for the positive control (test LED) and the total continuous illumination exposure (T.I. LED), for which the effect was evaluated as: LED

AP amplitude – first AP amplitude no LED. In order to reduce the probability of Type I error produced by multiple comparisons correction, statistical tests were made only for three light pulses (the first, 25th, and 50th) by using a unilateral one-sample Wilcoxon signed rank test (tested hypothesis, median effect <0). The σ risk level was set at 0.05 and Bonferroni–Holm correction was applied. Experiments were conducted on 24 neurons for each pattern of light stimulation and cell type (336 neurons in total). This sample size was determined based on a previously published experiment on MCs where continuous light stimulation reduced AP amplitude with ES = −1.2 (Ait Ouares et al., 2019) and takes into account the Bonferroni–Holm correction for 30 statistical comparisons. As a consequence, the statistical power to observe an effect as small as that produced by 1-s continuous light stimulation is estimated between 98% et 99% depending on the level of correction (calculated with G*Power 3.1.9.2; Faul et al., 2007). The 24 MCs were recorded from 57 mice. The homogeneity of the effect produced by the "Test LED" between the groups was assessed by one-way Kruskal–Wallis test. Exploratory analysis was performed to evaluate a possible difference between the average AP amplitude (over the 50 depolarizing steps) in the presence and in the absence of discontinuous light stimulation.

2.6.2 | Hypothesis 2 was tested as follows:

The general procedure was the same as for testing the hypothesis one except that AP latency was measured instead of AP amplitude.

Exploratory analysis was performed to evaluate whether 1P discontinuous blue light stimulation modifies other parameters of the AP such as AHP amplitude and action potential full width at half maximum (FWHM).

2.6.3 | Hypothesis 3 was tested as follows:

Light effect on membrane current was calculated on the median trace of the 15 recorded traces. For each of the 50 light pulses, the effect of light on membrane current was calculated as the difference between the average membrane current in the 1 s preceding the beginning of discontinuous light (the CTR period) and the average membrane current during the light period. For each of the three powers used, this resulted in the median light effect for each of the 50 pulses (i.e., effect of the first light pulse; ...; effect of the 50th light pulse). The values calculated for all recorded neurons were used for descriptive statistics by calculating the average population effect ± 95% CI as well as the Cohen's *d* ES (average of population effect/STD of population effect). Similar analyses were performed for the positive control (Test LED) and the total continuous illumination (T.I. LED), for which the effect was evaluated as the difference between the average membrane current during light stimulation and the average membrane current in the respective CTR period. Statistical test was performed only for three light pulses (the first, 25th, and 50th) by using a unilateral one-sample Wilcoxon signed rank test (tested hypothesis, median effect >0). The σ risk was set at 0.05 and a Bonferroni–Holm correction was applied. The experiment weas conducted on 24 neurons for each pattern of light stimulation and cell type (240 neurons in total). This sample size was determined based on a previously published experiment showing an effect size (ES) of continuous light stimulation on MC membrane current equal to 1 (Ait Ouares et al., 2019) and takes in account the Bonferroni–Holm correction for 30 statistical comparisons. Therefore, the statistical power to observe an effect as small as that produced by 1-s continuous light stimulation is between 91% et 99%, depending on the level of correction (calculated with G*Power 3.1.9.2). The 24 MCs were recorded from 51 different mice (i.e., different patterns were applied on slices coming from the same animal). The homogeneity between the groups produced by the "Test LED" was assessed by a one-way Kruskal–Wallis test.

2.6.4 | Hypothesis 4 was tested as follows:

For each of the 10 repetitions on each recorded neuron, the effect of light on AP frequency was calculated as the difference between the firing frequency in the LED condition and the firing frequency in the no LED condition. For each neuron, the median effect of light was calculated. The values calculated for all recorded neurons were used for descriptive statistics by calculating the average population effect ± 95% CI as well as the Cohen's d ES (average of population effect/STD of population effect). Statistical tests were performed using unilateral one-sample Wilcoxon signed rank test (tested hypothesis, median effect <0). The σ risk level was set at 0.05. The experiment was conducted on 15 neurons. This sample size was determined based on a previously published experiment on MCs and MSNs, in which continuous light stimulation reduced firing frequency with an ES = −1 at −1.6, respectively (Ait Ouares et al., 2019). Therefore, the statistical power to observe an effect as small as that produced by 1-s continuous light stimulation was between 97% and 99% (calculated with G*Power 3.1.9.2).

See Table S1 for a summary of statistical analysis.

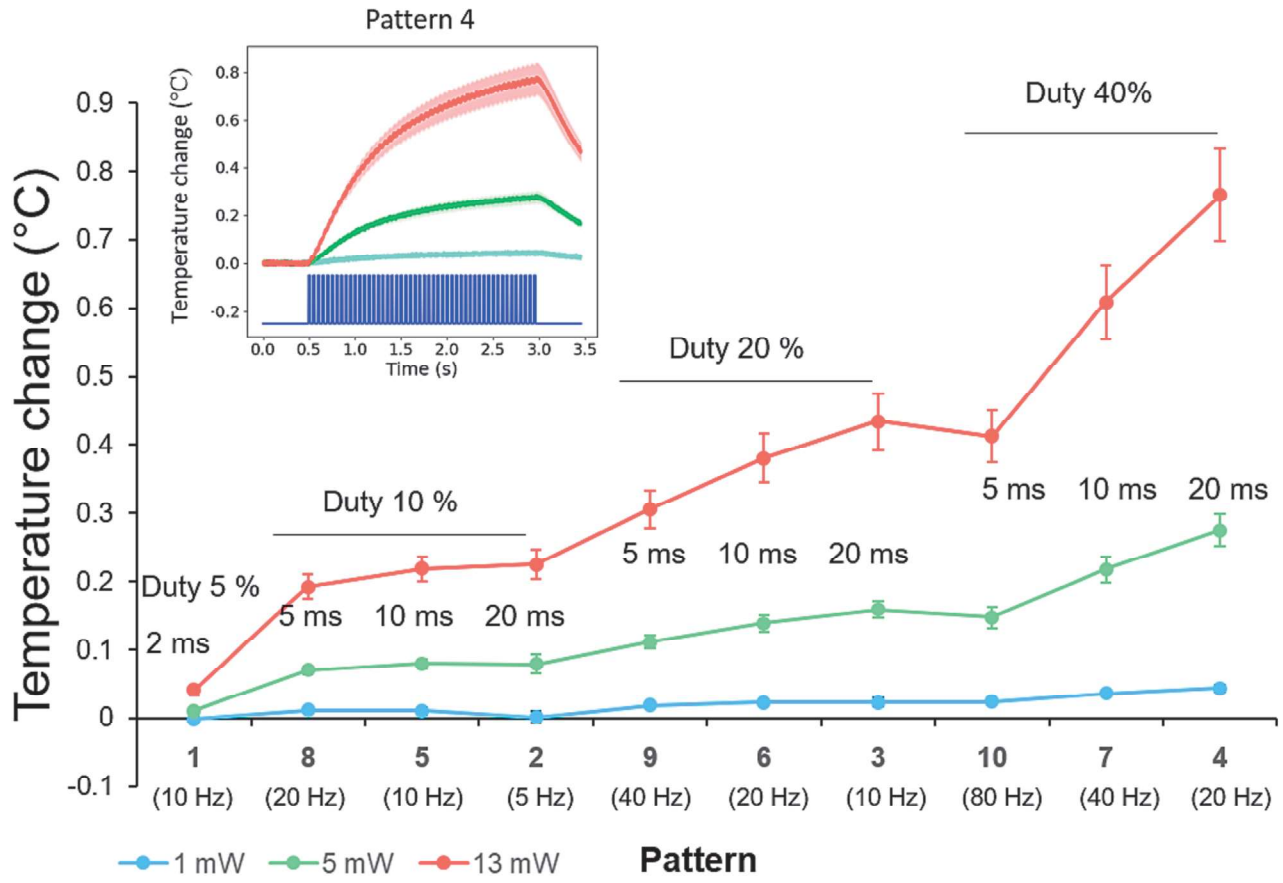

FIGURE 1 Discontinuous blue light produces warming of OB slices that increases with duty cycle and light pulse duration within each duty cycle. Data are ordered by duty cycle and light pulse duration. Vertical bars represent 95% CI. $N = 10$ slices. Inset: Temporal representation of the average temperature change produced by pattern 4. Blue bars on the bottom represent the light stimulation. Shadows on the traces represent 95% CI. Raw data and script for the analysis can be found here: https://osf.io/he9sw/ (data) https://osf.io/j295t/ (script).

The results obtained from procedure 1 were used for exclusion criteria based on Rm (see later) as well as for exploratory analysis aimed at correlating the eventual effect of light stimulation with Rm.

Analyses were performed with custom scripts (Python 3.7).

2.7 | Data sharing

All raw electrophysiological traces, scripts for the analysis, and raw data are accessible via the Open Science Framework website (https://osf.io/fe6t3/).

2.8 | Exclusion criteria

Cells were excluded from experiments when (i) their resting membrane potential (Vrest) was above −50 mV, (ii) the membrane resistance was higher than 1000 MΩ, and (iii) no AP could be elicited in the no light condition. Traces were excluded from the analysis when (i) the starting Vm (calculated in the 100 ms preceding the depolarizing current step) in the no light condition differed by more than 5 mV from the starting Vm in the light condition, (ii) there was an instability in membrane potential, and (iii) a degradation of neuronal whole-cell recording (depolarization of resting potential >10 mV, AP overshot below 0 mV, or access resistance >60 mΩ[2]).

3 | RESULTS

3.1 | Tissue temperature increases with light duty cycle and pulse duration during 1P discontinuous light stimulation (procedure 1)

We first evaluated the modification of tissue temperature when 50 blue light pulses were delivered to OB slices

[2]Revised from initial proposal of access resistance > 40 mΩ, after editorial approval on 13 Sept 2021. Analysis using 40 mΩ criteria lead to qualitatively similar results that are available at https://osf.io/amvkq.

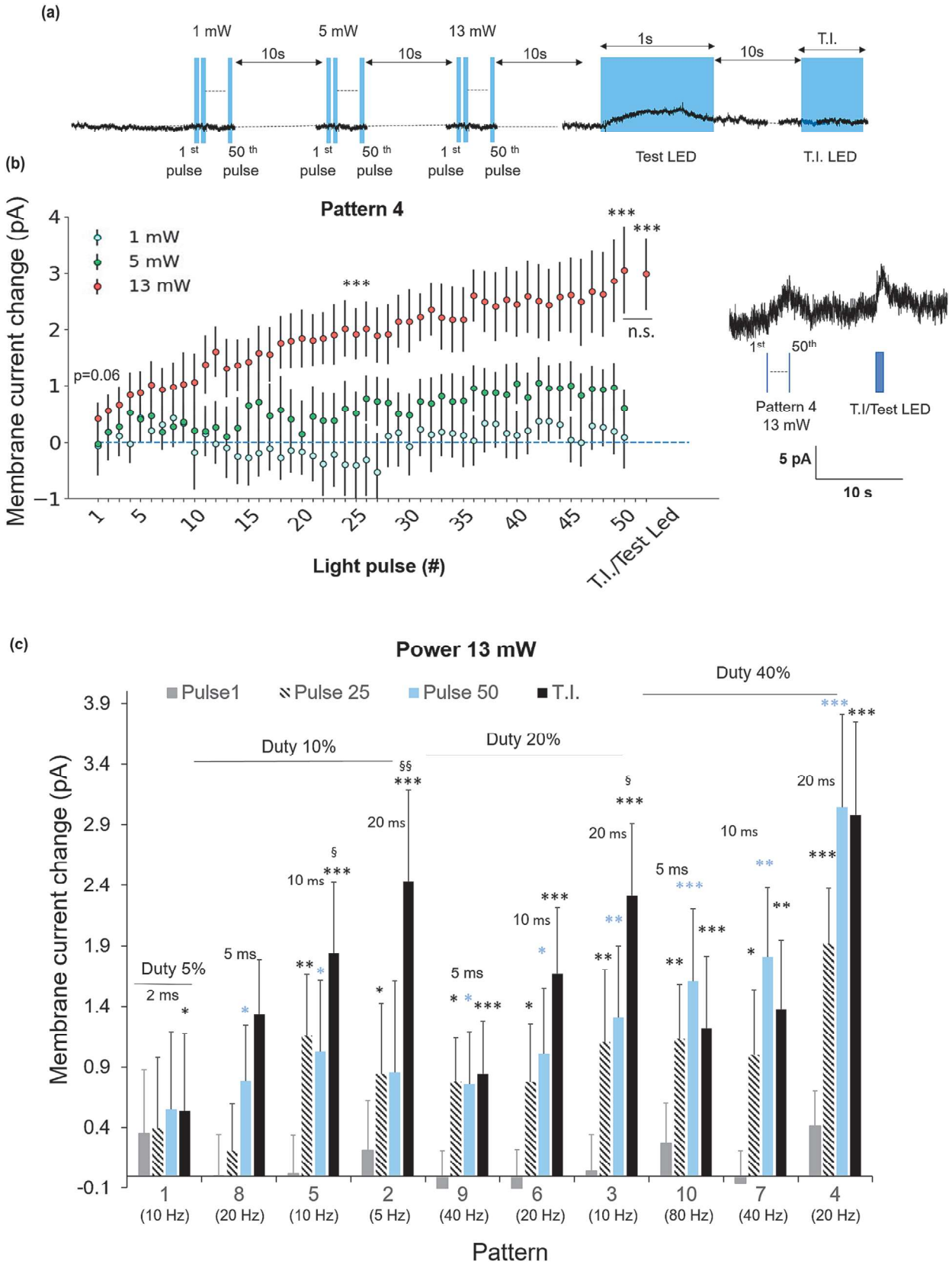

FIGURE 2 Legend on next page.

FIGURE 2 High power discontinuous blue light produces an outward current in MCs that increases with duty cycle. (a) Protocol used to assess the effect of patterned light on membrane current. (b, left) Quantification of the evolution of the light-induced current throughout the 50 steps for pattern 4. Statistical comparisons were performed for pulses 1, 25, and 50 and for T.I. LED; vertical bars represent 95% CI. (b, right) Representative trace showing the development of an outward current during light stimulation. (c) Quantification of the average currents produced by the first, 25th, and 50th pulse and T.I. LED for the 10 different patterns when light power is set to 13 mW. Pulse duration is indicated above each pattern. The frequency of light pulses is depicted below each pattern. The data are ordered by duty cycle and light pulse duration. Error bars represent 95% CI. * = $p < 0.05$,** = $p < 0.01$,*** = $p < 0.001$ compared with the control (ctr) period. § = $p < 0.05$, §§ = $p < 0.01$ compared with pulse 50. Raw data and script for the analysis can be found here: https://osf.io/hjxtg, https://osf.io/e6brs (data); https://osf.io/j295t/ (script).

following the stimulation patterns described in Table 1. The temperature of the tissue gradually increased over the 50 pulses for all patterns (Figure 1, inset). The higher the power, the duty cycle, and pulse duration, the more pronounced the temperature increase (Figure 1). Interestingly, temperature change did not appear to be correlated with the frequency of the stimulation within each duty cycle. At 13 mW, most of the patterns induced a temperature increase that overcame 0.1°C, a thermal condition that has been previously associated with modifications in neuronal activity (Ait Ouares et al., 2019; Owen et al., 2019).

3.2 | Discontinuous 1P blue light stimulation produces an outward current in MCs (procedure 3)

The effect produced by the 10 different patterns on MC membrane current was studied using the protocol depicted in Figure 2a. Whatever the pattern, light intensities of 1 mW had no effect, while for 5 mW, the light tended to produce an outward current that did not reach statistical significance (Figure 2b and Figures S1 and S2). This lack of effect appears mainly to result from the low statistical power produced by the correction for multiple comparisons (see p values before correction https://osf.io/e6brs). Moreover, the exploratory analysis performed by calculating the average effect produced over all 50 light pulses produced a small but significant outward current for all patterns (Table S2). When the light power was set at 13 mW, the light induced an outward current that tended to increase with pulse repetition (Figures 2b,c and S1). A significant effect was consistently observed at the 50th pulse for most of the patterns (Figure 2c). Similar to the effects of light on tissue temperature, the amplitude of the light-induced outward current increased with duty cycle. The effect of the pulse duration was less pronounced (Figure 2c). The difference between patterns cannot be attributed to sample variability because the effect produced by the test LED was the same for all patterns (Figure S1, Kruskal–Wallis test, $H = 0.79$, $p = 0.612$). For patterns with a high duty cycle, the effect produced by the continuous stimulation (TI LED) was not different from the effect produced by discontinuous light. However, for lower duty cycles, discontinuous stimulation produced a lower effect than continuous ones (Figure 2c). Interestingly, exploratory analysis showed a covariation between the effect produced by each pattern on tissue temperature and the generation of outward current (Figure 4a). These results suggest a causal link between the light effect on MC electrophysiological properties and the light-induced modification of tissue temperature, supporting previous findings (Ait Ouares et al., 2019; Owen et al., 2019).

3.3 | Discontinuous 1P blue light stimulation reduces AP amplitude without affecting AP latency in MCs (procedure 4)

The effect produced by the different patterns on AP properties was studied using the protocol depicted Figure 3a. Most of the recorded neurons were previously submitted to the voltage-clamp protocol shown in Figure 2a. Light stimulation induced a reduction in AP amplitude that reached a significant effect only for patterns 3, 4, 6, 7, and 8 (Figures 3b,c and S3). The lack of statistical significance of the other patterns is likely due to the low statistical power that follows the Bonferroni–Holm correction. Indeed, with the exception of pattern 1, all patterns had a p value lower than the α risk (0.05) before the correction (see https://osf.io/9z654/), a situation that has an extremely low probability of being due to the repetition of a type I error. Moreover, exploratory analyses for which the effect was assessed on all 50 APs showed a significant decrease in AP amplitude for all tested patterns (Table S3). Again, the light effect was higher for patterns that have a longer duty cycle. However, the covariation between the duty cycle and the AP amplitude reduction was less pronounced than the covariation between the duty cycle and the light-induced outward current shown in Figure 2. In addition, no clear relationship emerged between step duration and AP

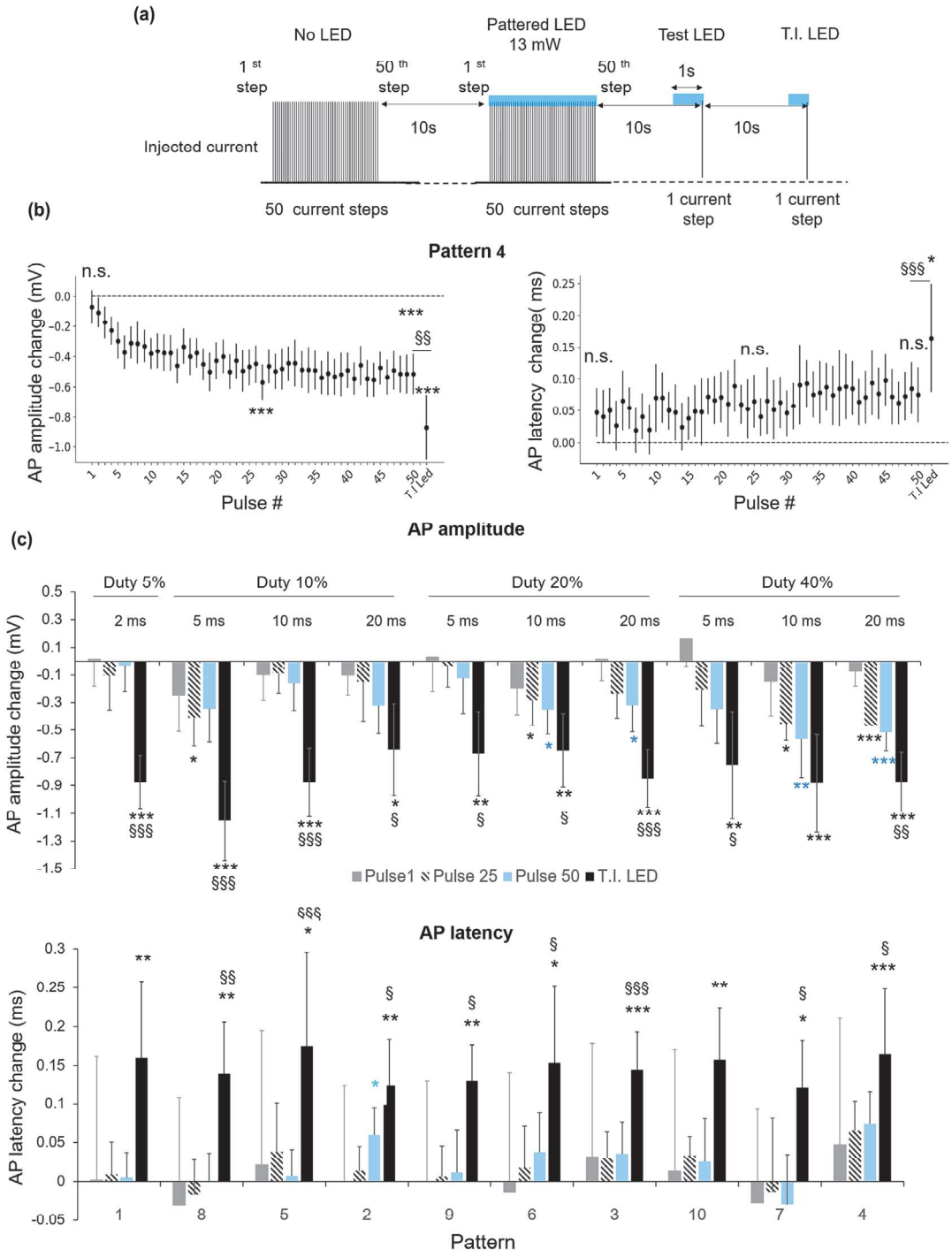

FIGURE 3 Discontinuous blue light reduces AP amplitude but has a negligible effect on AP latency in MCs. (a) Protocol used to assess the effect of patterned light on AP. (b) Quantification of the light-induced modification of AP amplitude (left) and latency (right) along the 50 steps. Average effect produced on 24 MCs by pattern 4. Statistical comparisons were performed for pulses 1, 25, and 50 and for T.I. LED; vertical bars represent 95% CI. (c) Average modification of AP amplitude (top) and latency (bottom) produced by the first, 25th, 50th light pulse and T.I.LED for the 10 different patterns. Light pulse duration is indicated above each pattern. The data are ordered by duty cycle and light pulse duration. Error bars represent 95% CI. * = $p < 0.05$,** = $p < 0.01$,*** = $p < 0.001$ compared with ctr period. § = $p < 0.05$, §§ = $p < 0.01$ compared with pulse 50. Raw data and script for the analysis can be found here: https://osf.io/6hbex, https://osf.io/9z654 (data); https://osf.io/j295t/ (script).

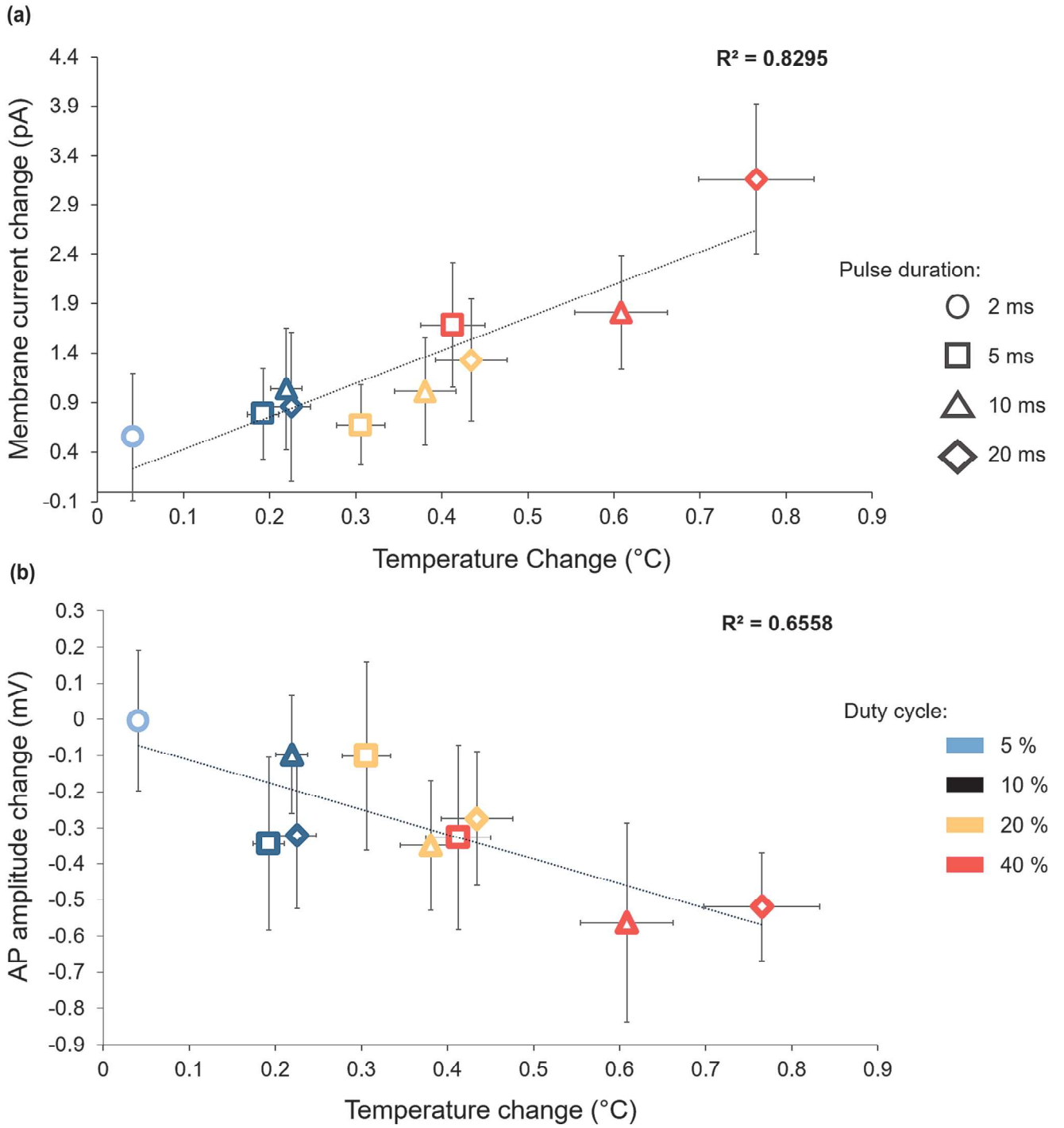

FIGURE 4 The outward current (a) and the reduction in AP amplitude (b) are correlated with the light-induced increase in tissue temperature. Error bars represent 95% CI. Temperature data from Figure 1. Current data from Figure 2 and AP data from Figure 3.

amplitude reduction. The effect of light on AP amplitude had a moderate covariation with the tissue temperature increase produced by the different patterns (Figure 4b). light did not alter AP latency (Figure 3c, bottom, and Figure S4). We further performed exploratory analysis to look for other eventual modifications produced by light on other AP parameters. In particular, we looked at the full width at half maximum (FWHM) and at the AHP amplitude. Both of these parameters were reduced by discontinuous stimulation (Table S3). To test whether light also alters APs during more physiological stimuli, we induced neuronal firing with longer pulses of current (2.5 s). We used only the pattern and power that produced the largest overall effect in previous tests (pattern

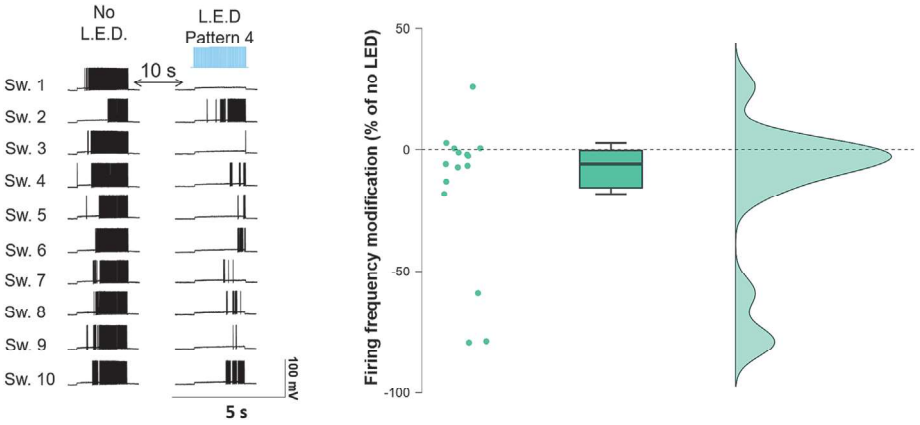

FIGURE 5 Discontinuous blue light stimulation reduces AP firing in some MCs. Left, example of a cell whose discharge frequency is strongly reduced by light. The experimental procedure was iterated 10 times for each MC (Sw: sweep). Right, quantification of the average AP frequency modification produced by patterned stimulation on 15 MCs illustrated by a Raincloud plot (probability of density distribution, boxplot and average frequency modification of individual MC, Jasp software). Raw data can be found here: https://osf.io/x48us.

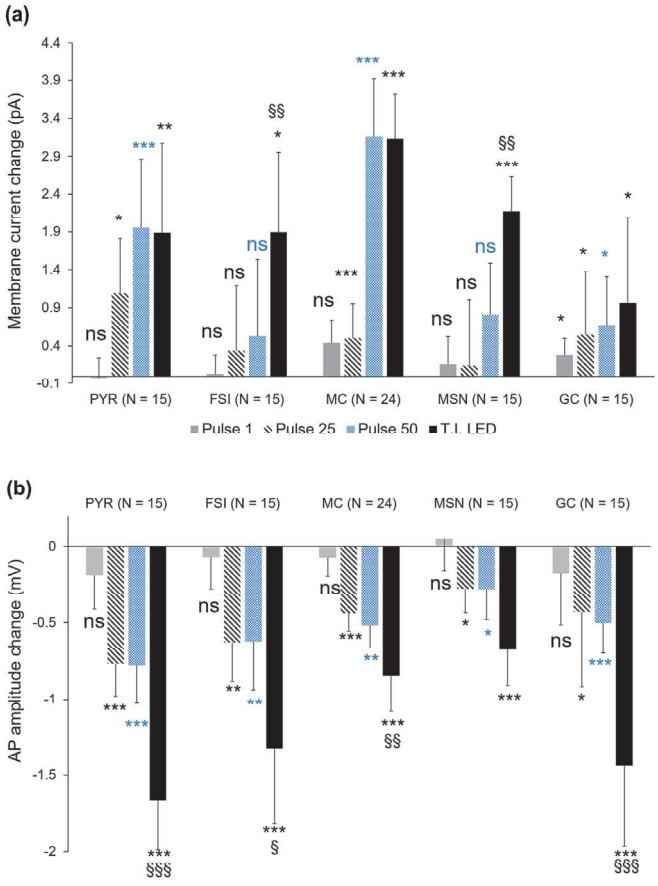

FIGURE 6 Discontinuous blue light stimulation induces an outward current and reduces AP amplitude in most of the neuronal types tested. Quantification of the average currents (a) and change in AP amplitude (b) induced by light stimulation at the first, 25th, and 50th pulse and T.I.LED by pattern 4 at 13 mW. Error bars represent 95% CI. * = $p < 0.05$, ** = $p < 0.01$, *** = $p < 0.001$ compared with ctr period. § = $p < 0.05$, §§ = $p < 0.01$ compared with pulse 50. Raw data and script for the analysis can be found here: https://osf.io/akh4j/ (data); https://osf.io/j295t/ (script).

4 at 13 mW). As shown in Figure 5, light stimulation had a heterogeneous action on MC population. The firing activity was mildly reduced or unaffected in around 80% of the recorded neurons and strongly reduced in the remaining cells. The average frequency modification was -16 ± 30 Hz ($N = 15$, $p = 0.013$).

3.3.1 | Effect of discontinuous 1P blue light stimulation on other neuronal types (procedures 3 and 4)

We next determined whether discontinuous light stimulation also affects the activity of GCs, PYRs, FSIs, and MSNs by using the pattern that produced the largest effect on MCs (pattern 4 at 13-mW power). While continuous light stimulation induced an outward current in all cell types (Ait Ouares et al., 2019), discontinuous stimulation had this effect only in PYRs, GCs, and MC (Figure 6a). Interestingly, in one of the recorded GC, we observed a clear inward current upon light stimulation (Figure S6). Discontinuous light reduced AP amplitude in all neuronal types, but this effect was less pronounced than that produced by continuous stimulation (Figure 6b). Similar to our observation for MCs, we did not find any effect of discontinuous light on AP latency (Figure S7).

4 | DISCUSSION

The main conclusion of this study is that a significant number of discontinuous light stimulation patterns, commonly used in optogenetic experiments, can affect

neuronal electrophysiological activity. However, their impact is, in general, smaller than that produced by continuous light stimulation. It also highlights how the different parameters of the stimulation impact the light action, providing several guidelines to minimize the artefactual effects associated with the use of light in neuroscientific investigations. Indeed, a bibliographic analysis done on the first 50 discontinuous patterns retrieved when using the query "Optogenetics" on PubMed showed that the light parameters investigated here are among the most commonly used in optogenetic experiments (https://osf.io/anvsj). We used the change in AP amplitude and latency and the generation of an outward current as a read-out for light action, all of which were modified by continuous light stimulation (Ait Ouares et al., 2019). We found that discontinuous light consistently reduced AP amplitude without significantly altering AP latency in all cell types and produced an outward current only in MCs, PYRs and GCs. The lack of statistical significance on AP latency is likely related to the low statistical power of the pre-registered analytical method, because exploratory analysis shown in Table S3 suggest that AP latency does indeed slightly increase during discontinuous light stimulation. The effects of light on membrane current and AP amplitude are small, with a change of only a few pA for membrane current and a ~0.5 mV reduction in AP amplitude for the pattern with the highest effect. However, even small variations in AP amplitude can consistently modify synaptic transmission (Rama et al., 2015). Moreover, we showed that the small modification of these two parameters is associated with a strong reduction in firing frequency for a subpopulation of MCs when neurons where depolarized to a membrane potential that allow spontaneous activity. A possible reason for the heterogeneity of this effect might be explained by a diversity of biophysical properties among MCs (Fourcaud-Trocmé et al., 2022; Padmanabhan & Urban, 2010). However, the effects of discontinuous light were in general lower than those produced by continuous stimulation, suggesting that discontinuous stimulation can reduce the artefactual effect of light. Both the induction of the outward current and the reduction in AP amplitude induced by discontinuous light occur rapidly after few pulses and quickly reach a plateau. Therefore, reducing the number of stimuli does not appear to be an optimal strategy to reduce the artefactual effect of light. On the other hand, the light effect can be attenuated by reducing the stimulation power, the duty cycle and, in some cases, the pulse duration. Note that varying the frequency of the light stimulation does not change the artefactual effects as long as the duty cycle is the same. This is particularly important for experiments whose goal is to induce high frequency firing by optogenetic stimulation. As a rule, we recommend adapting the pulse duration to the stimulation frequency in order to keep the duty cycle at or below 5%. Using a light power of 1 mW or less also appears to be an effective means of preventing unspecific effects during discontinuous stimulation compared with the higher powers, which induce an outward current (see Table S1). The reduction in AP amplitude induced by pattern 4 is observed in all cell types, whereas an outward current is induced only in FSIs and MSNs, suggesting a cell-specific effect of light. The greater reduction in the discharge frequency of FSIs induced by light compared with pyramidal neurons (Owen et al., 2019) also suggests a differential effect of light across cell types. However, we did not observe such a difference here where all experiments were done in the presence of ionotropic glutamatergic receptor antagonists. Because light appears to reduce glutamatergic synaptic transmission (Ait Ouares et al., 2019), the pronounced decrease in FSI firing observed by Owen et al. (2019) may be related to a reduction in their excitatory inputs. However, we cannot rule out the possibility that the weaker effect observed here is due to the presence of the tomato fluorescent protein in the recorded FSI. The covariation between the change in tissue temperature and the effect of light suggests a causal relationship between the two factors, as previously reported (Ait Ouares et al., 2019; Owen et al., 2019; Senova et al., 2017; Stujenske et al., 2015). The light-induced temperature changes observed in this study (between 0.1°C and 0.8°C) remain below the threshold for tissue damage but may modulate a set of voltage-dependent channels involved in neuronal discharge (Ait Ouares et al., 2019; Podgorski & Ranganathan, 2016). Our results suggest that light is able to modulate different type of K^+ channels beside the inwardly rectifying potassium channels (Kir) (Owen et al., 2019). For instance, the reduction in AP duration suggests an increase in Kv conductance's responsible for AP repolarization (Bean, 2007) while the reduction in AHP amplitude suggests an impact of light on the calcium- and voltage-dependent potassium channels (Sah & Faber, 2002). The light-induced reduction in AHP amplitude after a single AP contrasts with the increase in AHP measured at the end of a long depolarization that we observed previously (Ait Ouares et al., 2019). This result suggests that light may oppositely modulate the K^+ channels involved in the fast-medium and slow AHP. However, because the AHP in MCs is modulated by recurrent glutamatergic transmission (Duménieu et al., 2015), we cannot rule out that the light-induced reduction in AHP amplitude is partially due to the presence of ionotropic glutamatergic receptor antagonists. Finally, because AP initiation in MCs is promoted by hyperpolarizing events (Fourcaud-Trocmé et al., 2022), the light-induced decrease in AHP could also

contribute to the reduction of the firing frequency of these cells. Previous reports have shown that continuous 1P light stimulation produces similar inhibition of neuronal firing, regardless of the wavelength used (Ait Ouares et al., 2019; Owen et al., 2019). Therefore, we believe that our conclusions can be generalized to others wavelengths in the visible spectrum. The increase of tissue temperature produced by continuous 1P green light stimulation (3 and 15 mW) can yield to a decrease of firing activity in vivo that is sufficient to impact animal behaviour (Owen et al., 2019). Interestingly, as in our in vitro experiments, the heating effect induced by discontinuous 1P light stimulation in vivo decreases with low light power and low duty cycle (Senova et al., 2017), suggesting that acting on these two parameters could be an efficient strategy to reduce the artefactual effects produced by 1P light stimulation in vivo.

5 | CONCLUSIONS

Prevention of off-target effects during optogenetic stimulation is fundamental for reducing misinterpretation of experimental results. The use of discontinuous light at low power levels and/or duty cycle can achieve this goal. However, such conditions could reduce the efficiency of optogenetic protocols in neurons expressing first-generation opsins, a limitation that can be overcome by using new-generation large-conductance opsins such as ChRmine or ChroME (Marshel et al., 2019; Sridharan et al., 2022).

AUTHOR CONTRIBUTION

Anistasha Lightning: performed the experiments on cortical and hippocampal neurons, made the analysis and participated in the writing of the manuscript. Marie Bourzeix: performed the experiments on striatal neurons and participated in the writing of the manuscript. Corinne Beurrier: performed the experiments on striatal neurons and wrote the manuscript. Nicola Kuczewski: conceptualized and supervised the work, performed the experiment on MCs, made the script for the analysis and wrote the manuscript.

ACKNOWLEDGEMENTS

This work was supported by the Université Claude Bernard (Lyon 1), the CNRS and the INSERM.

CONFLICT OF INTEREST

The authors declare no conflicting financial or other interests.

DATA AVAILABILITY STATEMENT

All raw electrophysiological traces, scripts for the analysis, and raw data are accessible via the Open Science Framework website (https://osf.io/fe6t3/).

ORCID

Nicola Kuczewski https://orcid.org/0000-0003-1615-6344

PEER REVIEW

The peer review history for this article is available at https://publons.com/publon/10.1111/ejn.15927.

REFERENCES

Ait Ouares, K., Beurrier, C., Canepari, M., Laverne, G., & Kuczewski, N. (2019). Opto nongenetics inhibition of neuronal firing. *The European Journal of Neuroscience*, *49*, 6–26. https://doi.org/10.1111/ejn.14251

Bean, B. P. (2007). The action potential in mammalian central neurons. *Nature Reviews Neuroscience*, *8*, 451–465.

Duke, C. G., Savell, K. E., Tuscher, J. J., Phillips, R. A., & Day, J. J. (2020). Blue light-induced gene expression alterations in cultured neurons are the result of phototoxic interactions with neuronal culture media. *eNeuro*, *7*(1), ENEURO.0386-19.2019. https://doi.org/10.1523/ENEURO.0386-19.2019

Duménieu, M., Fourcaud-Trocmé, N., Garcia, S., & Kuczewski, N. (2015). Afterhyperpolarization (AHP) regulates the frequency and timing of action potentials in the mitral cells of the olfactory bulb: Role of olfactory experience. *Physiological Reports*, *3*(5), e12344. https://doi.org/10.14814/phy2.12344

Faul, F., Erdfelder, E., Lang, A.-G., & Buchner, A. (2007). G*Power 3: A flexible statistical power analysis program for the social, behavioral, and biomedical sciences. *Behavior Research Methods*, *39*, 175–191. https://doi.org/10.3758/BF03193146

Fourcaud-Trocmé, N., Zbili, M., Duchamp-Viret, P., & Kuczewski, N. (2022). After-hyperpolarization promotes the firing of mitral cells through a voltage dependent modification of action potential threshold. *eNeuro*, *9*(2), ENEURO.0401-21.2021. https://doi.org/10.1523/ENEURO.0401-21.2021

Friedmann, D., Hoagland, A., Berlin, S., & Isacoff, E. Y. (2015). A spinal opsin controls early neural activity and drives a behavioral light response. *Current Biology*, *25*(1), 69–74. https://doi.org/10.1016/j.cub.2014.10.055

Marshel, J. H., Kim, Y. S., Machado, T. A., Quirin, S., Benson, B., Kadmon, J., Raja, C., Chibukhchyan, A., Ramakrishnan, C., Inoue, M., Shane, J. C., McKnight, D. J., Yoshizawa, S., Kato, H. E., Ganguli, S., & Deisseroth, K. (2019). Cortical layer-specific critical dynamics triggering perception. *Science*, *365*, eaaw5202. https://doi.org/10.1126/science.aaw5202

Owen, S. F., Liu, M. H., & Kreitzer, A. C. (2019). Thermal constraints on in vivo optogenetic manipulations. *Nature Neuroscience*, *22*, 1061–1065. https://doi.org/10.1038/s41593-019-0422-3

Öztuna, D., Elhan, A. H., & Tüccar, E. (2006). Investigation of four different normality tests in terms of type 1 error rate and power under different distributions. *Turkish Journal of Medical Sciences*, *36*(1), 171–176.

Padmanabhan, K., & Urban, N. N. (2010). Intrinsic biophysical diversity decorrelates neuronal firing while increasing information content. *Nature Neuroscience*, *13*, 1276–1282. https://doi.org/10.1038/nn.2630

Podgorski, K., & Ranganathan, G. (2016). Brain heating induced by near-infrared lasers during multiphoton microscopy. *Journal of Neurophysiology*, *116*, 1012–1023. https://doi.org/10.1152/jn.00275.2016

Rama, S., Zbili, M., Bialowas, A., Fronzaroli-Molinieres, L., Ankri, N., Carlier, E., Marra, V., & Debanne, D. (2015). Presynaptic hyperpolarization induces a fast analogue modulation of spike-evoked transmission mediated by axonal sodium channels. *Nature Communications*, *6*, 10163. https://doi.org/10.1038/ncomms10163

Sah, P., & Faber, E. S. L. (2002). Channels underlying neuronal calcium-activated potassium currents. *Progress in Neurobiology*, *66*(5), 345–353. https://doi.org/10.1016/S0301-0082(02)00004-7

Senova, S., Scisniak, I., Chiang, C.-C., Doignon, I., Palfi, S., Chaillet, A., Martin, C., & Pain, F. (2017). Experimental assessment of the safety and potential efficacy of high irradiance photostimulation of brain tissues. *Scientific Reports*, *7*, 43997. https://doi.org/10.1038/srep43997

Sridharan, S., Gajowa, M. A., Ogando, M. B., Jagadisan, U. K., Abdeladim, L., Sadahiro, M., Bounds, H. A., Hendricks, W. D., Turney, T. S., Tayler, I., Gopakumar, K., Oldenburg, I. A., Brohawn, S. G., & Adesnik, H. (2022). High-performance microbial opsins for spatially and temporally precise perturbations of large neuronal networks. *Neuron*, *110*, 1139–1155. https://doi.org/10.1016/j.neuron.2022.01.008

Stujenske, J. M., Spellman, T., & Gordon, J. A. (2015). Modeling the spatiotemporal dynamics of light and heat propagation for in vivo optogenetics. *Cell Reports*, *12*, 525–534. https://doi.org/10.1016/j.celrep.2015.06.036

Tyssowski, K. M., & Gray, J. M. (2019). Blue light increases neuronal-activity-regulated gene expression in the absence of optogenetic proteins. *eNeuro*, *6*(5), ENEURO.0085-19.2019. https://doi.org/10.1523/ENEURO.0085-19.2019

Wang, M., Xu, Z., Liu, Q., Sun, W., Jiang, B., Yang, K., Li, J., Gong, Y., Liu, Q., Liu, D., & Li, X. (2019). Nongenetic optical modulation of neural stem cell proliferation and neuronal/glial differentiation. *Biomaterials*, *225*, 119539. https://doi.org/10.1016/j.biomaterials.2019.119539

SUPPORTING INFORMATION

Additional supporting information can be found online in the Supporting Information section at the end of this article.

How to cite this article: Lightning, A., Bourzeix, M., Beurrier, C., & Kuczewski, N. (2023). Effects of discontinuous blue light stimulation on the electrophysiological properties of neurons lacking opsin expression in vitro: Implications for optogenetic experiments. *European Journal of Neuroscience*, 1–15. https://doi.org/10.1111/ejn.15927

Study 1 Supplementary Tables and Figures

	Pattern 1			Pattern 2			Pattern 3			Pattern 4		
	1 mW	5 mW	13 mW	1 mW	5 mW	13 mW	1 mW	5 mW	13 mW	1 mW	5 mW	13 mW
Average I (pA)	-0.14	0.06	0.38	-0.06	0.52	0.72	0.12	0.09	1.13	0.04	0.59	1.89
95% CI	0.08	0.07	0.08	0.09	0.07	0.08	0.07	0.09	1.08	0.07	0.06	0.08
p_value	0.99	**0.048**	**$6*10^{-19}$**	0.88	**$5*10^{-49}$**	**$2*10^{-51}$**	0.07	**$1*10^{-13}$**	**$1*10^{-140}$**	**$3*10^{-5}$**	**$2*10^{-66}$**	**$5*10^{-85}$**
	Pattern 5			**Pattern 6**			**Pattern 7**			**Pattern 8**		
	1 mW	5 mW	13 mW	1 mW	5 mW	13 mW	1 mW	5 mW	13 mW	1 mW	5 mW	13 mW
Average I (pA)	-0.50	0.229	0.83	-0.3	0.19	0.71	0.13	0.38	0.97	0.2	0.22	0.37
95% CI	0.1	0.06	0.08	0.1	0.06	0.06	0.06	0.06	0.08	0.06	0.06	0.07
p_value	1	**$2*10^{-17}$**	**$2*10^{-82}$**	1	**$2*10^{-11}$**	**$2*10^{-80}$**	**0.0003**	**$1*10^{-34}$**	**$3*10^{-91}$**	**$1*10^{-7}$**	**$4*10^{-13}$**	**$5*10^{-25}$**
	Pattern 9			**Pattern 10**								
	1 mW	5 mW	13 mW	1 mW	5 mW	13 mW						
Average I (pA)	-0.27	0.19	0.37	0.18	0.89	0.89						
95% CI	0.06	0.05	0.12	0.06	0.07	0.04						
p_value	1	**$2*10^{-10}$**	**$2*10^{-40}$**	**$4*10^{-8}$**	**$2*10^{-31}$**	**$4*10^{-96}$**						

SUPPLEMENTARY TABLE S1. Light effect on the membrane current when the analysis is performed on the 50 light pulses.

	Pattern 1				Pattern 2				Pattern 3				Pattern 4			
	AP amplitude (mV)	AP latency (ms)	AHP amplitude (mV)	AP FWHM (µs)	AP amplitude (mV)	AP latency (ms)	AHP amplitude (mV)	AP FWHM (µs)	AP amplitude (mV)	AP latency (ms)	AHP amplitude (mV)	AP FWHM (µs)	AP amplitude (mV)	AP latency (ms)	AHP amplitude (mV)	AP FWHM (µs)
Average	-0.08	0.01	0	0.24	-0.21	0.03	-0.09	-3.69	-0.25	0.03	-0.09	-5.42	-0.43	0.06	-0.20	-8.96
95% CI	0.03	0.01	0.03	1.13	0.02	0.01	0.02	1.49	0.02	0.01	0.02	0.86	0.02	0.01	0.02	0.99
p_value	$2*10^{-9}$	$3*10^{-5}$	0.94	0.7	$9*10^{-56}$	$1*10^{-22}$	$4*10^{-19}$	$2*10^{-8}$	$7*10^{-73}$	$1*10^{-19}$	$2*10^{-20}$	$1*10^{-27}$	$5*10^{-190}$	$2*10^{-87}$	$4*10^{-94}$	$2*10^{-47}$
	Pattern 5				Pattern 6				Pattern 7				Pattern 8			
	AP amplitude (mV)	AP latency (ms)	AHP amplitude (mV)	AP FWHM (µs)	AP amplitude (mV)	AP latency (ms)	AHP amplitude (mV)	AP FWHM (µs)	AP amplitude (mV)	AP latency (ms)	AHP amplitude (mV)	AP FWHM (µs)	AP amplitude (mV)	AP latency (ms)	AHP amplitude (mV)	AP FWHM (µs)
Average	-0.08	0.02	-0.09	-3.80	-0.31	0.03	-0.08	-3.77	-0.44	-0.03	0.10	-6.60	-0.37	-0.01	-0.07	0.46
95% CI	0.02	0.01	0.02	1.76	0.02	0.01	0.04	0.85	0.04	0.0	0.05	1.03	0.03	0.01	0.02	0.64
p_value	$1*10^{-11}$	$6*10^{-10}$	$6*10^{-19}$	$3*10^{-9}$	$1*10^{-97}$	$7*10^{-4}$	0.002	$1*10^{-15}$	$1*10^{-98}$	1	0.01	$7*10^{-28}$	$2*10^{-92}$	0.9	$2*10^{-13}$	0.53
	Pattern 9				Pattern 10											
	AP amplitude (mV)	AP latency (ms)	AHP amplitude (mV)	AP FWHM (µs)	AP amplitude (mV)	AP latency (ms)	AHP amplitude (mV)	AP FWHM (µs)								
Average	-0.09	-0.01	0.12	-0.79	-0.20	0.03	-0.07	-5.23								
95% CI	0.04	0.01	0.06	0.79	0.03	0.01	0.05	1.55								
p_value	$6*10^{-24}$	0.9	0.5	0.01	$5*10^{-27}$	$8*10^{-10}$	0.9	$7*10^{-17}$								

SUPPLEMENTARY TABLE S2. Light effect on AP properties when the analysis is performed on the 50 light pulses.

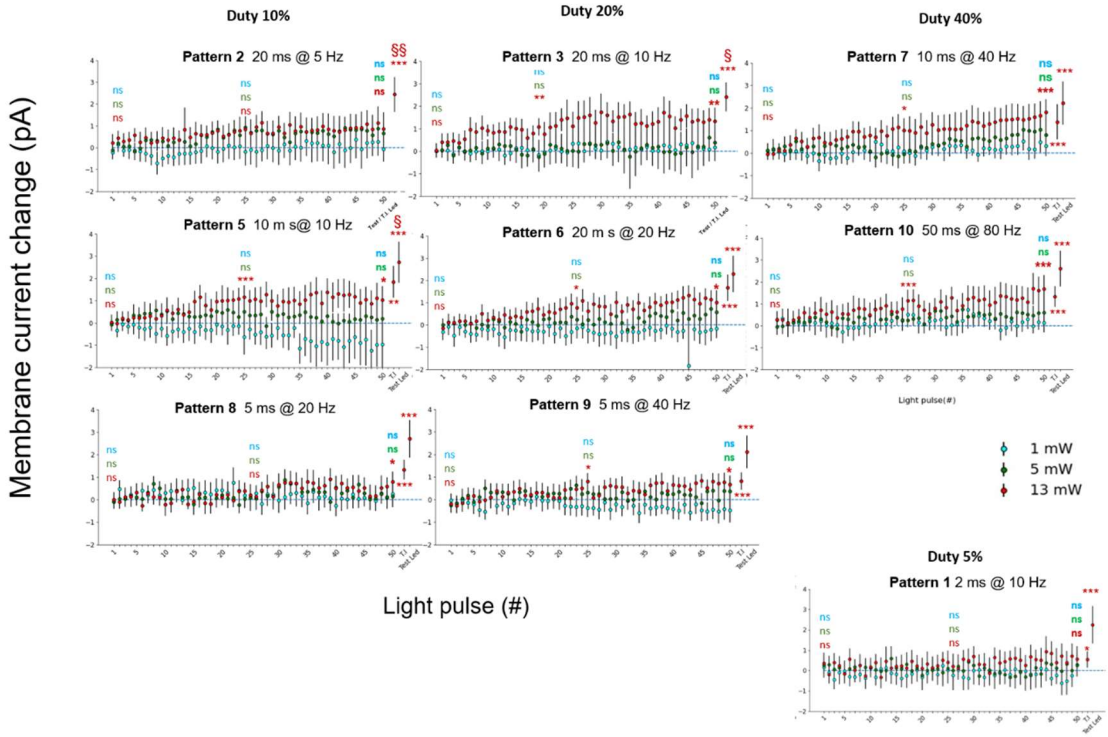

SUPPLEMENTARY FIGURE S1. Quantification of the light-induced current in MCs along the 50 steps for all the tested patterns except pattern 4. Average effect produced on 24 MCs at the three light powers. Statistical comparisons were performed for the pulses 1, 25 and 50 and for T.I. LED and Test LE. Vertical bars represent 95%. CI.
*=p<0.05, **= p<0.01, ***= p<0.001 compared to ctr period
§ =p<0.05, §§ = p<0.01 compared to pulse 50.

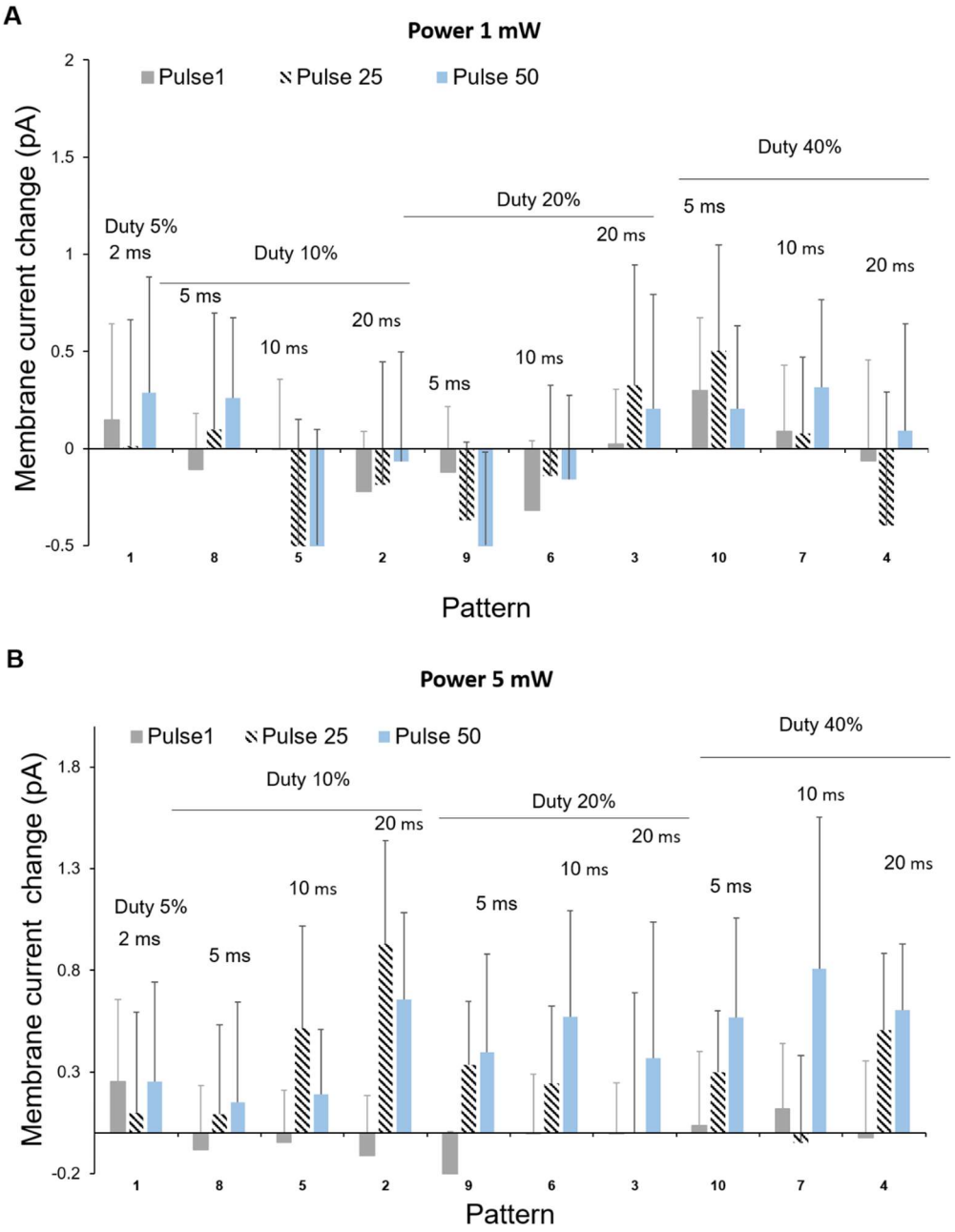

SUPPLEMENTARY FIGURE S2. Quantification of membrane current generated by patterned light at 1 (A) and 5mW (B). The graphs illustrate the average currents produced by the 1st, 25th and 50th pulse and T.I.LED for the ten different patterns. Data are ordered by duty cycle and light pulse duration. Error bars represent 95% CI. $p > 0.05$ for all the light effects. Raw data can be found here: https://osf.io/e6brs

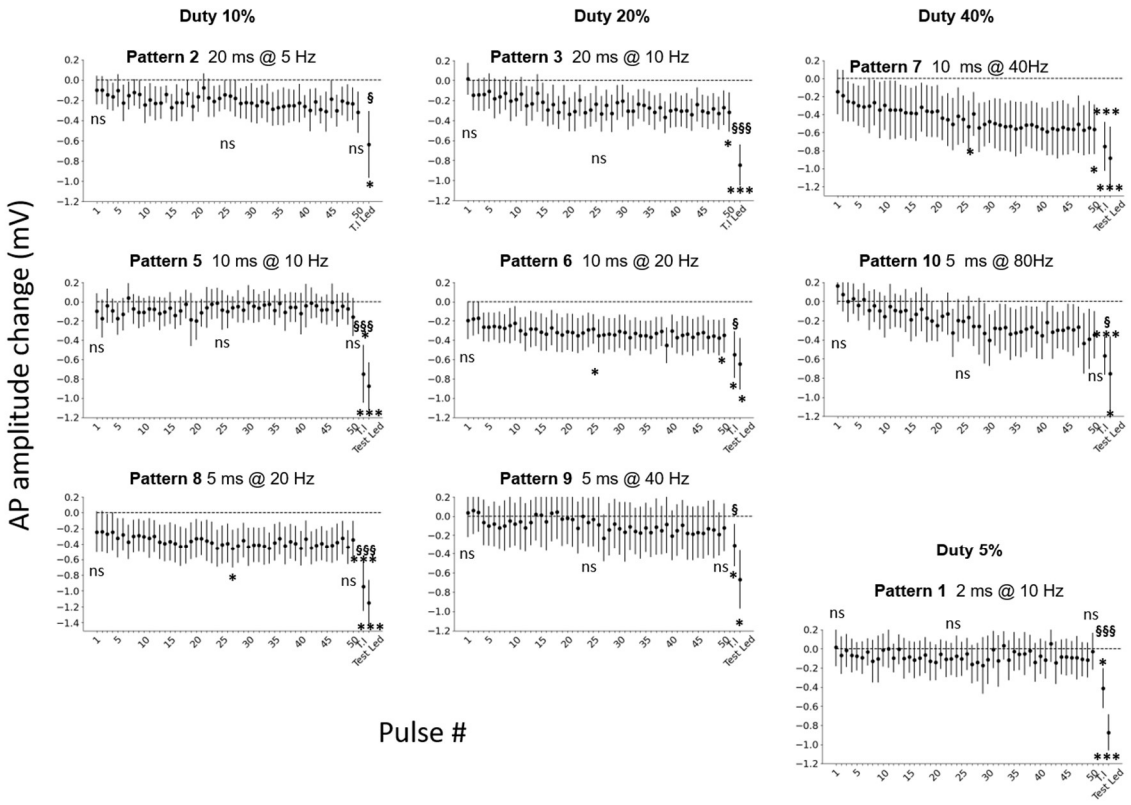

SUPPLEMENTARY FIGURE S3. Quantification of light-induced change in AP amplitude in MCs along the 50 steps for all tested patterns except pattern 4. N= 24 MCs per pattern. Error bars represent 95% CI.

*=p<0.05, **= p<0.01, ***= p<0.001 compared to ctr period.

§ =p<0.05, §§ = p<0.01, §§§ = p<0.001 compared to pulse 50.

Light power= 13 mW.

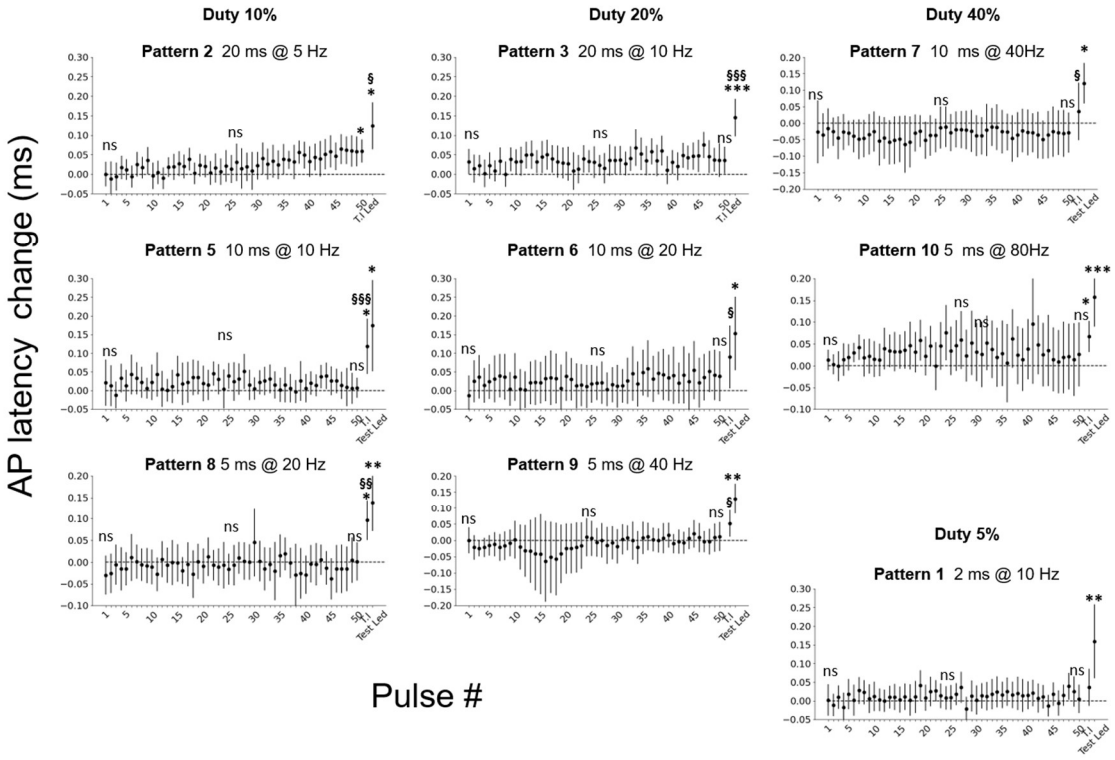

SUPPLEMENTARY FIGURE S4. Quantification of light-induced change in AP latency in MCs along the 50 steps for all tested patterns except pattern 4. Light power=13 mW. N= 24 MCs per pattern. Error bars represent 95% CI.

*=p<0.05, **= p<0.01, ***= p<0.001 compared to ctr period.

§ =p<0.05, §§ = p<0.01, §§§ = p<0.001 compared to pulse 50.

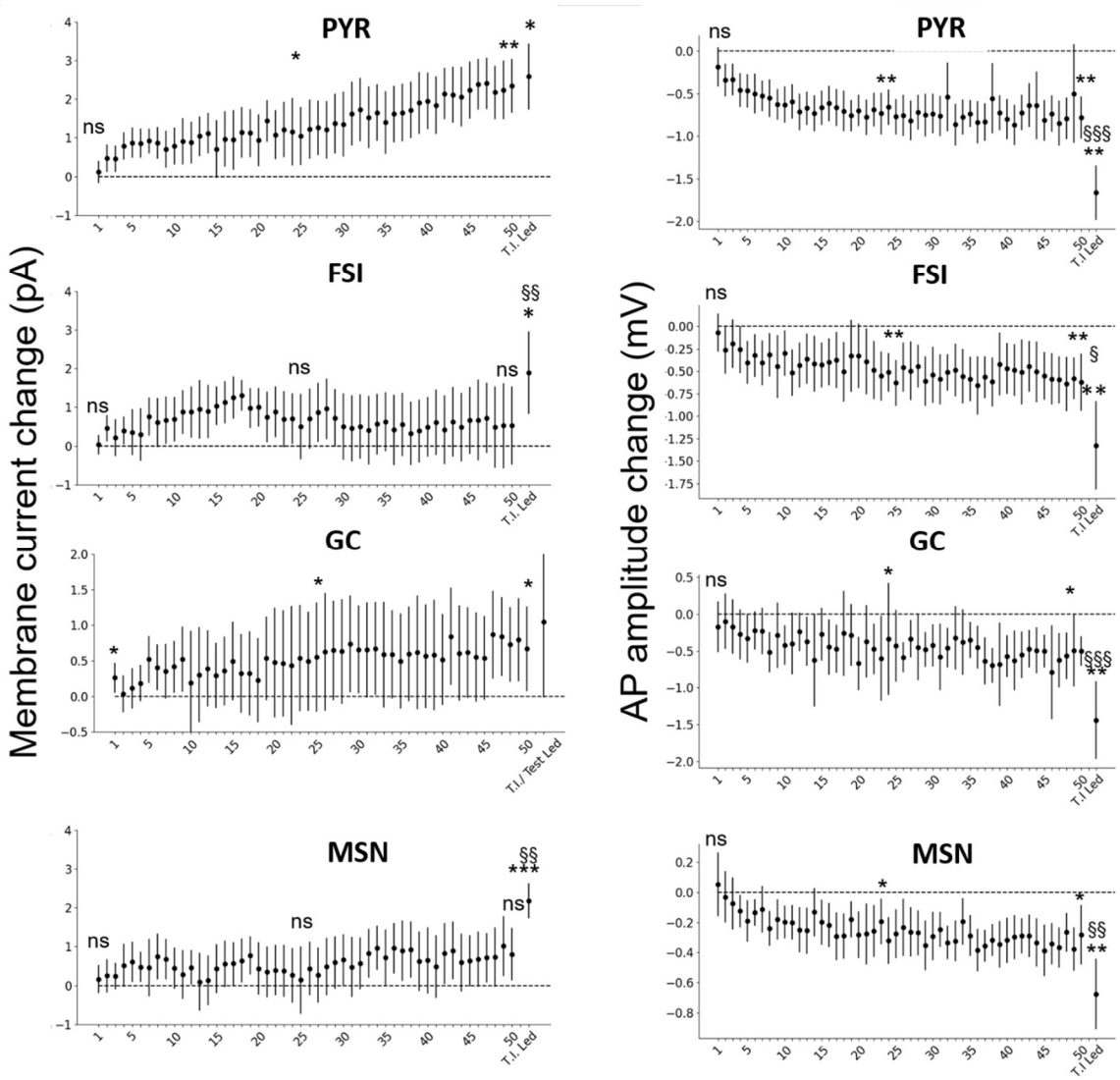

SUPPLEMENTARY FIGURE S5. Quantification of light-induced change in membrane current (left) and AP amplitude (right) for the different neuronal types. Error bars represent 95% CI.
*= p<0.05, **= p<0.0, ***= p<0.001 compared to ctr period.
§ =p<0.05, §§ = p<0.01, §§§ = p<0.001 compared to pulse 50.

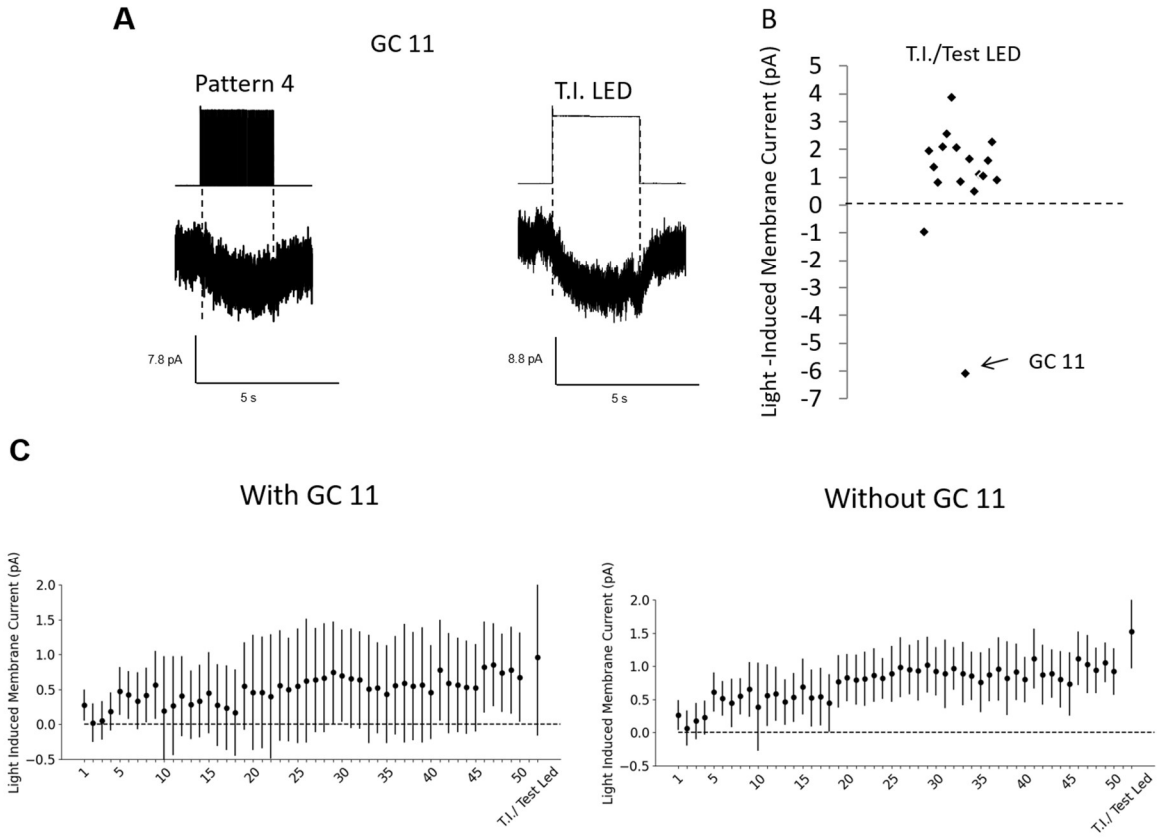

SUPPLEMENTARY FIGURE S6. Inward current is generated in one of the recorded GCs. **A)** average current generated by patterned and continuous light on 1 cell (GC 11). **B)** Quantification of the membrane current generated by the T.I. LED in GCs (n = 15). **C)** Quantification of the light-induced modification in membrane current in the presence (left) or in the absence (right) of GC 11 (substituted by a recording on a new GC). Error bars represent 95% CI.

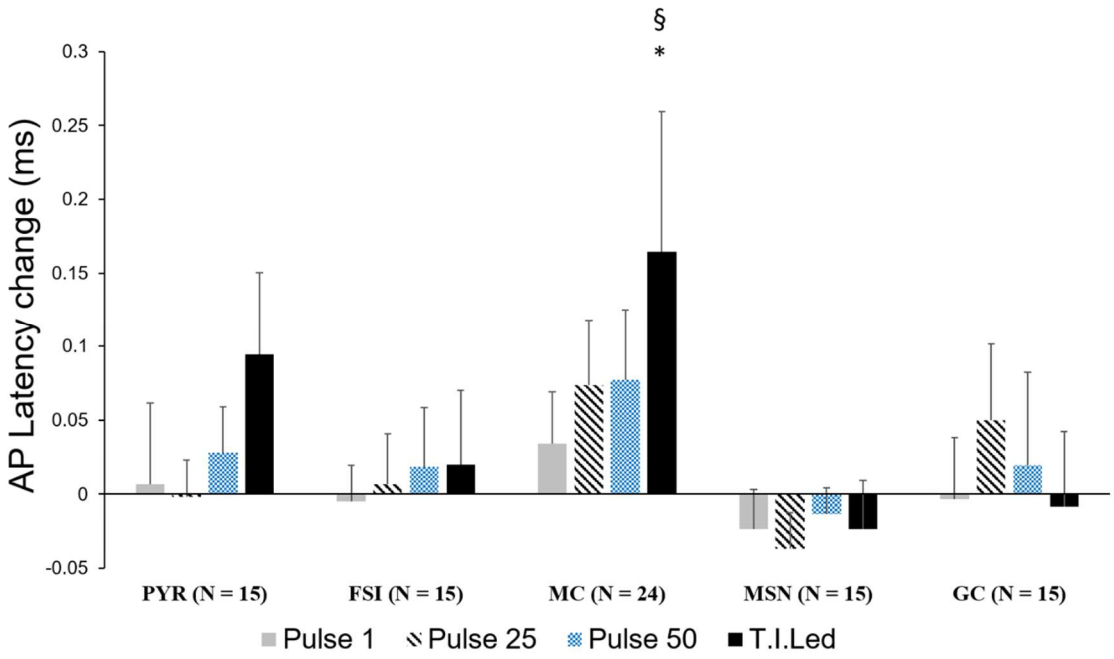

SUPPLEMENTARY FIGURE S7. Quantification of the average modification of AP latency produced at the 1st, 25th and 50th pulse and T.I.LED by pattern 4 at 13mW on the different cell types. Error bars represent 95% CI. *=p<0.05, **= p<0.01, ***=p<0.001 compared to ctr period. § =p<0.05, §§ = p<0.01 compared to pulse 50.
Raw data can be found here: https://osf.io/akh4j/

STUDY 2

MANUSCRIPT IN PREPARATION

LONG LASTING INHIBITION OF CORTICAL MOUSE AND HUMAN FIRING ACTIVITY PRODUCED BY BLUE LIGHT STIMULATION

LIGHTNING, Anistasha[1] ; **Di ROCCO**, Federico[2] ; **GUENOT**, Marc[2] ; **KUCZEWSKI,** Nicola[1]

1: Inserm U1028 - CNRS UMR5292 – UCBL

2: Pierre Wertheimer Hospital, 59 Bd Pinel, 69500 Bron, France and Woman-Mother-Child Hospital, 59 Bd Pinel, 69500 Bron, France

Corresponding author:

Nicola Kuczewski
Inserm U1028 - CNRS UMR5292 - UCBL
Centre Hospitalier Le Vinatier - Bâtiment 462 - Neurocampus
95 boulevard Pinel
69675 Bron Cedex
Tel. 0481106523e-mail: nicola.kuczewski@univ-lyon1.fr

Running title: Cortical Mouse and Human Inhibition with Blue Light

Total number of pages: 28

Total number of figures: 8

Total number of tables: 0

The total number of words in the whole manuscript: 7037

The total number of words in the Abstract: 192

Keywords: brain photostimulation, blue light stimulation, cortical neurons, electrophysiology, patch clamp, action potential

Acknowledgements: This work was supported by the Université Claude Bernard (Lyon 1), the CNRS and the INSERM. The authors would also like to thank Hajar **EL YAQOTI** and Fabrice **ABATE**, the research interns who assisted us at various stages of this project. H. EL YAQOTI assisted during procedure 2. F. ABATE assisted during procedure 6.

Conflict of Interest: The authors declare no conflicting financial or other interests.

Author contributions:

Abstract

Previous research demonstrates that continuous blue LED stimulation reduces action potential firing activity in several neuronal types in the mouse brain. While short lasting stimulation (1s) produces transient modifications of firing activity, longer stimulation (5-10s), appear to produce long lasting inhibition of neuronal activity. These results open the possibility that light stimulation could be adapted for therapeutic purposes in humans to treat the hyperexcitability associated with several neurological disorders, most notable epileptic syndromes. To investigate this possibly, patch clamp recording was performed both on mouse and human cortical neurons in slices to evaluate the effect of (5s) of continuous blue LED stimulation at 19mW. This stimulation produces a long-lasting inhibition of firing activity in most (73.7%) of cortical neurons recorded from mice and in a subset (68.8%) of human cortical neurons. These effects were associated with a membrane hyperpolarization. We also examined single evoked action potentials in voltage clamp mode to isolate the effects of the LED on sodium (Na^+) and potassium (K^+) currents, noting that the effect the LED has on Na^+ current appears to be more important for the overall modification of firing than the effect on the K^+ current.

Introduction

Previous research has demonstrated the efficacy of one-photon (1P) light stimulation in reducing neuronal action potential (AP) firing rate in several different neuronal subtypes in the CNS (Ait-Ouares et al., 2019; Owen, Liu, & Kreitzer, 2019; Lightning et al., 2023). This effect is typically transient, recovering after the LED is switched off, and appears to occur concomitant to a light-induced hyperpolarizing membrane current and changes to AP amplitude and latency (Ait-Ouares et al., 2019; Lightning et al., 2023). There is an ongoing investigation into the mechanisms responsible for the light effects on neuronal activity and most of the experimental evidence suggest that they are a consequence of tissue heating produced by the light (Stujenske, Spellman, & Gordon, 2015; Senova et al., 2017; Ait-Ouares et al., 2019; Owen, Liu, & Kreitzer, 2019; Lightning et al., 2023) along with possible GABA-mediated components (Leszkiewicz & Aizenman, 2003; Sun et al., 2020). Light induced hyperpolarization of membrane potential has been proposed to be due to the activation of inward rectifying potassium channels (K_{ir}) (Owen, Liu, & Kreitzer, 2019), while the light effect on the AP proprieties could be due to temperature mediated modification of voltage dependent Na^+ and K^+ channels (REF).

The effect of visible light stimulation on neuronal activity increases in tandem with increases in the light power and stimulation duration (Stujenske, Spellman, and Gordon, 2015; Senova et al., 2017, Ait-Ouares et al., 2019). Further, continuous LED stimulation produces a larger effect than pulsed LED stimulation (Lightning et al., 2023). Interestingly, in some of the Mitral Cells recorded on the olfactory bulb, long light stimulation (5-10s) was reported to produce an inhibition of firing activity that extend for several minutes beyond the stimulation period (Ait-Ouares et al., 2019). If confirmed and extended to other neuronal types, the long-lasting inhibition of neuronal activity produced by visible light opens the possibility to use light for therapeutic purposes to treat the neuronal hyperexcitability associated with several neurological disorders in humans. In the present report we investigate this possibility by looking at the effect produced by 5s blue light (19mW) stimulation of on the electrical activity of both mouse and human cortical neurons.

It is therefore important to better understand the physiological components of the effect that 1P blue LED stimulation is having before this line of pre-clinical questioning can continue. Here, we sought to develop an improved understanding of the effect of blue LED stimulation on neuronal activity *in vitro* as a compliment to previous work that demonstrated blue-light mediated reductions in AP firing activity for cortical pyramidal neurons (Ait-Ouares et al.,

2019) and related light-induced membrane hyperpolarization (Lightning et al., 2023). If this effect can also be made non-transient *in vitro*, then blue-LED mediated AP firing reduction may be adaptable into a non-invasive treatments for those disorders where the chief component is uncontrolled hyperexcitability.

Methods

Animals.

Male C57Bl6/J mice (Janvier Laboratories, France) aged between 60 and 90 days were used. All procedures were in accordance with European Union recommendations for animal experimentation (2010/63/UE). Mice were housed in groups of up to three in standard laboratory cages and were kept on a 12-hour light/dark cycle (at a constant temperature of 22°C) with food and water ad libitum.

Human Tissue.

For the investigation into human cortical neurons, we sourced living cortical tissue working with surgeons at two separate hospitals located in Bron, Auvergne-Rhône-Alpes, France[1]. Tissue was sourced from patients undergoing surgical treatment for drug resistant epilepsies or tumor removal (patients aged 3 – 54 years). All patients, or the guardians of patients where appropriate, gave their informed consent to the use of their excised cortical tissue for research purposes. This tissue come from cortical areas where tissue was already being removed as a normal part of the ongoing surgical procedure.

Electrophysiology.

Protocols for slice preparation and recordings of mouse cortical neurons.

Mice were anaesthetized with an intra-peritoneal injection of ketamine (50 mg/ml) and decapitated. The head was quickly immersed in ice-cold (2-4°C) artificial cerebrospinal fluid (CutACSF) with the following composition: 125 mM NaCl, 4 mM KCl, 25 mM NaHCO3, 0.5 mM $CaCl_2$, 1.25 mM NaH_2PO_4, 7 mM $MgCl_2$ and 5.5 mM (1g/L) glucose (pH = 7.4 oxygenated with 95 % O_2/5 % CO_2). The osmolarity of the solution was adjusted to between 300 and 320 mOsm with sucrose, an amount that settled on 20.4 mM (7g/L) of sucrose. The brain was removed from the dissected animal and the cerebellum and midbrain were removed using an

[1] Pierre Wertheimer Hospital, 59 Bd Pinel, 69500 Bron, France and Woman-Mother-Child Hospital, 59 Bd Pinel, 69500 Bron, France

Unger 4 cm razor blade (part No. SRB10), along with the olfactory bulb and approximately 1 - 2mm of the anterior cerebral cortex in order to create a flat plane for adherence to the vibratome chamber and preparation of the slices. Cortical coronal slices (400µm thick) were prepared with a vibratome (Leica) and cut in half to divide the hemispheres approximately along the corpus collosum. Slices were then incubated in a recovery chamber at 30 ± 1°C using an ACSF solution with a composition similar to the Cut ACSF, except for changes to $CaCl_2$ and $MgCl_2$ concentrations (1.2 mM and 0.7 mM, respectively). Slices were transferred to a recording chamber mounted on an upright microscope and continuously perfused with oxygenated ACSF (4 ml/min) at 36 ± 1°C. Neurons were visualized using a microscope (Zeiss axioscope) with a 40X objective (Zeiss Plan-APOCHROMAT). Data were acquired with the amplifier RK 400 BioLogic at full sampling frequency of 25 kHz using a 12-bit A/D-D/A converter (Digidata 1440A, Axon Instruments) and PClamp software (PClamp10, Axon Instruments). Patch-clamp whole-cell recordings were achieved with borosilicate pipettes having a resistance 4-9 MΩ and filled with: 126 mM K-gluconate, 5 mM KCl, 10 mM HEPES, 1 mM EGTA, 1 mM $MgCl_2$, 2 mM ATP-Na2, 0.3 mM GTP-Na3, and 10 mM phosphocreatine (pH = 7.3, 290 mOsm).

Protocol for slice preparation and recordings of human neurons.

Approximately $1cm^3$ of cortical tissue containing both grey and white matter was removed by the neurosurgeon and transferred to an improvised oxygenated transportation container containing ice cold (2 - 4°C) CutACSF solution with the following composition: 125 mM NaCl, 4 mM KCl, 25 mM $NaHCO_3$, 0.5 mM $CaCl_2$, 1.25 mM NaH_2PO_4, 7 mM $MgCl_2$, 5.5 mM (1g/L) glucose, 20.4 mM (7g/L) of sucrose. During transportation from the hospital to the research laboratory, the solution was continuously oxygenated (95% O_2, 5% CO_2) using a portable oxygen tank attached to the valve system of the improvised transportation container. The tissue along with the CutACSF was then transferred to a glass petri dish and cut as needed to adhere to the size of the vibratome chamber. Generally, the tissue was cut in a manner that allowed the slices to contain both grey and white matter for later orientation purposes under microscopy. Following this, slices (400µm thick) were prepared with the vibratome (Leica) and transferred to a recovery chamber at 30 ± 1°C, containing an ACSF solution with a composition similar to the Cut ACSF, except for changes to $CaCl_2$ and $MgCl_2$ concentrations (1.2 mM and 0.7 mM, respectively). Post-cut incubation and electrophysiology proceeded with exactly the same procedure as used for mouse cortical neurons.

Optical stimulation.

The light stimulation applied in this study is a 1 photon (1P) visible blue light stimulation peaked at 470 nm (emission spectrum between 430-495 nm), performed using a Dual Port OptoLED (CAIRN, UK) dichroic mirror 495 nm at a power of 19 mW measured at the output of the x40 objective. Power loss at the working distance (2.5 mm from the objective), due to the presence of ACSF, was empirically estimated at 13%. The average power density in the tissue was estimated by dividing the power at the working distance by the empirically measured illumination area (~ 7 mm^2). Calculating this and subtracting 13% of that value to account for the estimated power loss gives an average power density of ~2.4 mW/mm^2 for the 19mW blue LED.

Bath temperature in the recording chamber was measured and controlled by a ThermoClamp-1 device (Atomate Scientific).

Experimental procedure.

Procedure 1: Determination of light-induced tissue temperature change

Light induced temperature modification produced by LED stimulation was measured by placing the temperature probe connected to a ThermoClamp-1 device (Atomate Scientific) on cortical tissue beneath the microscope objective, which was held at the exact same distance as present in the electrophysiological experiments. The slices were stimulated with 19mW continuous blue light for 5s and the evolution of tissue temperature was recorded throughout Temperature modification was calculated as the difference between the average temperature during LED stimulation and the average temperature of the second preceding the light.

Procedure 2: Determination of the light effect on the action potential firing rate of cortical neurons.

This procedure was used for both mouse and human neurons. Cells were recorded in current-clamp mode at their resting membrane potential. In cases where spontaneous firing was present before recording began, a hyperpolarization of the membrane potential was produced by injecting negative current. To program the protocol and ensure consistent stimulation times, we divided the procedure into pre-defined sweeps **(supplementary figure 1).** The total time duration of each electrophysiological sweep was 38 seconds. During each sweep, two consecutive 5s trains of action potentials, separated by 15s, were generated with a 5s depolarizing step. 10 sweeps were recorded for each tested neuron before light stimulation as a control. Following the recording of the control sweeps, 10 or 6 sweeps were recorded, with the

first 5s train of action potentials generated concomitant with 5s of continuous blue light stimulation at the 19mW power level, and the second train of action potentials generated in the absence of light stimulation. 4s following the end of the second generation of action potentials, the neurons were subjected to an additional of 1s continuous light stimulation (procedure 4), which resulted in a total of 6s of light stimulation during each experimental sweep. The analysis was performed on the first train of each sweep by normalizing the firing rate on the of the median control AP firing rate using a custom python script (https://osf.io/6jqye/).

Procedure 3: Calculation of the membrane resistance (Rm)

The effect of light on Rm was determined both in current clamp and voltage clamp conditions.

Current clamp mode – A hyperpolarizing current step of -0.1 nA (duration 1s) occurred on every sweep prior to the injection of the depolarizing current described in procedure 1. The Rm was calculated on every sweep according to ohm's law $R=\Delta V/\Delta I$ where ΔV was the difference between the membrane potential measured in the last 100 ms of the hyperpolarization and the membrane potential of the 200 ms pre-step period.

Voltage clamp mode –. Cells were held at -70 mV in voltage-clamp mode. One step to -75 mV was generated (1s duration, 1Hz) and recorded on every sweep. The Rm was calculated on every sweep according to ohm's law $R=\Delta V/\Delta I$ where ΔV=-5mV and ΔI was the difference between the median current in the last 100 ms of the hyperpolarization and the median current in the 200 ms pre-step period. Access resistance A_R was calculated as $A_R=\Delta V/\Delta I_A$ where ΔI_A is the difference between the peak of transient current and the median current in the 200 ms pre-step period.

Procedure 4: Determination of light effect on membrane potential (Vm)

The effect of light stimulation on membrane potential was investigated by subtracting to the average Vm during the 1s light stimulation at the end of the sweep from the average Vm in the 1 second preceding the light stimulation.

Procedure 6: Determination of light effect on voltage dependent currents participating in the action potential generation

This procedure was applied only to mouse cortical neurons in voltage clamp mode (see **Supplementary Figure 2**). Neurons were held at -70mV. The Rm during this procedure in line

with the method described in procedure 3. Voltage command was used to produce an AP having the same shape as those AP recorded in current clamp configuration. The AP was preceded by itself repeated 10 times at -0.1 scale (i.e., inverted and reduced 10 times)

The fact that the range of voltage modification of the reduced AP is small (between -8.5 mV and +0.4 mV) ensures that it elicits only passive current. The total passive current that is produced during the generation of the AP was then calculated by the sum of the passive currents of the 10 reduced AP. This passive current was subtracted from the current record during the generation of the AP, allowing for the isolation of the active current that participates in the AP generation. This results in an inward, putative Na^+ and Ca^{2+} current associated with the AP depolarization and an outward, putative K^+ current associated with the afterhyperpolarization AHP (**supplementary figure 2**).

The control was established over 10 sweeps, followed by 6 sweeps with LED stimulation and a 25-minute post-led recovery period. Only the first of the two AP were analyzed. The eventual modification of the recorded currents produced by the modification of the access resistance (R_A) was corrected by multiplying the current trace of each sweep by the AR ratio (R_A first sweep/ R_A recorded sweep). The analysis was performed by a custom-written script.

Statistics:

Since the normality of the data was not known and normality tests have low statistical power for our low sample sizes (Öztuna *et al.*, 2006), non-parametric one-sample and paired sample Wilcoxon signed rank tests were used for the analysis (JASP software). Type I error probability was kept at 5%.

Data sharing.

All raw electrophysiological traces, scripts for the analysis and raw data are accessible via the Open Science Framework website (https://osf.io/6jqye/)

Exclusion criteria.

We excluded from analysis the following electrophysiological profiles:

1. Those cells that did not survive beyond the end of the LED stimulation period.

2. Cells for which there was instability of AP frequency along the different sweeps during control period.

3. For the action potential firing analysis: Individual sweeps within a cell's data where spontaneous firing activity occurred between current steps. The sweep was only excluded if the frequency of spontaneous firing was so high as to obscure the start and stop points of the current steps as read in the python script used for analysis.

4. For the Vm analysis: Individual sweeps within a cell's data where spontaneous action potential firing occurred during the 1s LED stimulation meant to measure light induced Vm modification.

Competing Interests: the authors declare no competing financial interests.

Results

Blue light stimulation produces a long-lasting modification of firing activity of mouse cortical neurons

The effect of 5s continuous blue light stimulation (19 mW) on tissue temperature modification was investigated by a thermal probe on cortical slices. Light-induced an increase of 1.8°C (95% CI [1.65, 1.97], Figure 1A). The effect of light on the firing activity of pyramidal cortical neuron was investigated using the protocol depicted in supplementary figure 1. Ten light stimuli (5s at 19 mW) produced an average decrease of firing activity (-31.6% ± 19.5% decrease compared to median control, SD = 43.4; Wilcoxon signed rank test, $p = 0.004$, $N = 19$) that lasts beyond the end of stimulation (-55.5% ± 34.3% between ~8 and ~13 minutes after the end of the stimulation [20-25 min total experiment time], $p = 0.013$, $N = 19$) (Figure 1B). The light effect was, however, heterogeneous, with the firing activity that increases by more than 10% from the control in 15% of neurons during LED stimulation and in 21% between ~8 and ~13 minutes after the end of the stimulation. Firing activity decreased more than 10% below the control in 73.6% of neurons during LED stimulation and 68.4% thereafter.

Light stimulation produced a heterogeneous modification of the membrane resistance (Figure 1C) with an average reduction during the led period that does not reach significance (-6.05 MΩ ± 6.34 MΩ, $p = 0.110$, $N = 19$). Interestingly, the modification of firing frequency correlates with the modification of the Rm both in the period of light stimulation (Spearman correlation, $r = 0.730$, $p < .001$, $N = 19$) and thereafter ($r = 0.727$, $p < .001$, $N = 18$). This suggests that the light effect on Rm could be a contributing mechanism on early and late modification in firing produced by light. No evident modifications in the resting membrane potential (V_{rest}) were produced by the light stimulation (Supplementary figure 3). As previously shown, light (1s) induced a hyperpolarization of the membrane potential (V_m) (one sample Wilcoxon signed-rank test: -0.323 mV ± 0.84mV, $p < .001$, $N = 19$) that does not

correlate with LED-induced AP firing reduction (Sparman correlation, r = 0.306, p = .202, N = 19; **Figure 1D**).

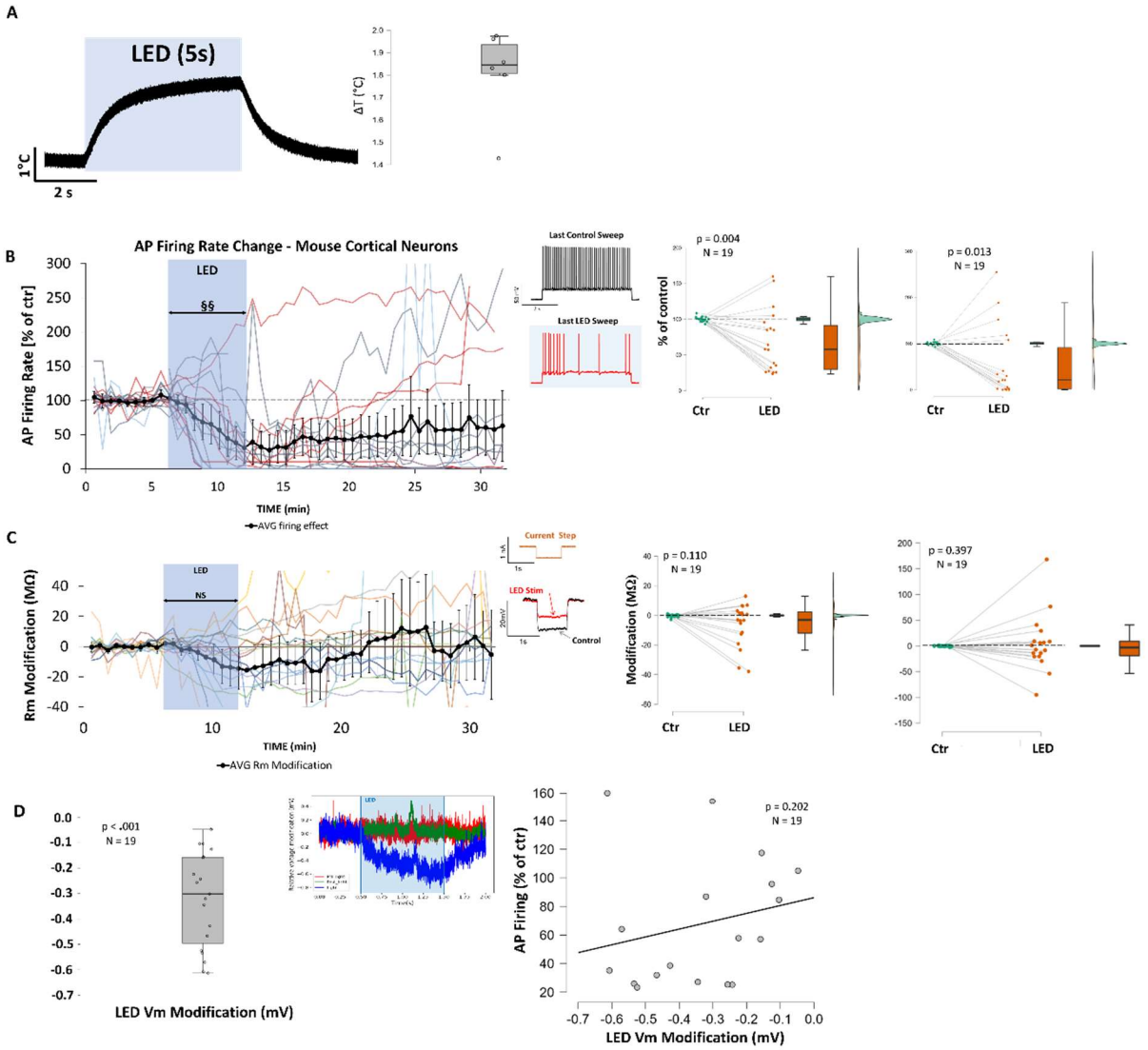

Figure 23. 5s 1P blue light stimulation raises tissue temperature and lowers AP firing rates in MOUSE cortical neurons but does not significantly lower Rm. Population average is represented in black; error bars represent 95% CI. Colored lines represent individual cell's behavior. N = 6 for temperature increases, N = 19 otherwise. §: p < .05; §§: p < .01; §§§: p< .001 **A)** Tissue temperature change during LED stimulation with population average change listed. Inlay: boxplot distribution of average temperature changes across 6 measured coronal slices. **B)** Left: AP firing rate evolution under and after LED stimulation with example of LED-induced AP firing rate change during electrical stimulation. Right: average control period firing behavior compared to average LED firing behavior with p-value listed (Paired Samples Wilcoxon Signed Rank Test, Ctrl > LED) and average control compared to average post-LED period between 20' and 25' (Paired Samples Wilcoxon Signed Rank Test, Ctrl > Post-LED) **C)** Left: Rm evolution under and after LED stimulation with example of LED-induced Rm change (bottom) and the current step used to generate the Rm measurement (top). Right: Average control period Rm compared to Rm under LED stimulation. **D)** Left: Distribution pf per-cell LED Vm evolution with example of the electrophysiology. Right: Correlation between LED Vm modification and LED AP firing rate change. Scripts and raw data for the analysis can be found here: **https://osf.io/6jqye/**

As evident from figure 1B (average trace) the effect of light on firing activity develops along the 10 light pulses, reaching its maximum effect at the last pulse, and does not recover back to the control period in the 32 minutes of recording time. We therefore wondered whether reducing the number of light stimuli to 6 would produce a lower effect capable of recovering to the initial firing frequency. As shown in figure 2, the average decrease in firing rate continued even after the light stimulation period with a reduction of 24.9% ± 26.2% during the LED (Wilcoxon signed rank test, $p = 0.078$ compared to ctr, $N = 7$; Figure 2B), and of 54.9% ± 31.6% in ~5 minutes that follow the LED stimulation ($p = 0.023$ compared to ctr, $N = 7$; Figure 2C). This suggests that the mechanisms responsible for the light effect required a few minutes to completely develop.

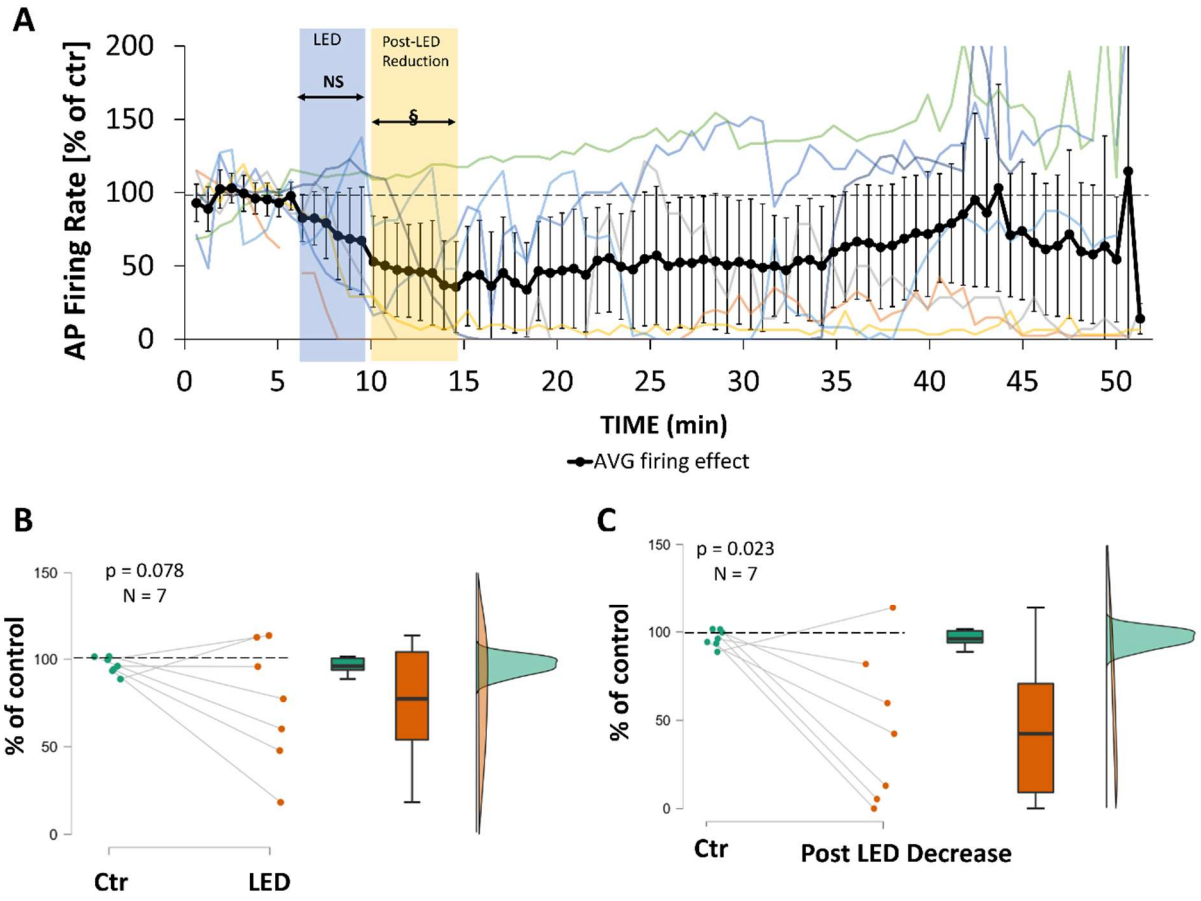

Figure 24. Reduced duration LED stimulation does not produce a significant effect during the LED, but AP firing reduction continues for approximately 5min after the LED has stopped. The activity reduction reaches significance in this post LED period. The neurons begin to recover toward baseline activity (on average) after about 25 minutes of rest in this condition. N = 7, §: $p < .05$; §§: $p < .01$; §§§: $p < .001$ **A)** AP firing rate evolution under and after reduced LED stimulation. Population average is represented in black; error bars represent 95% CI. Colored lines represent individual cell's behavior. **B)** Control period firing behavior compared to LED firing behavior with p-value listed. **C)** Control period firing behavior compared to post-LED reduction period firing (B&C: Paired Samples Wilcoxon Signed Rank Test, Ctrl > LED)

Light stimulation induces a long-lasting decrease of voltage dependent inward and outward currents participating in the AP

Both sodium (Na^+) and potassium (K^+) ion conductance across the membrane are important for AP generation. The activation of the sodium channel leads the cellular depolarization that becomes the AP following the attainment of the activation threshold, and the subsequent opening of voltage gated potassium channels triggers a K^+ efflux that repolarizes the neuron. The effect of light on firing activity could therefore be mediated by a modification of the functionality of voltage dependent K^+ and Na^+ channels. To elucidate this point, voltage clamp recordings were performed to isolate the voltage dependent outward (putative K^+) and inward (putative Na^+) currents produced when the membrane potential is experimentally modified to reproduce an AP representative of cortical pyramidal neuron activity (see methods and supplementary figure 2).

As shown in figure 3, most of the recorded neurons (6/8, 75%) show a transient increase in the outward currents during the 6-light stimulation (6 light pulses) (+10.3% ± 15.8%, $p = .46$, $N = 8$). However, a long-lasting reduction is observed thereafter (-42% ± 26.9%, $p = .039$, $N = 8$). On the other end, the inward currents start to decrease during light stimulation (-6%% ± 2.3%, $p < .001$, $N = 11$), with a maximal effect observed several minutes after the light stimulation (between 10-15', -27.2 ± 20%%, $p = .002$, $N = 11$). Similar to what was observed in the current clamp experiment, a heterogeneous effect of light on Rm was observed, with a predominate reduction in Rm at the 10–15-minute mark (-58.04MΩ ± 42.21 MΩ, $p = .027$, $N = 10$).

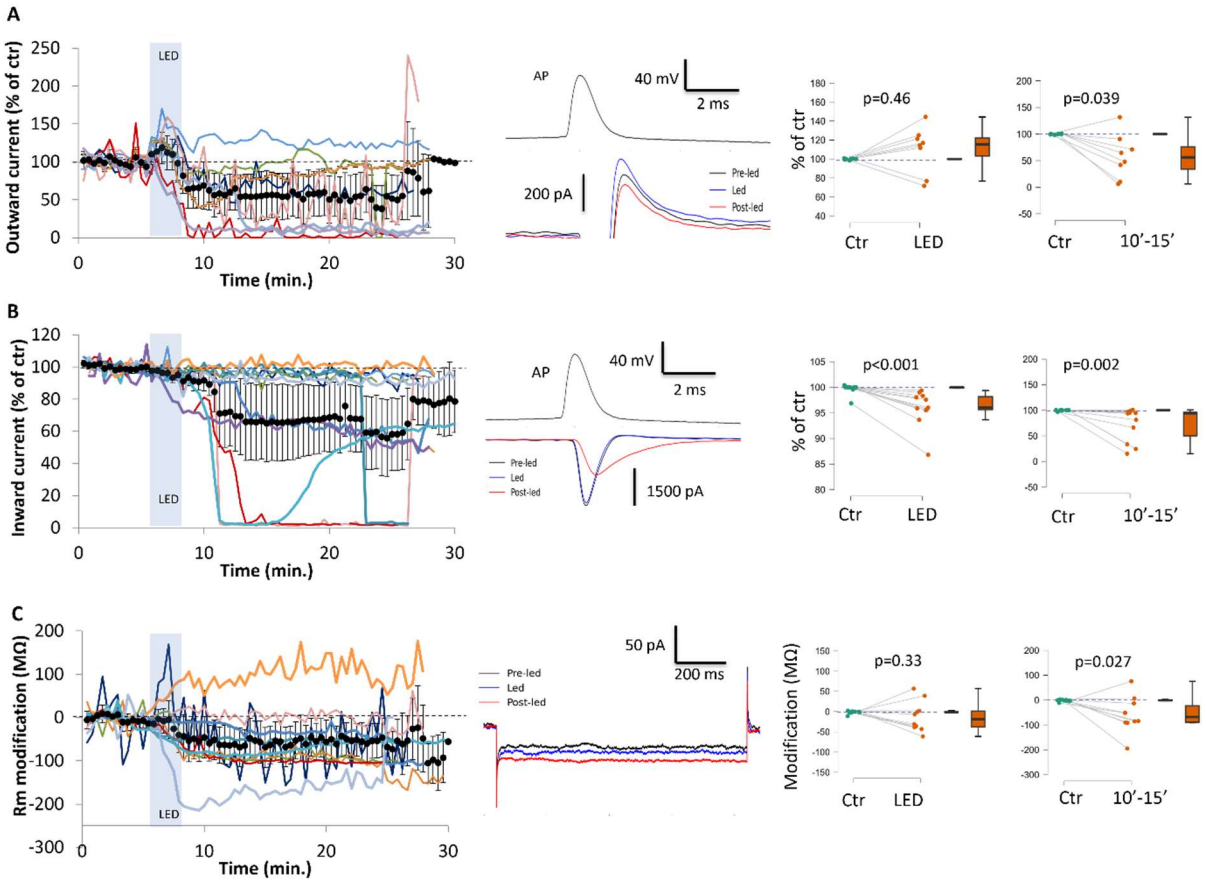

Figure 25. Blue light induced changes to K^+ outward current, and Na^+ inward current, and Rm in **MOUSE** cortical neurons, voltage clamp mode. Cation activity was measured via observations to the changes within a single evoked action potential. The population average change is presented in black, with the activity of all individual cells in the population presented in color to visualize behavior variability. N = 9, §§§: p<0.001 ; §§: p<0.01 ; §: p<0.05, Wilcoxon Signed Rank Test) **A)** Evolution of the outward K^+ current under blue LED stimulation. Left: visualization of the behavior of the outward current. Middle: Example trace showing how we measured the outward current following the AP. Right: raincloud plots showing the LED effect and the post LED effect (measured between 10' and 15' min total experiment time). **B)** Evolution of the inward Na^+ inward current under blue LED stimulation. Left: visualization of the behavior of the inward current. Middle: Example trace showing how we measured the inward current as a function of AP parameters. Right: raincloud plots showing the LED effect and the post LED effect (measured between 10' and 15'min total experiment time). **C)** Evolution of the Rm under LED stimulation in VC mode. Left: visualization of the behavior of the Rm. Middle: Example trace showing how we measured the Rm in voltage clamp mode. Right: raincloud plots showing the LED effect and the post LED effect (measured between 10' and 15'min total experiment time). Scripts and raw data for the analysis can be found here: **https://osf.io/6jqye/**

Blue light does not significantly reduce action potential firing activity in human cortical neurons

The effect of light on the firing activity of human pyramidal cortical neuron was investigated using the protocol depicted in supplementary figure 1. Ten light stimuli (5s at 19 mW) did not produce an average decrease of firing activity in these neurons (Wilcoxon signed rank test: -31.6% ± 19.5% decrease compared to median control, p = 0.004, N = 19) (Figure 4A). As in mouse cortical neurons, the light effect was heterogeneous, with the firing activity that increases by more than 10% from the control in 31% of neurons during LED stimulation and in 25% between ~2min30s and ~8min15s after the end of the stimulation. Firing activity decreased more than 10% below the control in 43.8% of neurons during LED stimulation and 56.2% thereafter.

Light stimulation produced a heterogeneous modification of the membrane resistance (Figure 4B) with an average increase during the led period that does not reach significance (1.9 MΩ ± 4.2 MΩ, p = 0.665, N = 14). Unlike in mouse cortical neurons, the light effect on human cortical neurons did not correlate with the light effect on the Rm during or after the LED. No evident modifications in the resting membrane potential (V_{rest}) were produced by the light stimulation. Interestingly, however, the light effect on the AP firing was correlated with the light effect on Vrest (Spearman correlation, r = 0.556, p =.028; supplementary figure 3). Blue light (1s) induced a hyperpolarization of the membrane potential in all but 2 neurons, but these two neurons displayed large depolarizations that ultimately resulted in a lack of statistical significance for the population (one-sample Wilcoxon signed rank test; 0.187 mV ± 0.575mV, p =.059, N = 14, Figure 4C). The membrane effect does not correlate with the LED effect on firing activity for human cortical neurons (Spearman correlation, r = 0.503, p = .069, Figure 4C).

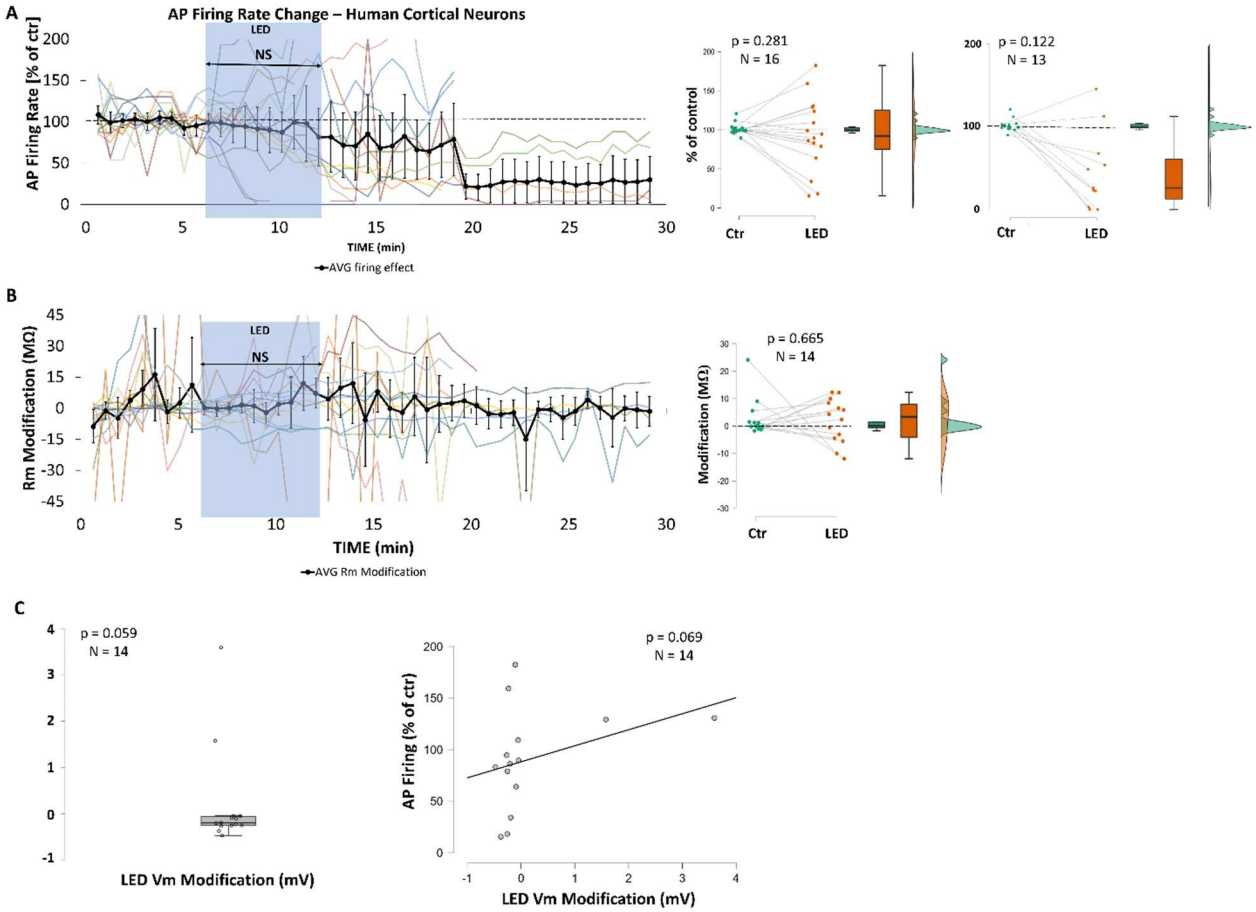

Figure 26. 1P blue light stimulation does not significantly lower AP firing rates or Rm in HUMAN cortical neurons. N = 16 for LED AP firing, N = 14 for Rm. §: p < .05; §§: p < .01; §§§: p< .001 **A)** Left: AP firing rate evolution under and after LED stimulation with example of LED-induced AP firing rate change during electrical stimulation. Right: average control period firing behavior compared to average LED firing behavior with p-value listed (Paired Samples Wilcoxon Signed Rank Test, Ctrl > LED) and average control compared to average post-LED period between 20' and 25' (Paired Samples Wilcoxon Signed Rank Test, Ctrl > Post-LED) **B)** Left: Rm evolution under and after LED stimulation with example of LED-induced Rm change (bottom) and the current step used to generate the Rm measurement (top). Right: Average control period Rm compared to Rm under LED stimulation. **C)** Left: Distribution pf per-cell LED Vm evolution. Right: Correlation between LED Vm modification and LED AP firing rate change. Scripts and raw data for the analysis can be found here: **https://osf.io/6jqye/**

Discussion

The primary conclusion of this study contains two parts. First, that 5s, 19mW, 1P blue-LED stimulation is capable of producing a long-lasting modification of neuronal firing activity in both human and mouse cortical neurons, with the majority of neurons in both species exhibiting at least a 10% decrease in firing either during the LED, as in mouse neurons (73.6%), or thereafter, as with human neurons (56.2%). The LED also produced a membrane hyperpolarization, in 100% of the mouse cortical neurons and 85.7% of human cortical neurons. While we did not observe an overall effect of the LED on human cortical neurons, it is worth noting that, in a sub population of these cells where the activity decreased to any degree under LED stimulation, the effect of the LED was significant (N = 11, supplementary figure 4).

We believe this discrepancy may be due to the lack of anatomical specificity in the experiments involving human neurons. The tissue came from various regions of the cortex, for which we received limited information from the healthcare teams. It was also exceedingly difficult to identify and stimulate the same neuronal subtype in the human slices due to the varying health, quality, and size of the tissues donated (e.g., some contained only grey matter, not all layers were present, the tissue contained only a few usable cells with ambiguous morphology due to poor health, etc.). Thus, while we are reasonably certain that the mouse cortical neurons were pyramidal cells from around layer 5, we cannot make the same statement about the human neurons. Indeed, previous work from our team has noted that different neuronal subtypes behave differently under blue light stimulation (Ait-Ouares et al., 2019; Lightning et al., 2023) and other work has demonstrated variability in light effect based on the region of the cortex (Owen et al., 2019; Stujenske, Spellman, & Gordon, 2015).

The second main conclusion here is that the effect of the light on AP firing appears to be mediated both by the modification of the passive membrane properties, in particular the

membrane resistance and the resting membrane potential, and by the modification of the voltage dependent currents involved in the AP generation. Of course, we cannot say that our light stimulation unilaterally resulted in a decrease in AP firing, as we observed some instances of LED-induced firing increase in both human (31%) and mouse (15%) neurons. However, regardless of the magnitude and direction of the activity change under LED stimulation, AP firing rate changes were correlated with both LED-based Rm changes in mouse neurons. All this said, we only demonstrated statistical significance for the reduction of AP firing in mouse cortical neurons, and the LED neither statistically significantly modified Rm nor Vrest in either species.

The lack of significance in the human cortical neurons, specifically, may be due to several factors, not least of which are differences in tissue health, the possibility of hypoxia during the transportation from the operating theater to the laboratory, and inter-patient variabilities. Indeed, this last point is the most likely, as the C57bl6 mice used in the experiments are an inbred strain designed to be genetically identical, but humans would of course not be free of genetic differences in the same way. The human neurons also had much larger cellular mortality rates during the experimentation, which we largely attribute to their overall poor levels of neuronal health compared to the mouse cortical tissue. We also observed two instances of strong LED-induced membrane depolarization in human cortical neurons that also increased AP firing activity. This demonstrates the need for more research with human tissues to investigate the effects of light on different neuronal subtypes with greater anatomical specificity than we were able to achieve here. This should ideally take place with live human tissues, but as this is exceedingly difficult to source, we suggest that cultured neurons may also provide insight in this area.

Consistent with previous results, we observed a LED-related tissue temperature increase (1.8°C), which was higher than the increases produced in other studies using lower

light power (<1°C, Ait-Ouares et al., 2019; Lightning et al., 2023). But this is consistent with the expectation that thermal propagation through the tissue will increase with increases to light power and light duration (Stujenske, Spellman, & Gordon, 2015; Senova et al., 2017). Despite the larger temperature increase, the temperature change remained within the rage of natural physiological fluctuation (2-3°C, Andersen & Moser, 1995) so we do not suspect any thermal toxicity to the neurons.

Concerning our conclusions related to ion flux – the effect of the light on Na^+ inward current was consistent with expectations. Indeed, we have observed blue-LED induced reductions to AP amplitude and increases to AP latency (Ait-Ouares et al., 2018; Lightning et al., 2023), and previous works have demonstrated that AP amplitude (decreased), duration (decreased), and latency (increased) are all affected by tissue temperature increase for both cortical and hippocampal neurons (Thompson et al., 1985; Volgushev et al., 2000a;b). It is also well established that these AP properties are intertwined with the Na^+ current (Huguenard & McCormick, 1994).

Light stimulation appears to have two opposite effects on outward (putative K^+) current: an increase during the LED stimulation and a long-lasting decrease thereafter. The current increase can be explained by the thermal effect on this current, which has been previously reported (Thompson, Musukawa, & Prince, 1985). The mechanism that could be behind the post light decrease in this potassium current is, for the moment, unknown. The decrease of the inward currents during LED stimulation is also compatible with known temperature-induced modifications of Na^+ current (Thompson, Musukawa, & Prince, 1985). The post LED reduction of the outward current is likely contributing to the lasting increase of firing observed in some cortical neurons, while the LED and post LED decrease of inward Na^+ currents are likely contributors to the long-lasting decrease of firing activity.

Conclusions

Understanding the longevity and mechanism of LED-induced AP firing effects is essential for determining if this type of brain stimulation has therapeutic merit. We have demonstrated that such an effect is non transient in both human and mouse cortical neurons *in vitro* and established that the reduction generally occurs concomitant to a save level of tissue temperature increase, membrane hyperpolarization, and changes to cation currents implicated in the action potential. While these results are promising, there is still a long way to go before research can determine whether blue-LED stimulation is therapeutically adaptable.

Indeed, some literature has, also described light-stimulation-induced membrane depolarization and increases to neuronal activity *in vivo* (Stujenske, Spellman, & Gordon, 2015; Owen, Liu, & Kreitzer, 2019), and thus we cannot rule out the possibility that the light effect may differ between *in vitro* and *in vivo* conditions. At the very least, it has been demonstrated that light can affect behavior *in vivo*. Specifically, Owen and colleagues (2019) demonstrated that green light stimulation of the striatum and inserted optical probe affected the behavior of mice *in* vivo. Fortunately, research has also shown that this level of invasiveness may not be necessary to induce a light effect in living mammals. Various wavelengths of visible and infrared (IR) light can penetrate the skulls of mice for transcranial brain light stimulation, with enough efficacy to evoke light-related effects to both neuronal physiology and observable behavior (Wu et al., 2012; Zhang et al., 2020). As with mice, visible and IR light are capable of penetrating the human skull (Litsher, D., & Litsher, G., 2013; Sun et al., 2016; Wang & Li, 2019), and transcranial laser light therapies (TLLT) using white, red, and IR light have been used as a treatment for various brain pathologies (Huang, 2022) such as mild traumatic brain injury (Naeser et al., 2016) and depression (Timonen et al., 2012).

REFERENCES

Ait-Ouares, K., Beurrier, C., Canepari, M., Laverne, G., & Kuczewski, N. (2019) Opto nongenetics inhibition of neuronal firing. *Eur. J. Neurosci.*, **49**, 6–26.

Andersen, P., & Moser, E. I. (1995). Brain temperature and hippocampal function. *Hipp.*, ***5*(6)**, 491–498. https://doi-org.docelec.univ-lyon1.fr/10.1002/hipo.450050602

Bates, D. A., & Mackillop, W. J. (1985). The effect of hyperthermia on the sodium-potassium pump in Chinese hamster ovary cells. *Rad. Res.*, **103**, 441–451. https://doi.org/10.2307/3576766

Huang L. D. (2022) Brighten the Future: Photobiomodulation and Optogenetics. *Focus: Amer. Psych. Pub., **20*(1)**, 36–44. https://doi.org/10.1176/appi.focus.20210025

Hodgkin, A. L., Huxley, A. F. (1952). A Quantitative Description of Membrane Current and Its Application to Conduction and Excitation in Nerve. *J. Physio., **117(4)**, 500–544. doi: 10.1113/jphysiol.1952.sp004764*

Hodgkin, A. L., & Katz, B. (1949). The Effect of Sodium Ions on the Electrical Activity of Giant Axon of the Squid. *J. Physio.*, ***(108)*1**, 37–77. doi: 10.1113/jphysiol.1949.sp004310.

Huguenard, J., & McCormick, D. (1994). Electrophysiology of the neuron. Oxford University Press, New York.

Leszkeiwicz, D., & Aizenman, E. (2003) Reversible modulation of GABAa receptor-mediated currents by lights is dependent on the redox state of the receptor. *Eur. J. Neurosci., **17***, 2077-2083. https://doi.org/10.1046/j.1460-9568.2003.02656.x

Lightning, A., Bourzeix, M., Beurrier, C., & Kuczewski, N. (2023) Effects of discontinuous blue light stimulation on the electrophysiological properties of neurons lacking opsin expression in vitro: Implications for optogenetic experiments. *Eur. J. Neurosci.*, **57**(6), 885–899. https://doi.org/10.1111/ejn.15927

Litsher, D., & Litscher, G. (2013) Laser therapy and stroke: Quantification of methodological requirements in consideration of yellow laser. *Int. J. Photo*. http://dx.doi.org/10.1155/2013/575798

Naeser, M. A., Martin, P. I., Ho, M. D., Krengel, M. H., Bogdanova, Y., Knight, J. A., ... & Koo, B. B. (2016) Transcranial, red/near-infrared light-emitting diode therapy to improve cognition in chronic traumatic brain injury. *Photomed. and las. Surg.*, ***34*(12)**, 610-626.

Owen, S.F., Liu, M.H., & Kreitzer, A.C. (2019) Thermal constraints on in vivo optogenetic manipulations. *Nat. Neurosci.*, **22**, 1061–1065.

Saucedo, C. L., Courtois, E. C., Wade, Z. S., Kelley, M. N., Kheradbin, N., Barrett, D. W., & Gonzalez-Lima, F. (2021) Transcranial laser stimulation: Mitochondrial and cerebrovascular effects in younger and older healthy adults. *Brain stim.*, ***14*****(2)**, 440–449. https://doi-org.docelec.univ-lyon1.fr/10.1016/j.brs.2021.02.011

Scharfman, H. E. (2007) The neurobiology of epilepsy. *Curr. Neuro. and Neurosci. Rep.*, *7*(4), 348-354.

Senova, S., Scisniak, I., Chiang, C.-C., Doignon, I., Palfi, S., Chaillet, A., Martin, C., & Pain, F.
(2017) Experimental assessment of the safety and potential efficacy of high irradiance photostimulation of brain tissues. *Sci. Rep.*, **7**, 43997.

Stujenske, J.M., Spellman, T., & Gordon, J.A. (2015) Modeling the Spatiotemporal Dynamics of Light and Heat Propagation for In Vivo Optogenetics. *Cell Rep.*, **12**, 525–534.

Sun, L., Liu, X., Li, X., & Li, M. (2020). Photosensitive inhibition of the GABA system in vitro. *Nature: Sci. Rep.*, ***10***. https://doi.org/10.1038/s41598-020-59915-2

Sun, L., Perakyla, J., Kovalainen, A., Ogawa, K. H., Karhunen, P. J., & Hartikainen, K. M. (2016) Human brain reacts to transcranial extraocular light. *PLoS ONE, **11*****(2)**.

Thomas, E. A., Hawkins, R. J., Richards, K. L., Xu, R., Gazina, E. V., and Petrou, S. (2009)
Heat opens axon initial segment sodium channels: a febrile seizure mechanism? *Ann. Neurol.*, **66**, 219–226.

Thompson, S. M., Masukawa, L. M., & Prince, D. A. (1985) Temperature dependence of intrinsic membrane properties and synaptic potentials in hippocampal CA1 neurons in vitro. *J. Neurosci.*, **5**, 817–824. https://doi.org/10.1523/JNEUROSCI.05-03-00817.1985

Timonen, M., Nissila, J., Liettu, A., Jokelainen, J., Jurvelin, H., Aunio, A., Rasanen, P., & Takala, T. (2012) Can transcranial brain-targetied bright light treatment via ear canals be effective in relieving symptoms in seasonal affective disorder? A pilot study. *Med. Hyp., **78***, 511-515. https://doi.org/10.1016/j.mehy.2012.01.019

Volgushev, M., Vidyasagar, T. R., Chistiakova, M., & Eysel, U. T. (2000a) Synaptic transmission in the neocortex during reversible cooling. *Neurosci.*, **98**, 9–22. https://doi.org/10.1016/ S0306-4522(00)00109-3

Volgushev, M., Vidyasagar, T. R., Chistiakova, M., Yousef, T., & Eysel, U. T. (2000b). Membrane properties and spike generation in rat visual cortical cells during reversible cooling. *J. Physio.*, **522**(Pt 1), 59–76. https://doi.org/10.1111/j.1469-7793.2000.0059m.x

Wang, P., & Li, T. (2019). Which wavelength is optimal for transcranial low-level laser stimulation?. *J. Biopho., **12*****(2)**, e201800173. https://doi.org/10.1002/jbio.201800173

Wu, Q., Xuan, W., Ando, T., Xu, T., Huang, L., Huang, Y.-Y., Dai, T., Dhital, S., Sharma, S.K., Whalen, M.J. and Hamblin, M.R. (2012) Low-Level Laser Therapy for Closed-Head Traumatic Brain Injury in Mice: Effect of Different Wavelengths. *Las. Surg. Med., **(44)***, 218-226. https://doi-org.docelec.univ-lyon1.fr/10.1002/lsm.22003

Zhang, K., D'Souza, S., Upton, B., Kernodle, S., Vemaraju, S., Nayak, G., Holt, A., Linne, C., Smith, A., Petts, N., Batie, M., Mukherjee, R., Tiwari, D., Burh, E., VanGelder, R., Gross, C., Sweeney, A., Sanchez-Guramaches, J., Seeley, R., & Lang, R. (2020) Violet-light suppression of thermogenesis by Opsin 5 hypothalamic neurons. *Nat., **(585)*****7825***, 420-425. doi:10.1038/s41586-020-2683-0.

Study 2 Supplementary Figures

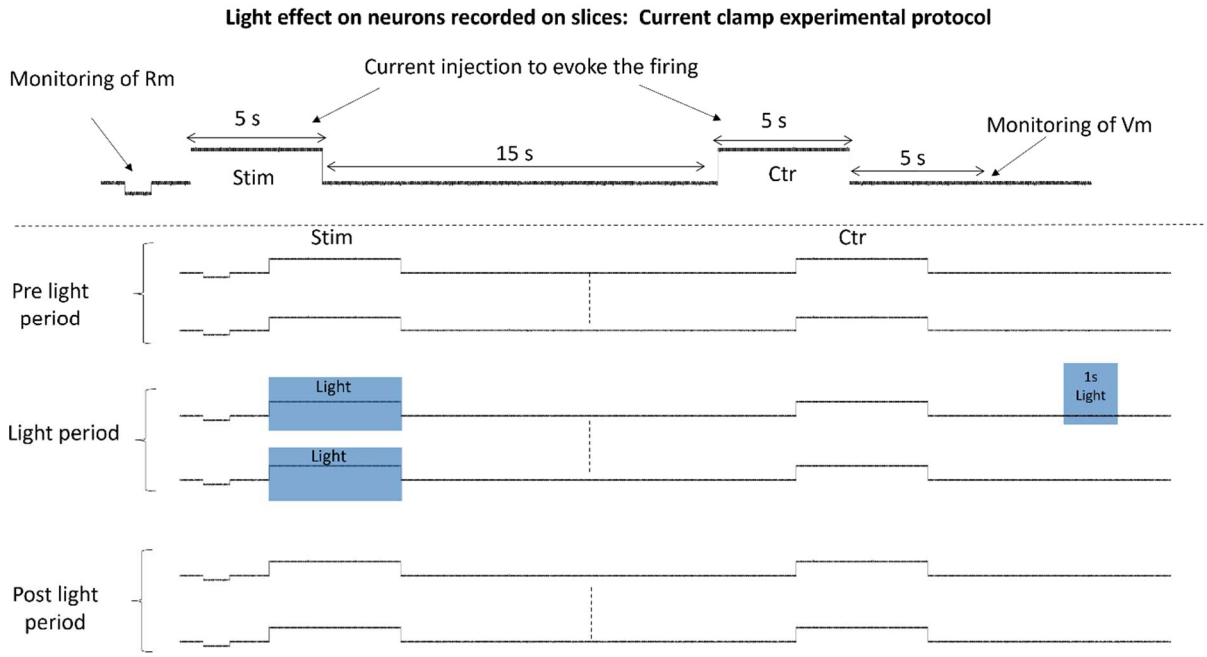

Supplementary Figure 1. Current clamp procedure used in the experiments, as described in the methods.

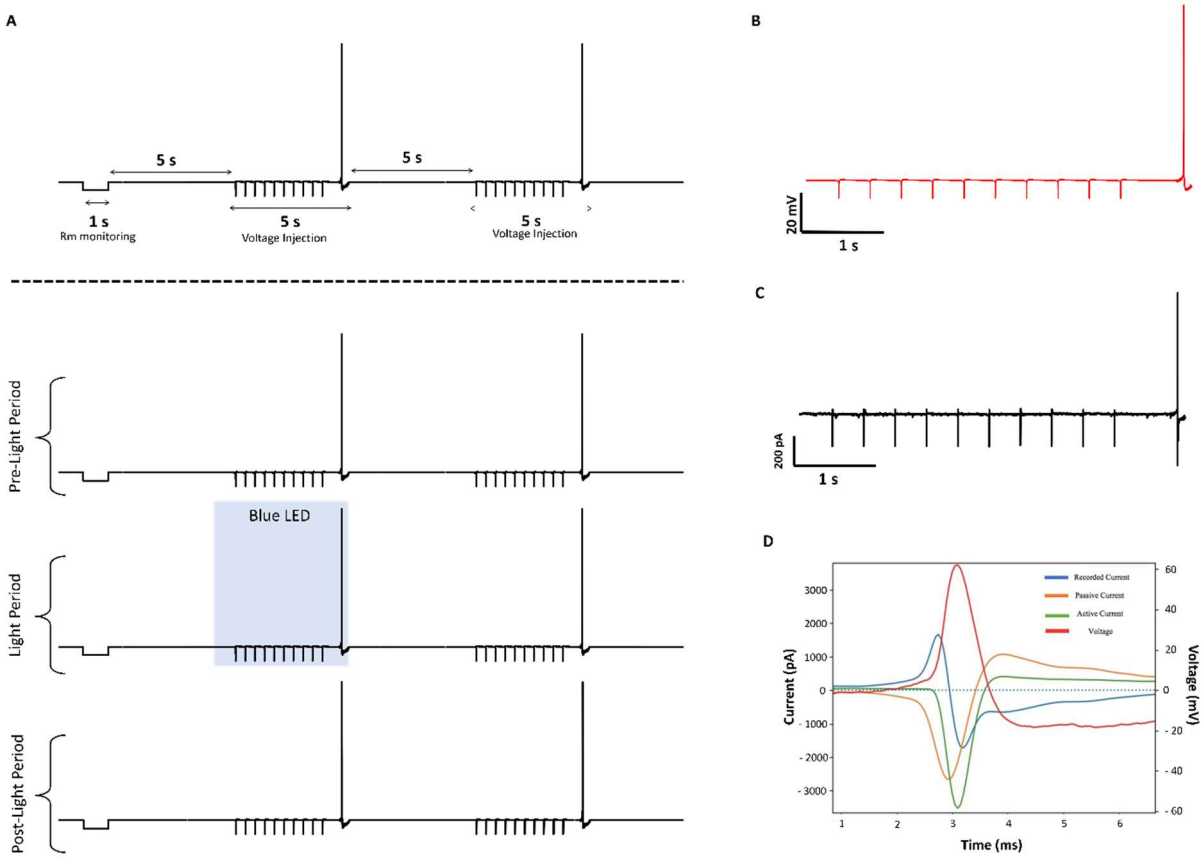

Supplementary Figure 2. Voltage clamp procedure used in the experiments, as described in the methods. **A)** Description of the procedure and example of pre-LED control, LED stimulation, and post-LED periods. **B)** Top, voltage modification applied to the recorded neurons, bottom, recorded currents. **C)** Example of the isolation of active current during AP generation (in red). Total passive current (in orange) was removed from recorded current (in blue) leaving the voltage dependent currents (in green)

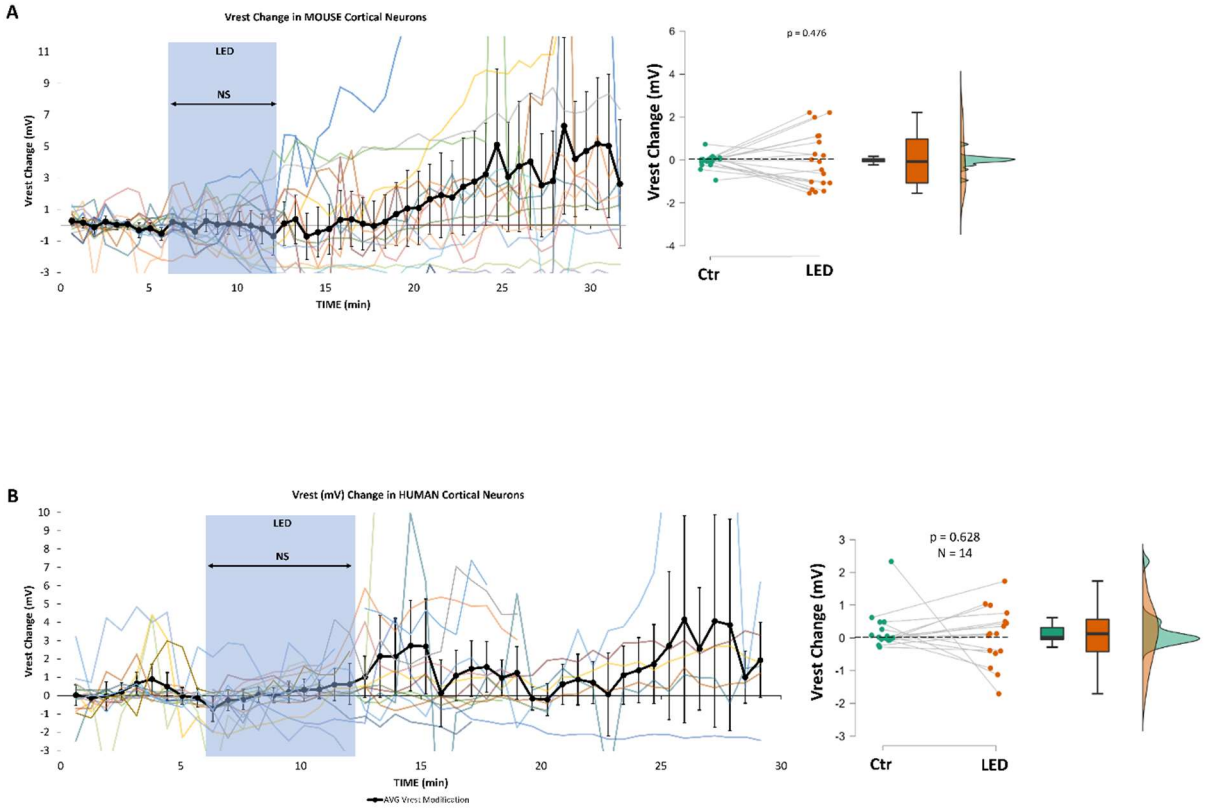

Supplementary Figure 3. Blue LED stimulation reduced AP firing activity in a subpopulation of HUMAN cortical neurons. This effect was non transient, as visualized by the error bars (95% CI), which did not cross back over the threshold of the control activity. N = 11, §: $p < .05$; §§: $p < .01$; §§§: $p < .001$ **A)** LED Vrest change in mouse cortical pyramidal neurons **B)** LED Vrest change in human cortical neurons

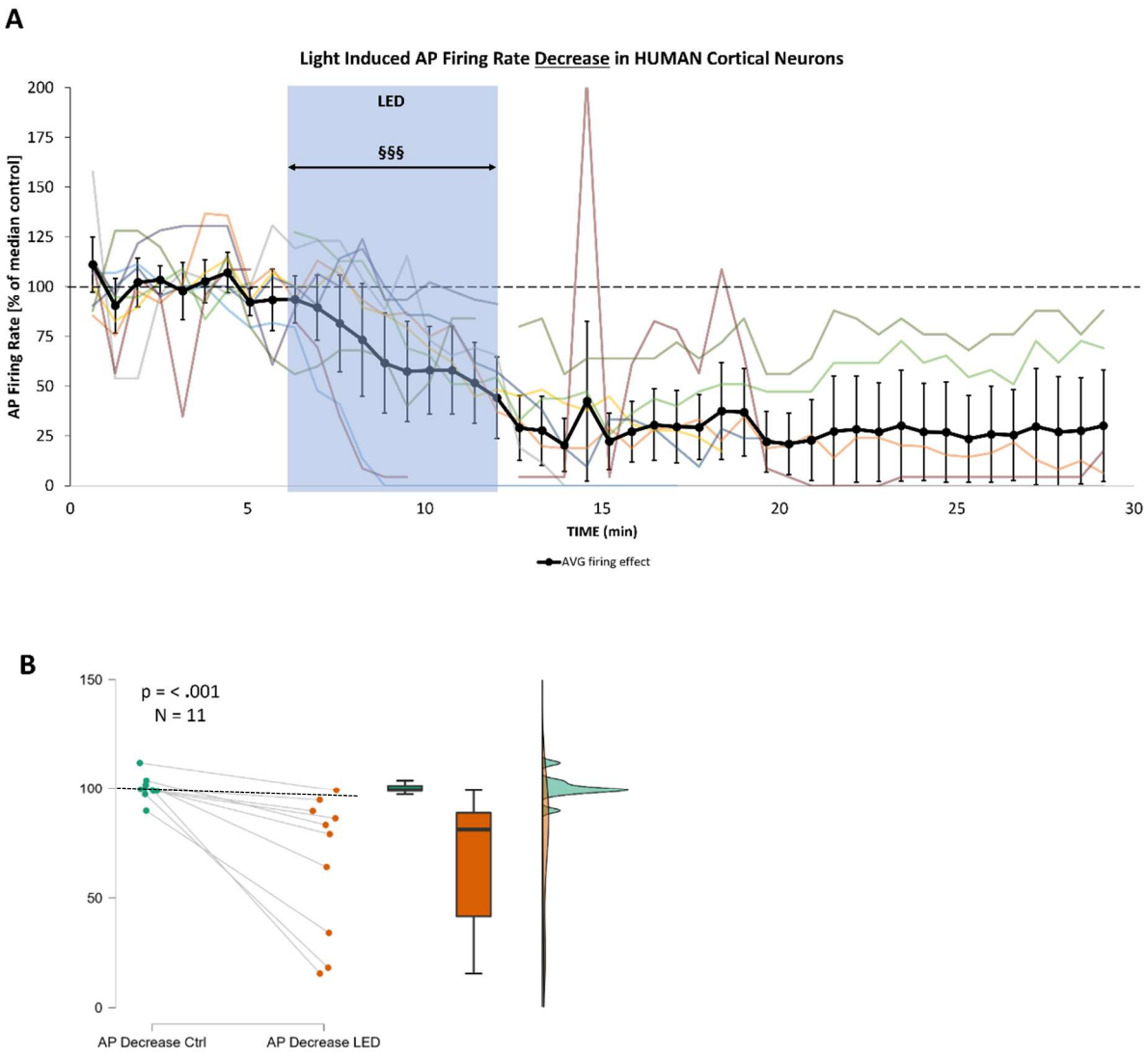

Supplementary Figure 4. Blue LED stimulation reduced AP firing activity in a subpopulation of HUMAN cortical neurons. This effect was non transient, as visualized by the error bars (95% CI), which did not cross back over the threshold of the control activity. N = 11, §: $p < .05$; §§: $p < .01$; §§§: $p < .001$ **A)** AP firing rate evolution under and after LED stimulation. Population average is represented in black. Colored lines represent individual cell's behavior. **B)** Average control period firing behavior compared to average LED firing behavior with p-value listed (Paired Samples Wilcoxon Signed Rank Test, Ctrl > LED)

DISCUSSION

Our work established a couple of key points concerning neuronal light sensibility. In the first study, we established that 1P blue light stimulation (λ = 470) may be producing artefacts for AP firing, AP amplitude, AP latency, and membrane polarization during optogenetic experimentation. However, using discontinuous (pulsed) light stimulation while keeping the power and duty cycle of the light low is a reasonable means to prevent this. Consistent with several other works presented in this thesis, we also established that light stimulation increases the tissue temperature as a function the light power and stimulation duration (Ait-Ouares et al., 2019; Senova et al., 2017), and additionally demonstrated that raising the duty cycle of pulsed light stimulation further increases temperature within these power levels. This tissue temperature increase occurs even for pulsed illumination.

Concerning continuous light's effect on neuronal activity and physiology, the first study established that continuous blue LED stimulation is capable of lowering AP firing frequency, lowering AP amplitude, and increasing AP latency in mouse olfactory MCs, even when the duty cycle and stimulation durations are low. This was also true for the induction of an outward hyperpolarizing current in MCs. However, we can only say that this occurred at 13mW light power, as 1mW and 5mW were not tested for continuous stimulation. We tested multiple neuronal subtypes in study 1, but all those other than olfactory MCs are only tested with a high power and high duty cycle pattern, termed pattern 4 (13mW, 40% duty cycle with a pulse length of 20ms) that had a continuous illumination time of 1s.

Continuous (1s) illumination of neurons under pattern 4 produced membrane hyperpolarization (when compared with the control period) in MCs, but also in cortical pyramidal neurons, fast spiking interneurons, MSNs in the striatum, and hippocampal granular

cells. The continuous blue LED also lowered AP amplitude in all cell types but did not change AP latency in any cell types except MCs. We did not measure the effect of the LED on AP firing rates for any neuronal types other than MCs.

The effect of the light stimulation in study 1 was typically transient for both pulsed and continuous stimulation. Even so, we were able to take the knowledge that 13mW light power produced neuronal effects even at low duty cycles and stimulation times ≤1s and conceive of the possibility of using these light-mediated changes in a therapeutic context. The first step of that was, of course, to see if we could establish a safe (read: non-thermo-toxic) and long-lasting AP firing reduction effect with higher light powers and greater stimulation times (19mW, 5s continuous stimulation). We achieved this in study 2 on mouse cortical pyramidal neurons but were not so successful with human cortical neurons. We were able to establish this long-lasting reduction in 68.8% of the human neurons, but this did not result in statistical significance for the whole neuronal population we tested. In tandem with results from study 1, we demonstrated a consistent LED induced membrane hyperpolarization that occurs in all in mouse cortical neurons tested. On the other hand, a clear light-induced membrane depolarization was produced in two (12.5%) human cortical neurons, while in the others light clearly hyperpolarized the Vm.

The heterogeneity of the effect of light on firing activity correlates with the light induced modification of Rm in mouse neurons suggesting that light effects are, in part, mediated by the modification of channels involved in passive membrane properties. But the long-lasting modification of the firing rate can also be ascribed to the light induced decrease of voltage dependent K^+ and Na^+ currents participating in the AP generation. As previously shown, a transient hyperpolarization of Vm was observed during light stimulation in all mice neurons and in the majority of human neurons. This effect has been proposed to be due to the activation of K_{ir} channels (Owen at al 2019). Although the mechanism behind this remains unknown, these effects mark a singularity in the physiology of some cortical human neurons compared to mice

neurons. These conclusions are interesting, but overall do not necessarily mean that this type of blue light stimulation can be therapeutically adaptable for epileptic disorders or other neurological conditions. Further establishing whether or not this is viable would require much more research. For this, I have some recommendations.

Future Investigative Directions

The future of research in this direction must contain both *in vitro* and *in vivo* elements. I have recommendations for both, but I will begin with *in vitro*, both because this is the logical first step and because we attempted to further the present investigation into therapeutic adaptability in this area. Using the methodology described by Losi et al. (2016), we attempted to induce seizure-like discharges (SLD) in the young rat (post-natal day 15-19) temporal cortex with puff application of NMDA. The animals were prepared and dissected in accordance with our previous methodologies for mice, and the ACSF solutions and perfusions were the same as in Losi (2016). We conducted some pilot experiments to determine (a) whether we could both produce and record NMDA induced SLD *in vitro* with our equipment and (b) whether we could visually identify any preliminary LED-induced reductions in SLD activity (same light stimulation parameters as in study 2). We first used single cell patch clamp to determine if we could reproduce Losi et al.'s (2016) results (Figure 23A) in this area. We were minimally successful, eliciting the response in only one attempt. However, this one success displayed a very similar result to the Losi study (Figure 23B). To test the effect of the LED, we then switched to cell-attached recording to monitor only AP at single cell level. In this configuration, we were not able to produce the same activity profile as the Losi study, as ours was much shorter in duration. The duration was so short as to not be truly representative of epileptic activity, but it was able to be evoked in the expected pattern: an initial burst of electrical activity under the NMDA, followed by a brief pause before the generation of late

firing. During the LED stimulation period, the slice was subjected to 10 pulses of 10s/19mW blue LED stimulation separated by 30s each. While immediately after the LED period the NMDA response was only slightly reduced, a complete loss of response was observed thereafter (Figure 23C, bottom).

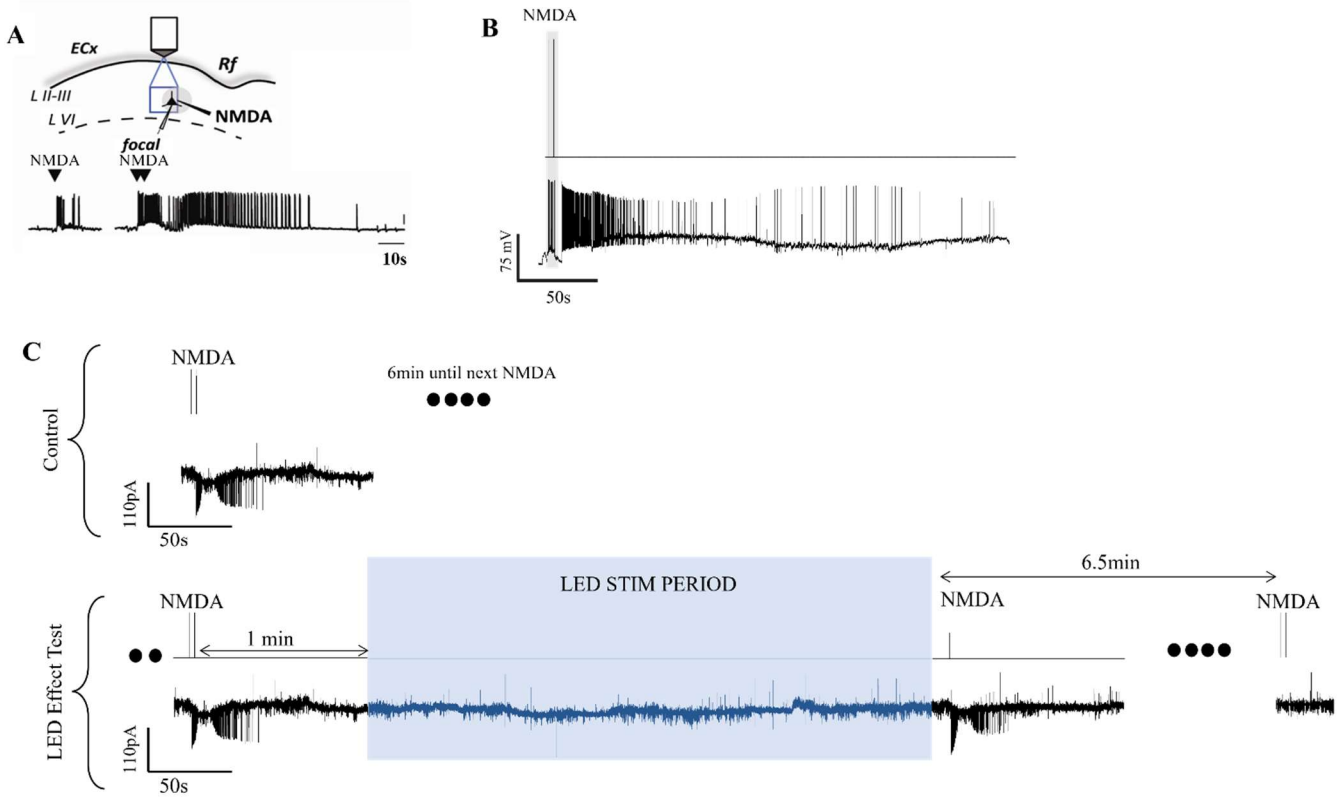

Figure 27. Pilot experiments on blue LED suppression of induced seizure-like discharge in the young rat temporal lobe. A) Top: experimental setup for the induction of SLD in the rodent temporal lobe via NMDA superfusion. Bottom: Recorded SLD activity in patched pyramidal neuron - per Losi et al., 2016. B) Our own preliminary results were not able consistently replicate the results. B) In one neuron in patch clamp, we were able to replicate the Losi results for patched cells. C) In cell attached recording, we were not able to replicate the activity profile (note the much shorter activity) but did observe some preliminary evidence of a delayed light effect. The top and bottom pieces are part of one continuous sweep.

The preliminary electrophysiology shows promise for the methodology as a proof of concept, and I am hopeful that the lab will be able to find more concrete and statistically significant evidence for blue-LED reduction in SLD as time progresses. There is a third line of *in vitro* investigation that would also prove useful, as it may have merit for establishing a way to predict how various neuronal subtypes will respond to blue-LED stimulation based on their baseline membrane physiology properties. This would be very useful, as establishing a therapeutic basis required the ability to predict how the brain will respond to the stimulation

under the realistic conditions of a living organism. This recommendation comes from the results of study 2, where exploratory analysis weakly suggested the potential for such a relationship.

Study 1 of this investigation and some previous works mentioned in the literature (Ait-Ouares et al., 2019; Owen, Liu, & Kreitzer, 2019) investigated various neuronal subtypes during their protocols. I recommend that future research similarly isolates various neuronal subtypes *in vitro*, recording the same baseline membrane physiology parameters and spontaneous firing activity we recorded in study 2 for the exploratory analysis (see study 2, supplementary table 3 for the complete list of variables). These studies could then use the same electrically evoked AP methodologies we used in studies 1 and 2 to discern the effect of light stimulation from 1P-blue LED (or other wavelengths and light stimulation types) on the firing, which could then be correlated with the membrane physiology data.

If a study like this were presented in isolation, computational analysis approaches using predictive modeling would theoretically be the ideal method of analysis, though there are incredible challenges to implementing such an approach in medical neurosciences, not the least of which being methodical constraints that separate pre-clinical work from real-world conditions, in addition to the lack of predictability for the normality of results (Bzdok & Ioannidis, 2019). Well established linear regression modeling could fill the gap (Bzdok & Ioannidis, 2019), but non-normal data remain a difficulty here as well. Fortunately, a correlation-based model may suffice as a component part of a pre-clinical investigation, so long as the results were reproducible and could be presented in tandem with other work investigating light-effects on factors such as SLD and with *in vivo* work that may be able to demonstrate that the light is not, in fact, making the hyperexcitability worse. This is a legitimate concern, as some studies (Stujenske Spellman, & Gordon, 2015) in addition to our own work in study 2 showed an increase in firing activity in principal cortical neurons when light stimulation was delivered within an *in vitro* animal model Thankfully, *in vivo* work may be able to abate some

of those concerns. Common pre-clinical mouse-models of epilepsy include both induced models, which use electrical stimulation or exposure to chemical compounds to cause mice to develop seizures, and genetic models, which generate missense and complex knockout mutations (often through the use of CRISPR:Cas9) to create genetically seizure-prone animals (Marshall, Gonzalez-Sulser, & Abbott, 2021). Induction models may be the most controllable and applicable for investigating light-stimulation effects; Indeed, while the genetic models have been historically useful in identifying associated molecular mechanisms, the genetic background of these mice can be variable, and it is often difficult to monitor and record seizures in these animals due to natural variations in the frequency and severity of episodes (Marshall, Gonzalez-Sulser, & Abbott, 2021).

Tethered telemetry (the insertion of a neural probe into the brain) in combination with an inserted optical LED probe, the combination often used in optogenetics to record *in vivo* electrophysiology could provide a methodological avenue to investigate light effects on induced epilepsy models. Wireless telemetry recording, which uses a wireless neurosensory probe and remains capable of transmitting full spectrum electrophysiological data while allowing the animal free movement (per developers Yin et al., 2014) could offer a viable solution for these investigations in genetic models, and indeed could be applied as a less restrictive recording method for induced models as well. This methodology has been further developed over the last 9 years, and wireless telemetry probes are now readily available for optogenetic experiments. Therefore, combining it with optical LED stimulation should pose no issue.

However, part of the goal of developing a light therapy for epileptic hyperexcitability is making the treatment minimally- or non-invasive. Deep brain stimulation probes are, of course, acceptably used in neuropathic treatments, the most well-known perhaps being with Parkinson's disease, but such invasive means should not be relied upon if they can be avoided. Light in the visual and IR spectrums are capable of penetrating the skulls of both humans and

mice (see section 1.1d). Further, white light therapy delivered vis the ear canals seem to improve depressive symptoms, and emotional cognition (Sun et al., 2016; Timonen et al., 2012) and transcranial laser light therapy has shown promise for improving both TBI recovery and cognitive function (Huang, 2022). These effects are all, however, results of increases to activity. LED-induced activity increase in naïve mouse brain has been shown capable of producing behavioral consequences *in vivo* (Owen, Liu, & Kreitzer, 2019). It appears to be currently unknown (a) whether light stimulation can trigger activity reductions in the mouse brain *in vivo* and (b) whether transcranial light stimulation is capable of this in in less invasive manner.

There are several ways to investigate one or the other, or indeed to investigate both simultaneously. I propose that one such method could make use of behavioral assays that evaluate animal task success rate. Given our study 1 results concerning activity reduction in mouse olfactory MCs in tandem with the Ait-Ouares (2019) study's similar findings in that neuronal type, I propose that an olfaction detection task could be easily adapted for this purpose. One of the original plans for moving the present investigation into *in vivo* territory was, in fact, just such an experiment. Mice would be trained to identify limonene-marked radial maze arms, being granted a food reward upon successful identification of the correct arm (Figure 24A). A transcranial blue light optical probe would be affixed to the test group of mice, and they would perform the task concomitant to transcranial blue LED stimulation, which would then allow the team to compare success rates as a way of discerning the presence of LED-induced olfactory bulb suppression (Figure 24B, below).

The options for future investigative directions presented here are just some examples of the options available. I have provided some summative recommendations that I hope will aid in framing the continuing ideas of my current team and others that seek to continue this investigation.

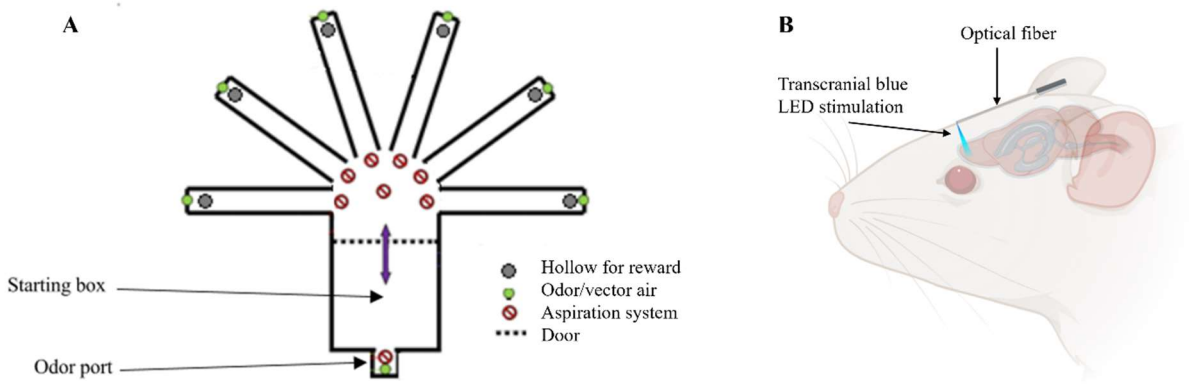

Figure 28. Proposed adaptation of task-based behavioral studies to identify any transcranial blue LED effect in mouse olfaction. A) Typical radial maze experimental design. B) Model of transcranial LED placement, affixed with veterinary glue.

Conclusions

The applicability of naïve neuronal sensibility in therapeutic avenues is a complex and evolving topic. Though there has been much evolution in the medical adaptability of light in areas such as TLLT, other options for using light to treat neural pathologies are still in in the pre-clinical conceptualization phase. Our results and those presented throughout this thesis show promise for this area, but need to push much further before pre-clinical ideas can develop viability, especially considering epileptic syndromes. The results from this investigation have been positive, and it is thus my sincere hope that the line of questioning continues to develop. Even if blue-light stimulation does not become an answer to drug-resistant epilepsies and other pathological hyperexcitability, I am certain that the scientific process will persevere, and that results from this line of questioning will join the chain of inspiration for the research that ultimately produces medical solutions.

BIBLOGRAPHIC REFERENCES

Ait-Ouares, K., Beurrier, C., Canepari, M., Laverne, G., & Kuczewski, N. (2019). Opto nongenetics inhibition of neuronal firing. *European Journal of Neuroscience*, 1-21. https://doi.org/10.1111/ejn.14251

Acharya, A. R., Vandekerckhove, B., Larsen, L. E., Delbeke, J., Wadman, W. J., Vonck, K., Carette, E., Meurs, A., Vanfleteren, J., Boon, P., Missinne, J., & Raedt, R. (2021). *In vivo*blue light illumination for optogenetic inhibition: effect on local temperature and excitability of the rat hippocampus. *Journal of neural engineering*, *18*(6). https://doi-org.docelec.univ-lyon1.fr/10.1088/1741-2552/ac3ef4

Aravanis, A.M., Wang, L.P., Zhang, F., Meltzer, L.A., Mogri, M.Z., Schneider, M.B., & Deisseroth, K. (2007). An optical neural interface: in vivo control of rodent motor cortex with integrated fiberoptic and optogenetic technology. *Journal of Neural Engineering (4)*, S143–S156. http://dx.doi.org/10.1088/1741-2560/4/3/S02

Arsonval, A. D. (1891). La fibre musculaire est directement excitable par la lumiere. CR Soc. Biol, 43, 318-320.

Arvanitaki, A., & Chalazonitis, N. (1961). *Excitatory and inhibitory processes initiated by light and infra-red radiations in single identifiable nerve cells (giant ganglion cells of Aplysia)*. Pergamon Press.

Arvanitaki, A., Chalazonitis, N., & Costa, H. (1964). Excitation of the Giant Neuron by Crossed Exponential Transmembranal Currents (Aplysia Fasciata). *Comptes Rendus Des Seances de La Societe de Biologie et de Ses Filiales*, *158*, 2373–2377.

Balaban, P., Esenaliev, R., Karu, T., Kutomkina, E., Letokhov, V., Oraevsky, A., & Ovcharenko, N. (1992). He-Ne laser irradiation of single identified neurons. *Lasers in surgery and medicine*, *12*(3), 329-337.

Barrett, D. W., & Gonzalez-Lima, F. (2013). Transcranial infrared laser stimulation produces beneficial cognitive and emotional effects in humans. *Neuroscience 230*, 13-23. https://doi-org.docelec.univ-lyon1.fr/10.1016/j.neuroscience.2012.11.016

Blackshaw, S., & Snyder, S. H. (1999). Encephalopsin: A novel mammalian extraretinal opsin discretely localized in the brain. *The Journal of Neuoscience, 19*(10), 3681-3690.

Blanco, N. J., Maddox, W. T., & Gonzalez-Lima, F. (2015). Improving executive function using transcranial infrared laser stimulation. *Journal of Neuropsychology, 11*(1), 14-25. https://doi.org/10.1111/jnp.12074

Booth, J., Von Muralt, A., & Stampfli, R. (1950). The photochemical action of ultra-violet light on isolated single nerve fibres. *Helvetica physiologica et pharmacologica acta*, *8*(2), 110-127.

Boyden, E.S. (2011). A history of optogenetics: The development of tools for controlling brain circuits with light. *F1000 Biology Reports, 3*(11). DOI: 10.3410/B3-11

Boyden, E. S., Zhang, F., Bamberg, E., Nagel, G., & Deisseroth, K. (2005). Millisecond-timescale, genetically targeted optical control of neural activity. *Nature Neuroscience, 8*, 1263–1268. https:// doi.org/10.1038/nn1525

Byrne, J.H. (Ed.), Heidelberger, R. (Ed.), & Waxham, M. N. (Ed.). (2014). *From molecules to networks: An introduction to cellular and molecular neuroscience*. Academic Press.

Bzdok, D., & Ioannidis, J. P. A. (2019). Exploration, Inference, and Prediction in Neuroscience and Biomedicine. *Trends in neurosciences*, *42*(4), 251–262. https://doi-org.docelec.univ-lyon1.fr/10.1016/j.tins.2019.02.001

Cardin, J. A., Carlen, M., Meletis, K., Knoblich, U., Zhang, F., Deisseroth, K., et al. (2009). Driving fast-spiking cells induces gamma rhythm and controls sensory responses. Nature 459, 663–667. doi: 10.1038/nature08002

Chen, W., Li, C., Liang, W., Li, Y., Zou, Z., Xie, Y., Liao, Y., Yu, L., Lin, Q., Huang, M., Li, Z., Zhu, X. (2022). The roles of optogenetics and technology in neurobiology: A review. *Frontiers in Aging Neuroscience, 14*, doi: 10.3389/fnagi.2022.867863

Christie, I. N., Wells, J. A., Southern, P., Marina, N., Kasparov, S., Gourine, A. V., & Lythgoe, M. F. (2013). fMRI response to blue light delivery in the naive brain: implications for combined optogenetic fMRI studies. *Neuroimage*, *66*, 634-641. https://doi-org.docelec.univ-lyon1.fr/10.1016/j.neuroimage.2012.10.074

Deisseroth, K. (2015). Optogenetics: 10 years of microbial opsins in neuroscience. Nature Neuroscience, 18, 1213–1225. https://doi. org/10.1038/nn.4091

Deng, W., Goldys, E. M., Farnham, M. M. J., & Pilowski, P. M. (2014). Optogenetics, the intersection between physics and neuroscience: Light stimulation of neurons in physiological conditions. American Journal of Physiology: Regulatory, Integrative, and Comparative Physiology, 307. https://doi.org/10.1152/ajpregu.00072.2014

Duke, A. R., Jenkins, M. W., Lu, H., McManus, J. M., Chiel, H. J., & Jansen, E. D. (2013). Transient and selective suppression of neural activity with infrared light. Scientific Reports, 3. https://doi.org/10.1038/srep02600

Fenno, L., Yizhar, O., & Deisseroth, K. (2011). The development and application of optogenetics. Annual Review of Neuroscience, 34, 389–412. https://doi.org/10.1146/annurev-neuro-061010-113817

Feng, H. J., Kao, C., Gallagher, M. J., Jansen, E. D., Mahadevan-Jansen, A., Konrad, P. E., & Macdonald, R. L. (2010). Alteration of GABAergic neurotransmission by pulsed infrared laser stimulation. *Journal of neuroscience methods*, *192*(1), 110–114. https://doi-org.docelec.univ-lyon1.fr/10.1016/j.jneumeth.2010.07.014

Fischer, R. M., Fontinha, B. M., Kirchmaier, S., Steger, J., Bloch, S., Inoue, D., Panda, S., Rumpel, S., & Tessmar-Raible, K. (2013). Co-expression of VAL- and TMT-opsins uncovers ancient photosensory interneurons and motorneurons in the vertebrate brain. *PLoS Biol, 11*(6): e1001585. https://doi.org/10.1371/journal.pbio.1001585

Fisher, R. S., Scharfman, H. E., & deCurtis, M. (2014). How can we identify ictal and interictal abnormal activity?. *Advances in experimental medicine and biology*, *813*, 3–23. https://doi-org.docelec.univ-lyon1.fr/10.1007/978-94-017-8914-1_1

Fork, R. L. (1971). Laser Stimulation of Nerve Cells in Aplysia. *Science*, *171*(3974), 907–908. http://www.jstor.org/stable/1731369

Frankenhauser, B., & Moore, L. (1963). The effect of temperature on the sodium and potassium permeability changes in the myelinated nerve fibres of xenopus laevis. *Journal of Physiology, 169*, 431-437.

Friedman, D., Hoagland, A., Berlin, S., & Isacoff, E. Y.G (2015). A spinal opsin controls early neural activity and drives a behavioral light response. *Current Biology*, *25*, 69-74. http://dx.doi.org/10.1016/j.cub.2014.10.055

Gong, J., Yuan, Y., Ward, A., Kang, L., Zhang, B., Wu, Z., Peng, J., Feng, Z., Liu, J., & Xu, X. Z. S. (2016). The c. elegans taste receptor homolong LITE-1 is a photoreceptor. *Cell, 167*, 1252-1263. http://dx.doi.org/10.1016/j.cell.2016.10.053

Gutiérrez-Menéndez, A., Marcos-Nistal, M., Méndez, M., & Arias, J. L. (2020). Photobiomodulation as a promising new tool in the management of psychological disorders: A systematic review. *Neuroscience & Biobehavioral Reviews, 119*, 242–254. https://doi.org/10.1016/j.neubiorev.2020.10.002

Hallett, R. A., Zimmerman, S. P., Yumerefendi, H., Bear, J. E., and Kuhlman, B. (2016). Correlating in vitro and in vivo activities of light-inducible dimers: a cellular optogenetics guide. *ACS Synth. Biol. 5*, 53–64. doi: 10.1021/acssynbio.5b00119

Hardie, R. C., & Franze, K. (2012). Photomechanical responses in drosophilia photoreceptors. *Science, 338*. https://doi.org/10.1126/science.1222376

Henley, C. (2021). *Foundations of Neuroscience*. Michigan State University Libraries. https://openbooks.lib.msu.edu/neuroscience/

Hamblin, M. R. (2016). Shining light on the head: Photobiomodulation for brain disorders. *BBA Clinical, 6*, 113-124. http://dx.doi.org/10.1016/j.bbacli.2016.09.002

Hamblin, M. R. (2018). Mechanisms and Mitochondrial Redox Signaling in Photobiomodulation. *Photochemistry and photobiology*, *94*(2), 199–212. https://doi-org.docelec.univ-lyon1.fr/10.1111/php.12864

Hodgkin, A. L., Huxley, A. F. (1952a). A Quantitative Description of Membrane Current and Its Application to Conduction and Excitation in Nerve. *The Journalof Physiology, 117(4), 500–544. doi: 10.1113/jphysiol.1952.sp004764.*

Hodgkin, A. L., Huxley, A. F. (1952b). Currents carried by sodium and potassium ions through the membrane of the giant axon of Loligo. *The Journal of Physiology, 116(4)* doi: 10.1113/jphysiol.1952.sp004717.

Hodgkin, A. L., & Katz, B. (1949). The Effect of Sodium Ions on the Electrical Activity of Giant Axon of the Squid. *The Journal of Physiology*, *(108)*1, 37–77. doi: 10.1113/jphysiol.1949.sp004310.

Huang L. D. (2022). Brighten the Future: Photobiomodulation and Optogenetics. *Focus: American Psychiatric Publishing, 20*(1), 36–44. https://doi.org/10.1176/appi.focus.20210025

Huguenard, J., & McCormick, D. (1994). Electrophysiology of the neuron. Oxford University Press, New York.

Jiang, S., Wu, X., Rommelfanger, N., Ou, Z., & Hong, G. (2022) Shedding light on neurons: Optical approaches to neuromodulation. *National Science Review, (9)*. https://doi.org/10.1093/nsr/nwac007

Kashio, M., & Tominaga, M. (2022). TRP channels in thermosensation. *Current opinion in neurobiology*, *75*, 102591. https://doi-org.docelec.univ-lyon1.fr/10.1016/j.conb.2022.102591

Kim, J., & Connors, B. (2012). High temperatures alter physiological properties of pyramidal cells and inhibitory interneurons in hippocampus. *Frontiers in Cellular Neuroscience, 6*. https://doi.org/10.3389/fncel.2012.00027

Leszkeiwicz, D., & Aizenman, E. (2003). Reversible modulation of GABAa receptor-mediated currents by lights is dependent on the redox state of the receptor. *European Journal of Neuroscience, 17*, 2077-2083. https://doi.org/10.1046/j.1460-9568.2003.02656.x

Lightning, A., Bourzeix, M., Beurrier, C., & Kuczewski, N. (2023). Effects of discontinuous blue light stimulation on the electrophysiological properties of neurons lacking opsin expression in vitro: implications for optogenetic experiments. *European Journal of Neuroscience, 57*(6), 885-899. https://doi.org/10.1111/ejn.15927

Litsher, D., & Litscher, G. (2013). Laser therapy and stroke: Quantification of methodological requirements in consideration of yellow laser. *International Journal of Photoenergy*. http://dx.doi.org/10.1155/2013/575798

Liu, Y., Lopez-Santiago, L. F., Yuan, Y., Jones, J. M., Zhang, H., O'Malley, H. A., Patino, G. A., O'Brien, J. E., Rusconi, R., Gupta, A., Thompson, R. C., Natowicz, M. R., Meisler, M. H., Isom, L. L., & Parent, J. M. (2013). Dravet syndrome patient-derived neurons suggest a novel epilepsy mechanism. *Annals of neurology*, *74*(1), 128–139. https://doi-org.docelec.univ-lyon1.fr/10.1002/ana.23897

Losi, G., Marcon, I., Mariotti, L., Sessolo, M., Chiavegato, A., & Carmignoto, G. (2016). A brain slice experimental model to study the generation and the propagation of focally-induced epileptiform activity. *Journal of neuroscience methods*, *260*, 125–131. https://doi-org.docelec.univ-lyon1.fr/10.1016/j.jneumeth.2015.04.001

Lyon Epilepsy Institute (2016, September 8). *Epilepsy*. Fondation-Idee. https://www.fondation-idee.org/L-epilepsie_a39.html

Marshall, G. F., Gonzalez-Sulser, A., & Abbott, C. M. (2021). Modelling epilepsy in the mouse: challenges and solutions. *Disease models & mechanisms*, *14*(3), dmm047449. https://doi-org.docelec.univ-lyon1.fr/10.1242/dmm.047449

Mie, G. (1908). Beiträge zur Optik trüber Medien, speziell kolloidaler Metallösungen. *Annalen der Physik*, *330 (3)*. 377–445. doi:10.1002/andp.19083300302.

Meisler, M. H., Kearney, J., Ottman, R., & Escayg, A. (2001). Identification of epilepsy genes in human and mouse. *Annual review of genetics*, *35*, 567–588. https://doi-org.docelec.univ-lyon1.fr/10.1146/annurev.genet.35.102401.091142

Naeser, M. A., Martin, P. I., Ho, M. D., Krengel, M. H., Bogdanova, Y., Knight, J. A., ... & Koo, B. B. (2016). Transcranial, red/near-infrared light-emitting diode therapy to improve cognition in chronic traumatic brain injury. *Photomedicine and laser surgery*, *34*(12), 610-626.

Nilius, B., & Szallasi, A. (2014). Transient receptor potential channels as drug targets: from the science of basic research to the art of medicine. *Pharmacological reviews*, *66*(3), 676–814. https://doi-org.docelec.univ-lyon1.fr/10.1124/pr.113.008268

Nissila, J., Manttari, S., Sarkoija, T., Tuominen, H., Takala, T., Timonen, M., & Saarela, S. (2012). Encephalopsin (OPN3) protein abundance in the adult mouse brain. *Journal of Comparative Physiology, 198*, 833-839. https://doi.org/10.1007/s00359-012-0754-x

Noether, E. (1918). "Invariante Variationsprobleme"

- **Noether, E.** [Translated by Tavel, M.] (1971). "Invariant Variation Problems". *Transport Theory and Statistical Physics*. *1*(3): 186–207. doi:10.1080/00411457108231446

Nortje, J., & Menon, D. K. (2004). Traumatic brain injury: physiology, mechanisms, and outcome. *Current opinion in neurology*, *17*(6), 711–718. https://doi-org.docelec.univ-lyon1.fr/10.1097/00019052-200412000-00011

Orchardson, R., Peacock, J. M., & John Whitters, C. (1997). Effect of pulsed Nd: YAG laser radiation on action potential conduction in isolated mammalian spinal nerves. *Lasers in Surgery and Medicine: The Official Journal of the American Society for Laser Medicine and Surgery*, *21*(2), 142-148. DOI: 10.1002/(SICI)1096-9101(1997)21:2<142::AID-LSM5>3.0.CO;2-Q

Owen, S. F., Liu, M. H., & Kreitzer, A. C. (2019). Thermal constraints on in vivo optogenetic manipulations. *Nature Neuroscience*. https://doi.org/10.1038/s41593-019-0422-3

Passarella, S., & Karu, T. (2014). Absorption of monochromatic and narrow band radiation in the visible and near IR by both mitochondrial and non-mitochondrial photoacceptors results in photobiomodulation. *Journal of photochemistry and photobiology*. *B, Biology, 140*, 344–358. https://doi-org.docelec.univ-lyon1.fr/10.1016/j.jphotobiol.2014.07.021

Pastore, D., Greco, M., & Passarella, S. (2000). Specific helium-neon laser sensitivity of the purified cytochrome c oxidase. *International journal of radiation biology*, *76*(6), 863–870. https://doi-org.docelec.univ-lyon1.fr/10.1080/09553000050029020

Pennes, H. H. (1948). Analysis of tissue and arterial blood temperatures in the resting human forearm. *Journal of applied physiology, 1*(5). https://doi-org.docelec.univ-lyon1.fr/10.1152/jappl.1998.85.1.5

Pierroz, V., & Folcher, M. (2018). From photobiomodulation to optogenerapy, recent advances in NIR light photomedicine applications. *Journal of Molecular Genetics and Medicine, 2*(1:10). http://www.imedpub.com/journal-molecular-genetics-medicine/

Podgorski, K., & Ranganathan G. (2016). Brain heating induced by near infrared lasers during multiphoton microscopy. *Journal of Neurophysiology, 116*, 1012-1023. https://doi.org/10.1152/jn.00275.2016

Portela, A., Vasallo, G., Campi, M., Guardado, M. I., Stewart, P. A., Gimeno, A. L., Jenerick, H., & Rozzell, T. C. (1978). Temperature effects on the properties of the Hodgkin-Huxley propagated action potential model determined by computed solutions and phase-plane analysis. *Acta physiologica latino americana*, *28*(6), 271–307.

Provencio, I., Jiang, G., DeGrip, W.J., Hayes, W.P., & Rollag, M.D. (1998). Melanopsin: An opsin in melanophores, brain, and eye. *PNAS USA (95)*, 340-345

Prüss, H., Derst, C., Lommel, R., & Veh, R. W. (2005). Differential distribution of individual subunits of strongly inwardly rectifying potassium channels (Kir2 family) in rat brain. *Brain research. Molecular brain research*, *139*(1), 63–79. https://doi-org.docelec.univ-lyon1.fr/10.1016/j.molbrainres.2005.05.006

Ragsdale D. S. (2008). How do mutant Nav1.1 sodium channels cause epilepsy?. *Brain research reviews*, *58*(1), 149–159. https://doi-org.docelec.univ-lyon1.fr/10.1016/j.brainresrev.2008.01.003

Rhee, A. Y., Gong, L., Wells, J., Kao, J. P. Y. (2008). Photostimulation of sensory neurons of the rat vagus nerve. *Proc. SPIE BiOS (6854), Optical Interactions with Tissue and Cells XIX*. https://doi.org/10.1117/12.772037

Richardson, R. T., Ibbotson, M. R., Thompson, A. C., Wise, A. K., & Fallon, J. B. (2020). Optical stimulation of neural tissue. Healthcare technology letters, 7(3), 58–65. https://doi.org/10.1049/htl.2019.0114

Richter, C., & Tan, X. (2014). Photons and neurons. *Hearing Research, 311*. http://dx.doi.org/10.1016/j.heares.2014.03.008

Rungta, R. L., Osmanski, B., Boido, D., Tanter, M., & Charpak, S. (2017). Light controls cerebral blood flow in naïve animals. *Nature Communications*. https://doi.org/10.1038/ncomms14191

Saucedo, C. L., Courtois, E. C., Wade, Z. S., Kelley, M. N., Kheradbin, N., Barrett, D. W., & Gonzalez-Lima, F. (2021). Transcranial laser stimulation: Mitochondrial and cerebrovascular effects in younger and older healthy adults. *Brain stimulation*, *14*(2), 440–449. https://doi-org.docelec.univ-lyon1.fr/10.1016/j.brs.2021.02.011

Scharfman, H. E. (2007). The neurobiology of epilepsy. *Current neurology and neuroscience reports*, *7*(4), 348-354.

Senova, S., Scisniak, I., Chiang, C., Doignon, I., Palfi, S., Chaillet, A., Martin, C., & Pain, F. (2017). Experimental assessment of the safety and potential efficacy of high irradiance photostimulation of brain tissues. *Nature Scientific Reports*. DOI: 10.1038/srep43997

Somjen, G. G. (2001). Mechanisms of spreading depression and hypoxic spreading depression-like depolarization. *Physiological reviews*, *81*(3), 1065–1096. https://doi-org.docelec.univ-lyon1.fr/10.1152/physrev.2001.81.3.1065

Stujenske, J. M., Spellman, T., & Gordon, J. A. (2015). Modeling the spatiothermal dynamics of light and heat propagation for in vivo optogenetics. *Cell Reports, 12*, 525-534. http://dx.doi.org/10.1016/j.celrep.2015.06.036

Sun, L., Perakyla, J., Kovalainen, A., Ogawa, K. H., Karhunen, P. J., & Hartikainen, K. M. (2016). Human brain reacts to transcranial extraocular light. *PLoS ONE, 11*(2).

Sun, L. Liu, X., Li, X., & Li, M. (2020). Photosensitive inhibition of the GABA system in vitro. *Nature Scientific Reports, 10*(3133). https://doi.org/10.1038/s41598-020-59915-2

Tarttelin, E. E., Bellingham, J., Hankins, M. W., Foster, R. G., & Lucas, R. J. (2003). Neuropsin (OPN5): a novel opsin identified in mammalian neural tissue. *FEBS Letters, 554*, 410-416. https://doi.org/10.1016/s0014-5793(03)01212-2

Thiery, E., Thomas, S., Vacher, S., Delezoide, A. L., Delabar, J. M., & Créau, N. (2003). Chromosome 21 KIR channels in brain development. *Journal of neural transmission. Supplementum*, (67), 105–115. https://doi-org.docelec.univ-lyon1.fr/10.1007/978-3-7091-6721-2_9

Thompson, S., Masukawa, L., & Prince, D. (1985). Temperature dependence of intrinsic membrane properties and synaptic potentials in hippocampal CA1 neurons in vitro. *The Journal of Neuroscience, 5*(3), 817-824.

Timonen, M., Nissila, J., Liettu, A., Jokelainen, J., Jurvelin, H., Aunio, A., Rasanen, P., & Takala, T. (2012). Can transcranial brain-targetied bright light treatment via ear canals be effective in relieving symptoms in seasonal affective disorder? A pilot study. *Medical Hypotheses, 78*, 511-515. https://doi.org/10.1016/j.mehy.2012.01.019

Vennekens, R., Menigoz, A., & Nilius, B. (2012). TRPs in the Brain. *Reviews of physiology, biochemistry and pharmacology*, *163*, 27–64. https://doi-org.docelec.univ-lyon1.fr/10.1007/112_2012_8

Volgushev, M., Vidyasagar, T. R., Chistiakova, M., & Eysel, U. T. (2000a). Synaptic transmission in the neocortex during reversible cooling. Neuroscience, 98, 9–22. https://doi.org/10.1016/ S0306-4522(00)00109-3

Volgushev, M., Vidyasagar, T. R., Chistiakova, M., Yousef, T., & Eysel, U. T. (2000b). Membrane properties and spike generation in rat visual cortical cells during reversible cooling. *Journal of Physiology*, *522*(Pt 1), 59–76. https://doi.org/10.1111/j.1469-7793.2000.0059m.x

Wade, P. D., Taylor, J., & Siekevitz, P. (1988). Mammalian cerebral cortical tissue responds to low-sensitivity visible light. *Proceedings of the National Academy of Sciences, USA, 85*(23)*,* 9322-9326. https://doi.org/10.1073/pnas.85.23.9322

Wang, L., Jacques, S. L., & Zheng, L. (1995). MCML – Monte Carlo Modeling of light transport in multi-layered tissues. *Computer methods and programs in biomedicine, 47*, 131-146. https://doi-org.docelec.univ-lyon1.fr/10.1016/0169-2607(95)01640-F

Wang, P., & Li, T. (2019). Which wavelength is optimal for transcranial low-level laser stimulation?. *Journal of biophotonics, 12*(2), e201800173. https://doi.org/10.1002/jbio.201800173

Wang, X., Wanniarachchi, H., Wu, A., Gonzalez-Lima, F., & Liu, H. (2021). Transcranial photobiomodulation and thermal stimulation induce distinct topographies of EEG alpha and beta power changes in healthy humans. Scientific reports, 11(1), 18917. https://doi.org/10.1038/s41598-021-97987-w

Wesselmann, U., Kerns, J. M., & Rymer, W. Z. (1994). Laser effects on myelinated and nonmyelinated fibers in the rat peroneal nerve: a quantitative ultrastructural analysis. *Experimental neurology*, *129*(2), 257-265. https://doi.org/10.1006/exnr.1994.1168

Williams, S. C. P., & Deisseroth, K. (2013). Optogenetics. *Proceedings of the National Academy of Sciences of the United States of America, 110*, 16287. https://doi.org/10.1073/pnas.1317033110

Wong-Riley, M. T., Liang, H. L., Eells, J. T., Chance, B., Henry, M. M., Buchmann, E., Kane, M., & Whelan, H. T. (2005). Photobiomodulation directly benefits primary neurons functionally inactivated by toxins: role of cytochrome c oxidase. *The Journal of biological chemistry*, *280*(6), 4761–4771. https://doi-org.docelec.univ-lyon1.fr/10.1074/jbc.M409650200

World Health Organization (2023, February 9). *Epilepsy*. WHO Newsroom. https://www.who.int/news-room/fact-sheets/detail/epilepsy

Wu, Q., Xuan, W., Ando, T., Xu, T., Huang, L., Huang, Y.-Y., Dai, T., Dhital, S., Sharma, S.K., Whalen, M.J. and Hamblin, M.R. (2012). Low-Level Laser Therapy for Closed-Head Traumatic Brain Injury in Mice: Effect of Different Wavelengths. *Lasers in Surgery and Medicine, (44)*, 218-226. https://doi-org.docelec.univ-lyon1.fr/10.1002/lsm.22003

Yang, F., Cui, Y., Wang, K., Zheng, J. (2010) Thermosensitive TRP channel pore turrent is part of the temperature activation pathway. *PNAS Biological Sciences, 107*(15), 7083-7088. https://doi.org/10.1073/pnas.1000357107

Yao, J. P., Hou, W. S., and Yin, Z. Q. (2012). Optogenetics: a novel optical manipulation tool for medical investigation. *International Journal Ophthalmology, 5*, 517–522. doi:10.3980/j.issn.2222-3959.2012.04.22

Yin, M., Borton, D. A., Komar, J., Agha, N., Lu, Y., Li, H., Laurens, J., Lang, Y., Li, Q., Bull, C., Larson, L., Rosler, D., Bezard, E., Courtine, G., & Nurmikko, A. V. (2014). Wireless neurosensor for full-spectrum electrophysiology recordings during free behavior. *Neuron*, *84*(6), 1170–1182. https://doi-org.docelec.univ-lyon1.fr/10.1016/j.neuron.2014.11.010

Yizhar, O., Fenno, L. E., Davidson, T. J., Morgri, M., & Deisseroth, K. (2011). Optogenetics in Neural Systems. *Neuron (71)*. http://dx.doi.org/10.1016/j.neuron.2011.06.004

Yu, F. H., Mantegazza, M., Westenbroek, R. E., Robbins, C. A., Kalume, F., Burton, K. A., Spain, W. J., McKnight, G. S., Scheuer, T., & Catterall, W. A. (2006). Reduced sodium current in GABAergic interneurons in a mouse model of severe myoclonic epilepsy in infancy. *Nature neuroscience*, *9*(9), 1142–1149. https://doi-org.docelec.univ-lyon1.fr/10.1038/nn1754

Zhang, K., D'Souza, S., Upton, B., Kernodle, S., Vemaraju, S., Nayak, G., Holt, A., Linne, C., Smith, A., Petts, N., Batie, M., Mukherjee, R., Tiwari, D., Burh, E., VanGelder, R., Gross, C., Sweeney, A., Sanchez-Guramaches, J., Seeley, R., & Lang, R. (2020). Violet-light suppression of thermogenesis by Opsin 5 hypothalamic neurons. *Nature, (585)*7825, 420-425. doi:10.1038/s41586-020-2683-0.

Zhu, Z., Bolt, E., Newmaster, K., Osei-Bonsu, W., Cohen, S., Cuddapah, V. A., Gupta, S., Paudel, S., Samanta, D., Dang, L. T., Carney, P. R., & Naik, S. (2022). SCN1B Genetic Variants: A Review of the Spectrum of Clinical Phenotypes and a Report of Early Myoclonic Encephalopathy. *Children (Basel, Switzerland)*, *9*(10), 1507. https://doi-org.docelec.univ-lyon1.fr/10.3390/children9101507